RETURN TO DES

JOURNAL OF THE AERONAUTICAL SCIENCES

VOLUME 15 APRIL, 1948 NUMBER 4

CONTENTS

Low-Drag and Suction Airfoils ..... SYDNEY GOLDSTEIN 189

Warping and Shear Lag in Closed Cylindrical Shells ..... LEON BESKIN 221

Low-Speed Flutter and Its Physical Interpretation ..... M. A. BIOT AND LEE ARNOLD 232

The Analysis of a Circular Ring with Propped Floor Beam ..... J. S. TAYLOR AND S. S. GILL 237

High-Speed Flow Through Cambered Rotating Grids ..... FRANK L. WATTENDORF 243

Letters to the Editor 231, 236

THE JOHN CRERAR LIBRARY APR 21 1948

Published by the
INSTITUTE OF THE AERONAUTICAL SCIENCES, INC.

JOURNAL OF THE AERONAUTICAL SCIENCES

Editor: HUGH L. DRYDEN, *Director of Aeronautical Research, N.A.C.A.*

Associate Editor: ROBERT R. DEXTER *Associate Editor:* BERNEICE H. JARCK

The Institute of the Aeronautical Sciences publishes monthly the JOURNAL OF THE AERONAUTICAL SCIENCES and the AERONAUTICAL ENGINEERING REVIEW.

The JOURNAL OF THE AERONAUTICAL SCIENCES prints papers of scientific and technical interest to Institute members and subscribers. In general, it provides an opportunity for specialists to publish articles disclosing new knowledge and new applications in the field of the aeronautical sciences. The JOURNAL restricts itself to the aeronautical aspects of advances in science and engineering, and papers printed have either been submitted directly to the JOURNAL or have been previously presented at a meeting of the Institute.

The AERONAUTICAL ENGINEERING REVIEW keeps members and subscribers informed regarding the contents of new books and current periodicals in the field of aeronautics. It reviews new developments in the aircraft industry and reports on progress from house organs and catalogs published by aircraft and engine manufacturers and other companies engaged in aeronautical activities. It publishes papers on applied engineering and aircraft production. News of Institute activities is published in the REVIEW.

Statements and opinions expressed in the JOURNAL are to be understood as individual expressions of the authors and not those of the Institute.

SUBSCRIPTION RATES

Journal of the Aeronautical Sciences
Published Monthly

United States and Possessions		Foreign Countries Including Canada (American Currency Rates)	
1 Year	$12.00	1 Year	$13.00
Single Copies	1.50	Single Copies	1.50

Aeronautical Engineering Review
Published Monthly

United States and Possessions		Foreign Countries Including Canada (American Currency Rates)	
1 Year	$3.00	1 Year	$3.50
Single Copies	0.50	Single Copies	0.50

Notices of change of address should be sent to the Institute at least 30 days prior to actual change of address.

Manuscripts for publication, proofs, and all correspondence should be addressed to the Editorial Office of the JOURNAL.

Correspondence regarding subscriptions may be addressed to Publication Office, 20th and Northampton Sts., Easton, Pa., or to the Editorial Office of the JOURNAL OF THE AERONAUTICAL SCIENCES, 2 East 64th Street, New York 21, New York.

Copyright, 1948, by the Institute of the Aeronautical Sciences, Inc.

Entered as Second Class Matter at the Post Office, Easton, Pa., May 1, 1937. Acceptance for mailing at a special rate of Postage provided for in the Act of August 24, 1912. Authorized April 29, 1937.

INS

JOHN K

SMITH J
C. L. J
R. P. L
EARL D

S. PAUL

BENNET

E. E. A
LAWRE
REX B.
WILLIA
W. A. I
VICTOR

WALTE
FRANK
RALPH
KENNE
R. H. I
R. PAU

JOHN C.
JOHN N
W. A. M
FRANK
E. U. C

H. H. A
FRANK
SIR GE
JAMES
DONALI
HUGH I

E. E. A
HART C
W. A. I
E. L. C
DONAL
SHERM

IRA H.
JOHN I
E. E. A
HARRY
KARL
J. L. A
PAUL S
RALPH
P. R. I
WELLI
REX H
G. M.
DON R
HENRY
WILLI
GEORG
LYMA
W. G.
WILLI
CHARI
KENN
CHARI
ALLA
FRANI
CHARI
KARL
EMER
JOHN
RALP
LUIS
SMITH
I. P.
WALT
C. S.
IVAN
WILL
C. L.
FRED

INSTITUTE of the AERONAUTICAL SCIENCES

President
JOHN K. NORTHROP

Vice-Presidents
SMITH J. DE FRANCE
C. L. JOHNSON
R. P. LANSING
EARL D. OSBORN

Director
S. PAUL JOHNSTON

Executive Vice-President
BENNETT H. HORCHLER

Past-Presidents
J. C. HUNSAKER
CHARLES L. LAWRANCE
DONALD W. DOUGLAS
GLENN L. MARTIN
CLARK B. MILLIKAN
T. P. WRIGHT
GEORGE W. LEWIS
JAMES H. DOOLITTLE
FRANK W. CALDWELL
HALL L. HIBBARD
HUGH L. DRYDEN
R. H. FLEET
CHARLES H. COLVIN
ARTHUR E. RAYMOND
P. R. BASSETT

Secretary
ROBERT R. DEXTER

Treasurer
SHERMAN M. FAIRCHILD

Controller
JOSEPH J. MAITAN

Counsel
ALLAN D. EMIL

COUNCIL

E. E. ALDRIN
LAWRENCE D. BELL
REX B. BEISEL
WILLIAM BOLLAY
W. A. M. BURDEN
VICTOR E. CARBONARA
FRANK O. CARROLL
CHARLES H. COLVIN
JAMES H. DOOLITTLE
C. C. FURNAS
LEROY R. GRUMMAN
J. A. HERLIHY
JEROME LEDERER
JOHN C. LESLIE
JACK MASON
C. KENNETH RAZAK
L. B. RICHARDSON
RUSSELL G. ROBINSON
GEORGE S. SCHAIRER
ERNEST G. STOUT
A. J. THIEBLOT

ADVISORY COMMITTEE

WALTER BEECH
FRANK W. CALDWELL
RALPH S. DAMON
KENNETH S. M. DAVIDSON
R. H. FLEET
R. PAUL HARRINGTON
R. M. HAZEN
HALL L. HIBBARD
J. C. HUNSAKER
TH. VON KÁRMÁN
THOMAS A. KNOWLES
I. M. LADDON
GROVER LOENING
GLENN L. MARTIN
CLARK B. MILLIKAN
THOMAS A. MORGAN
ARTHUR E. RAYMOND
F. W. REICHELDERFER
LAURANCE S. ROCKEFELLER
T. CLAUDE RYAN
EDWARD P. WARNER

HONORARY MEMBERS

JOHN C. ADAMS
JOHN N. BROWN
W. A. M. BURDEN
FRANK O. CARROLL
E. U. CONDON
L. C. CRAIGIE
IRA C. EAKER
HARRY F. GUGGENHEIM
HENRY G. HOUGHTON
GEORGE C. KENNEY
CURTIS E. LE MAY
GEORGE B. PEGRAM
E. M. POWERS
J. LAURENCE PRITCHARD
ARTHUR W. RADFORD
F. W. REICHELDERFER
H. B. SALLADA
CARL SPAATZ
L. C. STEVENS
NATHAN F. TWINING

HONORARY FELLOWS

H. H. ARNOLD
FRANK W CALDWELL
SIR GEOFFREY DE HAVILLAND
JAMES H. DOOLITTLE
DONALD W. DOUGLAS
HUGH L. DRYDEN
W. F. DURAND
SIR RICHARD FAIREY
SIR ROY FEDDEN
J. C. HUNSAKER
SIR MELVILL JONES
GEORGE W. LEWIS
GLENN L. MARTIN
GEORGE J. MEAD
SIR FREDERICK HANDLEY PAGE
D. R. PYE
IGOR I. SIKORSKY
SIR GEOFFREY TAYLOR
TH. VON KÁRMÁN
EDWARD P. WARNER
T. P. WRIGHT

BENEFACTORS

E. E. ALDRIN
HART O. BERG (Deceased)
W. A. M. BURDEN
E. L. CORD
DONALD W. DOUGLAS
SHERMAN M. FAIRCHILD
SIR RICHARD FAIREY
R. H. FLEET
FLORENCE GUGGENHEIM (Deceased)
C. D. HANSCOM
JOHN P. V. HEINMULLER
ALEXANDER KLEMIN
PAUL KOLLSMAN
BELLA C. LANDAUER
WILLIAM LANDAUER
GROVER LOENING
EDMUND C. LYNCH (Deceased)
F. W. MAGIN
GLENN L. MARTIN
GEORGE J. MEAD
S. A. REED (Deceased)
LAURANCE S. ROCKEFELLER
EDWARD P. WARNER

AMERICAN FELLOWS

IRA H. ABBOTT
JOHN D. ACKERMAN
E. E. ALDRIN
HARRY G. ARMSTRONG
KARL ARNSTEIN
J. L. ATWOOD
PAUL S. BAKER
RALPH S. BARNABY
P. R. BASSETT
WELLWOOD E. BEALL
REX B. BEISEL
G. M. BELLANCA
DON R. BERLIN
HENRY A. BERLINER
WILLIAM BOLLAY
GEORGE W. BRADY
LYMAN J. BRIGGS
W. G. BROMBACHER
WILLIAM G. BROWN
CHARLES P. BURGESS
KENNETH CAMPBELL
CHARLES H. CHATFIELD
ALLAN CHILTON
FRANKLIN R. COLLBOHM
CHARLES H. COLVIN
KARL T. COMPTON
EMERSON W. CONLON
JOHN W. CROWLEY, JR.
RALPH S. DAMON
LUIS DE FLOREZ
SMITH J. DE FRANCE
J. P. DEN HARTOG
WALTER S. DIEHL
C. S. DRAPER
IVAN H. DRIGGS
WILLIAM K. EBEL
C. L. EGTVEDT
FREDERIC FLADER
CHARLES FROESCH
JACK FRYE
GARLAND FULTON
LESTER D. GARDNER
RICHARD C. GAZLEY
MICHAEL E. GLUHAREFF
MELVIN N. GOUGH
LEROY R. GRUMMAN
HAROLD R. HARRIS
R. M. HAZEN
ALBERT F. HEGENBERGER
EDWARD H. HEINEMANN
S. D. HERON
HALL L. HIBBARD
L. S. HOBBS
PAUL E. HOVGAARD
WILLIAM HOVGAARD
ROBERT INSLEY
EASTMAN N. JACOBS
C. L. JOHNSON
S. PAUL JOHNSTON
ALEXANDER KARTVELI
PAUL H. KEMMER
CARLETON KEMPER
J. H. KINDELBERGER
OTTO B. KIRCHNER
ARTHUR L. KLEIN
ALEXANDER KLEMIN
W. B. KLEMPERER
PAUL KOLLSMAN
OTTO C. KOPPEN
B. V. KORVIN-KROUKOVSKY
S. M. KRAUS
ARNOLD M. KUETHE
I. M. LADDON
E. S. LAND
CHARLES L. LAWRANCE
JEROME LEDERER
JOHN G. LEE
JOHN C. LESLIE
CHARLES A. LINDBERGH
WILLIAM LITTLEWOOD
GROVER LOENING
ALBERT E. LOMBARD
F. A. LOUDEN
W. RANDOLPH LOVELACE, II
EUGENE E. LUNDQUIST
R. D. MACCART
JOHN R. MARKHAM
ERLE MARTIN
WM. H. MCAVOY
C. J. MCCARTHY
J. S. MCDONNELL
CLARK B. MILLIKAN
ROBERT J. MINSHALL
JOSEPH S. NEWELL
ALFRED S. NILES
JOHN K. NORTHROP
ARTHUR NUTT
SHATSWELL OBER
ROBERT R. OSBORN
W. BAILEY OSWALD
GEORGE A. PAGE, JR.
F. W. PAWLOWSKI
F. W. PENNOYER, JR.
A. A. PRIESTER
ARTHUR E. RAYMOND
F. W. REICHELDERFER
ELLIOTT G. REID
H. J. E. REID
H. C. RICHARDSON
L. B. RICHARDSON
RUSSELL G. ROBINSON
LEONARD B. ROOT
C. E. ROSENDAHL
ADDISON M. ROTHROCK
W. R. SEARS
WILLIAM T. SCHWENDLER
FRANCIS R. SHANLEY
JAMES M. SHOEMAKER
MAC SHORT
IGOR ALEXIS SIKORSKY
ABE SILVERSTEIN
SELDEN B. SPANGLER
ELMER A. SPERRY, JR.
JOHN STACK
ROBERT M. STANLEY
WILLIAM B. STOUT
HARRY A. SUTTON
C. FAYETTE TAYLOR
EDWARD S. TAYLOR
PHILIP B. TAYLOR
TH. THEODORSEN
T. E. TILLINGHAST
S. TIMOSHENKO
L. B. TUCKERMAN
RALPH H. UPSON
J. PARKER VAN ZANDT
J. G. VINCENT
RICHARD VON MISES
FRANK L. WATTENDORF
P. V. H. WEEMS
FRED E. WEICK
R. D. WEYERBACHER
JOHN B. WHEATLEY
ANDREW V. WILLGOOS
DONALD H. WOOD
ROBERT J. WOODS
JOHN E. YOUNGER
ALBERT F. ZAHM
STEPHEN J. ZAND

Corporate Members
of the
Institute of the Aeronautical Sciences

Academy of Aeronautics, Inc.
Casey Jones School of Aeronautics

Aero Insurance Underwriters

Aerojet Engineering Corporation

Aeroproducts Division, General Motors Corporation

Aeroquip Corporation

Agawam Aircraft Products, Inc.

Airborne Instruments Laboratory, Inc.

Airchox Company Division, Joyce Aviation, Inc.

Aircraft Radio Corporation

AiResearch Manufacturing Company, Division of The Garrett Corporation

Allis-Chalmers Manufacturing Company

Allison Division, General Motors Corporation

Aluminum Company of America

American Airlines System

American Bosch Corporation

American Overseas Airlines, Inc.
Iceland Airport Corporation (Subsidiary)

American Phenolic Corporation

Associated Aviation Underwriters

Atlas Supply Company

Baker Steel & Tube Company

Beech Aircraft Corporation

Bell Aircraft Corporation

Bendix Aviation Corporation
Bendix International Division
Bendix Products Division
Bendix Radio Corporation
Eclipse-Pioneer Division
Friez Instrument Division
Pacific Division
Scintilla Magneto Company

The BG Corporation

Boeing Airplane Company
Seattle Division
Wichita Division

Breeze Corporations, Inc.
Aircraft Standard Parts Company, Inc.
Aldrich Company
Anderson Stove Company, Inc.
Federal Laboratories, Inc.
Foundry Service, Inc.

Cal-Aero Technical Institute, A Division of Grand Central Airport Company

Cessna Aircraft Company

Chandler-Evans Division, Niles-Bement-Pond Company

Chase Aircraft Company, Inc.

Chase National Bank of the City of New York

The Cleveland Graphite Bronze Company

The Cleveland Pneumatic Tool Company
Automotive-Aircraft Division

Clifford Manufacturing Company, Division of Standard-Thomson Corporation

Consolidated Vultee Aircraft Corporation
Fort Worth Division
Stinson Aircraft Division

Continental Motors Corporation

Curtiss-Wright Corporation
Airplane Division
Propeller Division
Wright Aeronautical Corporation Division

Doak Aircraft Company, Inc.

Douglas Aircraft Company, Inc.
El Segundo Plant
Long Beach Plant
Santa Monica Plant

The Dow Chemical Company

Dzus Fastener Company, Inc.

Eastern Air Lines, Inc.

Eaton Manufacturing Company
Dynamatic Corporation (Subsidiary)
Eaton-Wilcox-Rich Ltd. (Subsidiary)

Thomas A. Edison, Incorporated, Instrument Division

Edo Corporation

Electrol Incorporated

Ethyl Corporation

Fairchild Camera & Instrument Corporation
Fairchild Aerial Surveys, Inc.

Fairchild Engine and Airplane Corporation
Al-Fin Division
Fairchild Aircraft Division
Fairchild Personal Planes Division
Fairchild Pilotless Plane Division
NEPA Division
Ranger Aircraft Engines Division
Stratos Corporation (Subsidiary)

Federal Telephone and Radio Corporation
Federal Electric Manufacturing Company, Ltd.
Federal Telecommunication Laboratories, Inc. (Partial Subsidiary)
Firestone Aircraft Company
General Aviation Equipment Company, Inc.
General Electric Company
Aircraft Gas Turbine Division
Aviation Divisions
General Tire and Rubber Company of California, Research and Development Division
The B. F. Goodrich Company
The Goodyear Tire & Rubber Company
Goodyear Aircraft Corporation
Grumman Aircraft Engineering Corporation
W. &. L. E. Gurley
The International Nickel Company, Inc.
Irving Air Chute Company, Inc.
Jack & Heintz Precision Industries, Inc.
Johns-Manville Sales Corporation
Walter Kidde & Company, Inc.
Kollsman Instrument Division, Square D Company
Lavelle Aircraft Corporation
Lear Incorporated
Link Aviation, Inc.
The Liquidometer Corporation
Lockheed Aircraft Corporation
Airquipment Company (Subsidiary)
Lockheed Air Terminal (Subsidiary)
Lockheed Aircraft Overseas Corporation (Subsidiary)
Lockheed Aircraft Service, Inc. (Subsidiary)
Longines-Wittnauer Watch Company, Inc.
The Glenn L. Martin Company
GLM Chemical Division
Rotawings Division
Warren McArthur Corporation
McDonald Aircraft Corporation
Minneapolis-Honeywell Regulator Company
Brown Instrument Company (Subsidiary)
Moore Drop Forging Company
National City Bank of New York
National Credit Office, Inc.
North American Aviation, Inc.
North American Aviation, Inc., of Texas
Northrop Aircraft, Inc.
Northwest Airlines, Inc.
Owens-Corning Fiberglas Corporation
Pan American World Airways System
The Parker Appliance Company
Pesco Products Division, Borg-Warner Corporation
Phillips Petroleum Company
Pure Oil Company
Radioplane Company
Republic Aviation Corporation
A. V. Roe Canada Limited
John A. Roebling's Sons Company
Rohr Aircraft Corporation
Ryan Aeronautical Company
Shell Oil Company, Inc.
Simmonds Aerocessories, Inc.
Skydyne, Inc.
Socony-Vacuum Oil Company, Inc.
Solar Aircraft Company
Sperry Gyroscope Company Division of The Sperry Corporation
Square D Company
Standard Oil Company of California
Standard Oil Company (Indiana)
Standard Oil Company of New Jersey
The Texas Company
Thompson Products, Inc.
Tinnerman Products, Inc.
Union Carbide and Carbon Corporation
Bakelite Corporation
Electro Metallurgical Company
Haynes Stellite Company
The Linde Air Products Company
National Carbon Company, Inc.
United Air Lines, Inc.
United Aircraft Corporation
Chance Vought Aircraft Division
Hamilton Standard Propellers Division
Pratt & Whitney Aircraft Division
Sikorsky Aircraft Division
United Aircraft Export Corporation
United Aircraft Service Corporation
United States Aviation Underwriters, Inc.
United States Rubber Company
Dominion Rubber Company, Ltd.
Vickers, Inc.
Warner Aircraft Corporation
The Weatherhead Company
Angola, Indiana Division
Columbia Products Division
Houma Division
The Weatherhead Company of Canada (Subsidiary)
Westinghouse Electric Corporation
Aviation Gas Turbine Division
Industrial Electronics Division
Marine & Aviation Sales Department
Small Motor Division, Aviation Sales
Weston Electrical Instrument Corporation
Wyman-Gordon Company
Young Radiator Company

EDITORIAL COMMITTEE

HUGH L. DRYDEN, *Chairman*

Aerodynamics

Francis Clauser
Howard Emmons
R. Paul Harrington
R. T. Jones
W. B. Klemperer
Otto C. Koppen
John G. Lee
H. P. Liepmann
H. F. Ludloff
John R. Markham
Clark B. Millikan
Shatswell Ober
W. Bailey Oswald
Allen E. Puckett
Elliott G. Reid
H. J. E. Reid
Russell Robinson
L. E. Root
G. B. Schubauer
W. R. Sears
John Stack
Th. von Kármán
Richard von Mises

Air Transport

A. W. Dallas
Charles Froesch
J. A. Herlihy
Otto E. Kirchner
John C. Leslie

Aircraft Design

W. E. Beall
Rex B. Beisel
W. K. Ebel
Hall L. Hibbard
C. L. Johnson
I. M. Laddon
C. J. McCarthy
Fred E. Weick
Robert J. Woods

Physiologic Problems

H. G. Armstrong
Louis H. Bauer
Eugene Du Bois
W. Randolph Lovelace, II
Ross A. McFarland
A. D. Tuttle

Aircraft Propulsion

George W. Brady
Frank W. Caldwell
L. S. Hobbs
E. E. Johnson
Joseph Keenan
R. P. Kroon
Arthur Nutt
Hans Reissner
Abe Silverstein
C. Fayette Taylor
E. S. Taylor
P. Taylor

Structures and Materials

W. B. Bleakney
E. W. Conlon
J. P. Den Hartog
L. H. Donnell
E. C. Hartmann
N. J. Hoff
E. E. Lundquist
C. F. Nagel, Jr.
J. S. Newell
Alfred S. Niles
W. Ramberg
E. Reissner
F. R. Shanley
H. W. Sibert
C. R. Strang
S. Timoshenko
H. S. Tsien
Chi-Teh Wang

Meteorology

C. F. Brooks
D. M. Little
E. J. Minser
F. W. Reichelderfer
H. C. Willett

Fuels and Oils

A. L. Beall
J. H. Doolittle
Graham Edgar
R. T. Goodwin
S. D. Heron
A. M. Rothrock

Instruments

Allan G. Binnie
W. G. Brombacher
J. Callahan
Charles H. Colvin
C. S. Draper
O. E. Esval
David W. Moore
W. A. Reichel
C. F. Savage
O. Hugo Schuck
R. Sylvander

Rotating Wing Aircraft

Robert Coleman
G. Horvay
Alexander Klemin
Ralph McClarren
R. H. Miller
R. H. Prewitt
Igor I. Sikorsky
Robert A. Wolf

Vibration and Flutter

Lee Arnold
M. A. Biot
William Bollay
Chieh-Chien Chang
J. P. Den Hartog
Manfred Rauscher

Flight Testing

W. K. Ebel
R. R. Gilruth
Melvin N. Gough
Robert Stanley
E. A. Stout

I.A.S. REPRESENTATIVES TO OTHER ORGANIZATIONS

Aircraft Industries Association of America, Inc.—CHARLES MARCUS

American Association for the Advancement of Science—J. C. HUNSAKER

American Society of Mechanical Engineers—CHARLES H. COLVIN

American Standards Association—P. R. BASSETT

Engineering Society of Detroit—DONALD C. HUNT, GEORGE TWENEY

Greater New York Safety Council—WILLIAM LITTLEWOOD

Daniel Guggenheim Medal Board of Award—CHARLES H. COLVIN, GROVER LOENING, S. PAUL JOHNSTON

Institute of Radio Engineers—L. M. HULL

Manufacturers Aircraft Association—ARTHUR E. RAYMOND

National Aeronautic Association—WILLIAM R. ENYART

National Fire Protection Association—E. E. ALDRIN

National Research Council Engineering Division—HUGH L. DRYDEN

National Safety Council—JEROME LEDERER

New York Museum of Science and Industry—LESTER D. GARDNER

Society of Automotive Engineers—STEPHEN J. ZAND

JOURNAL OF THE AERONAUTICAL SCIENCES

VOLUME 15 APRIL, 1948 NUMBER 4

Low-Drag and Suction Airfoils

The Eleventh Wright Brothers Lecture

SYDNEY GOLDSTEIN*

University of Manchester, England

(1) Introduction

I SHOULD LIKE FIRST TO SAY how much I appreciate the honor of being invited to deliver the Wright Brothers Lecture. To anyone whose work is associated in any way with the aeronautical sciences, it must be a source of pride and gratification to be invited to be a chief participant in one of the greatest occasions in the world of aeronautical research, an occasion designed in honor of the two great pioneers, Wilbur and Orville Wright. In my own case these feelings are shared with a feeling of humility and of my own unworthiness for the task.

The story I am to tell in this lecture is still incomplete. It is largely the story of the researches carried out in Great Britain arising from an idea due to Dr. A. A. Griffith. This idea is at once very general and very simple. When, at a sufficiently high Reynolds number, a fluid flows along an immersed solid surface, a boundary layer is formed; if the flow in the boundary layer cannot be controlled, harmful results may follow; the boundary layer may be removed by suction in an attempt to avoid these harmful results. Griffith's idea was that if boundary-layer suction is to be applied, the shape of the solid surface should be specially designed. It is the application of this idea to airfoil design which forms the main subject of this lecture and it may be as well to stress that this does not include a discussion of the effects of suction on conventional airfoil shapes, or on any shapes not specially designed for the purpose; such a discussion should really be separate, since the amount of common ground is not large.

Part of the story has been excellently told already by Mr. Relf in his Wilbur Wright Memorial Lecture to the Royal Aeronautical Society in 1946: I shall try to fill in some of the details, as far as they are known at present.

In assessing the probable performance of a suction wing, the state of the boundary layer (turbulent or laminar) at the slot through which part of it is to be sucked away is of great importance. It is therefore advisable to spend a short time on a discussion of the principles of the ordinary laminar-flow or low-drag wing, and of the present position with regard to obtaining laminar boundary layers in flight. Some mention of the principles is moreover necessary in order really to understand why a suction wing gives a theoretical prospect of better performance than the best low-drag wing without suction.

The work described in this lecture was all carried out in the Aerodynamics Division of the National Physical Laboratory or at the Royal Aircraft Establishment, and I am indebted to the Directors of these establishments and to the relevant government departments (the Ministry of Supply and the Department of Scientific and Industrial Research) for permission to use the results. I should also like to thank Mr. W. A. Mair for assistance with the preparation of the diagrams.

(2) Low-Drag Wings

The principle underlying the design of low-drag wings is simply to design to keep as much of the boundary layer laminar as possible without boundary-layer separation before the trailing edge. The transition to turbulence should be as far aft as possible, without any risk of the boundary layer separating; apart from stalling incidences, this risk is greatest, at the Reynolds numbers of flight, at moderately large lifts with the boundary layer made accidentally turbulent at the leading edge by some form of accidental roughness. The whole matter is therefore bound up with transition to turbulence in boundary layers and with turbulent boundary-layer separation, both matters which, to this

Presented before the Institute of the Aeronautical Sciences in the U.S. Chamber of Commerce Auditorium, Washington, D.C., December 17, 1947.

* Beyer Professor of Applied Mathematics. Also, Chairman, Aeronautical Research Council.

day, are very imperfectly understood. Although, thanks largely to the excellent wind-tunnel researches by the N.A.C.A. in this country, much is known of the performance and behavior of low-drag wings, the basis for a complete physical understanding of the processes involved has not yet been constructed. Mathematical researches in Germany and experimental researches at the National Bureau of Standards, corroborated by researches at the California Institute of Technology, have certainly laid a basis for understanding the instability of laminar boundary layers, but it is abundantly clear that this instability is not itself the same thing as, nor need it necessarily lead to, transition to turbulence. Apart from the deeper physical reasons, this is clear from the fact that low drags, indicating a large extent of laminar boundary-layer flow, have been obtained in wind tunnels in this country up to Reynolds numbers of 30 to 50 millions, and also from the flight experiments at the Royal Aircraft Establishment, Farnborough, mentioned later. The physical processes leading to transition are still largely unknown, and the same is certainly true of turbulent boundary-layer separation. We are therefore at present forced to rely on certain overall experimental results, which fortunately give us much of what is needed for practical purposes.

The first such result is that on a smooth, true surface a boundary layer may be kept laminar if the velocity outside the boundary layer is increasing, and the pressure is decreasing, in the direction of flow, but that transition to turbulence takes place very soon when there is an adverse pressure gradient. Thus low-drag wings should be designed so that, at the design lift coefficient, and over as wide a range of lift coefficients as possible, the velocity outside the boundary layer rises from the front stagnation point to a position as far back along the wing as possible. A second overall experimental result, however, must now be taken into account at once—namely, that the larger the unfavorable pressure gradient the greater the risk of boundary-layer separation. The further back the position of maximum velocity, and therefore of maximum suction, the smaller is the fraction of the chord over which the pressure recovery, which must occur before the trailing edge is reached, can take place; the greater therefore, for a given maximum suction (which is related to the thickness of the wing), is the unfavorable pressure gradient over the rear of the wing; and so the greater is the danger of boundary-layer separation. For any normal wing thickness there is therefore a limit imposed by these considerations on the position of maximum suction. From a consideration of the American experimental results, Mr. Richards[1] has deduced rough rules for the maximum rate of velocity decrease that should be allowed over the rear of a wing if the danger of turbulent boundary-layer separation at moderately high lifts, with the wing accidentally roughened and the boundary layer made turbulent at the leading edge, is to be avoided; if U is the velocity of the wing relative to the undisturbed air, c the chord of the wing, and q the relative velocity of the air just outside the boundary layer and the wing at a distance x along the chord from the leading edge, then, for example, a rough criterion is that at a lift coefficient of 0.95 the nondimensional adverse velocity gradient $-(c/U)(dq/dx)$ at seven-tenths of the chord from the leading edge should not exceed 1.27, at any rate when the maximum suction is at half chord.

In practice a further limitation is set, not only to the length of laminar boundary layer which can be achieved, but also to the length that should be aimed at, by roughness and waviness of the surface. Beyond certain quite small limits it is known from experiment that even with a favorable pressure gradient roughnesses, or waviness due to manufacturing limitations, will induce, a transition to turbulence in the boundary-layer flow. If transition occurs forward of the position of maximum velocity, the drag of the wing will be greater than if the maximum velocity had been designed to be at the position of transition, since there will be a greater area with a large velocity outside the boundary layer in the turbulent region, and this produces increased skin-friction drag. The aerodynamic design of the wing and the probable state of the surface should therefore be matched so that the transition occurs at, or just aft of, the position of maximum suction.

The properties of low-drag wings that have been mentioned are all relevant to a consideration of suction wings; other properties, such as maximum lift and the behavior of control surfaces, need not detain us, though some remarks on designing for maximum lift will be made later.

(3) Flight Tests on Low-Drag Wings

Two series of flight tests have been carried out at the Royal Aircraft Establishment. One[2] was on a Kingcobra (P 63), the wing having an N.A.C.A. 662x-116 section at the root and 662x-216 section at the tip, so the maximum suction at the design lift coefficient is at 60 per cent of the chord from the leading edge and the maximum thickness-chord ratio is nearly 16 per cent. The profile drag was measured at a section 137 in. from the aircraft centerline. The results are summarized in Fig. 1. With the surface in the state in which it was received a drag coefficient of 0.0075 to 0.0080 was found; the reduction of roughness by smoothing yielded a drag coefficient of 0.005 to 0.006 near $C_L = 0.2$, with sharp rises on both sides of that lift coefficient. A test portion about 3 ft. in span was then very carefully prepared in order to decrease the waviness of the surface. The test portion was cleaned down to the metal surface, and was given two coats of primer paint, and then a paint-type filler was sprayed on; local areas found to be low were specially filled, and the wing was rubbed down with special curved rubbing blocks with strips of carborundum paper (grade 280C) held over the

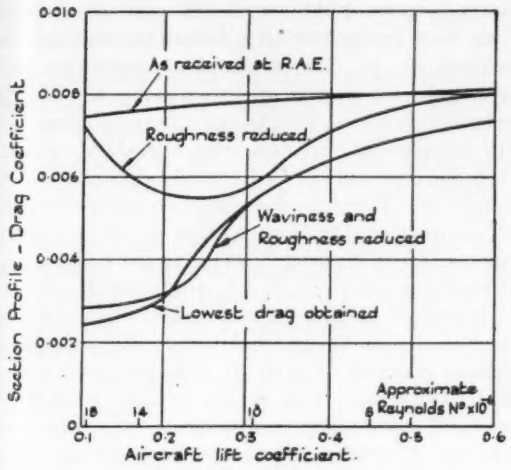

FIG. 1. Measured profile-drag coefficient of a section of a wing of a Kingcobra aircraft.

curved surfaces. The drag was now greatly reduced, as shown in Fig. 1; a drag coefficient of 0.0028 was obtained at $C_L = 0.1$, and the lowest drag recorded (with the surface polished) was 0.00245. The surface waviness was measured with an Ames dial, which could be read to $^1/_{5,000}$ in., and which was mounted on a base supported at points 2 in. apart. The measurements on the test section as received and in the final condition are shown in Fig. 2. The measurements were static measurements made on the ground; deflections in flight were not measured. It appears that on a wing of this type, at the Reynolds numbers of the tests (up to 18 millions), a very low drag is obtainable if the fluctuations on the front portion of the surface can be reduced to $^1/_{1,000}$ in. measured on a 2-in. gage; larger fluctuations may be allowed further back.

It may be noted that the use of paint and filler, by itself, does not necessarily reduce waviness, since they may be rubbed down in such a way that the final surface, while smooth, follows the waviness of the metal surface.

In order to obtain the results shown in Fig. 1 it was necessary not to pick up flies and other insects during the take-off and climb. If encountered, flies would stick to the surface, generally over the first 10 per cent of the chord; in the words of the original report, "the flies on hitting the surface disintegrate and are found in the form of small parts of the flies' bodies stuck to the surface with a particularly potent glue." Transition to turbulence is, of course, produced by the resulting "roughness," and the drag may thereby be raised by 50 to 100 per cent. In the earlier months of the year (March and April) flies could be avoided by flying before 9 a.m. G.M.T., but with the approach of warmer weather some other method had to be found. A large sheet of paper, 3 ft. wide, was placed over the leading edge and covered the test portion on the top and bottom surfaces to 30 per cent of the chord from the leading edge; the paper was kept in position by adhesive tape at the edges; a loop of string round the paper at the leading edge had its free end in the cockpit. No flies were encountered above 5,000 ft., and when this height was reached the pilot pulled the string and tore the paper along the leading edge; the wind then blew off the two halves of the paper from the top and bottom surfaces of the wing, leaving a clean surface free from parts of flies' bodies.

Apart from flies no other trouble was encountered. No trouble resulted from the effects of dust or water. Water may be used to wash the wings if they are polished, and rain has no subsequent effect on the value of the drag. Polishing the surface has very little effect on the drag, but the use of wax polish is advisable if the wings are to be washed.

Once the surface had been prepared it did not deteriorate (except at the skin-joint) over a period of six months, during which 50 flights, occupying about 40 hours, were made and the aircraft was exposed to weather for about 200 hours. During the remainder of the time it was kept in a hangar, but no special precautions were taken against weathering.[3] The difficulty at the skin-joint, where a gap between the two skins of 5 to 10 thousandths of an inch was filled with filler, which had to be rubbed down frequently, was probably caused by variations in the gap under load, and could be avoided by redesigning the joint.

Experience on another aircraft, which in fact was left in the open for over 2 years, suggested that quite long exposure to weather would not by itself cause serious deterioration of the surface.

There are, of course, other aspects of the problem of the maintenance of low-drag wings besides the effect of

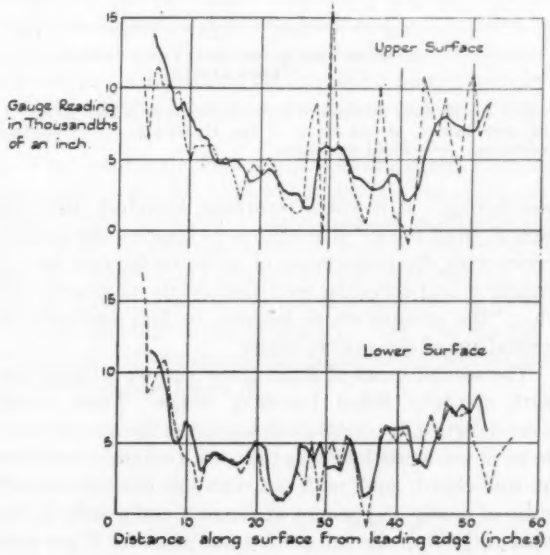

FIG. 2. Surface waviness measurements with a 2-in. gauge on the test section of the wing of the Kingcobra. ------Original condition. ——Final condition.

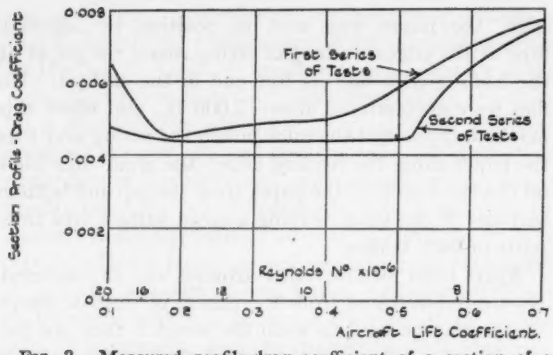

FIG. 3. Measured profile-drag coefficient of a section of a moderately low-drag wing fitted to a Hurricane aircraft. First series, as received; second series, with waviness reduced.

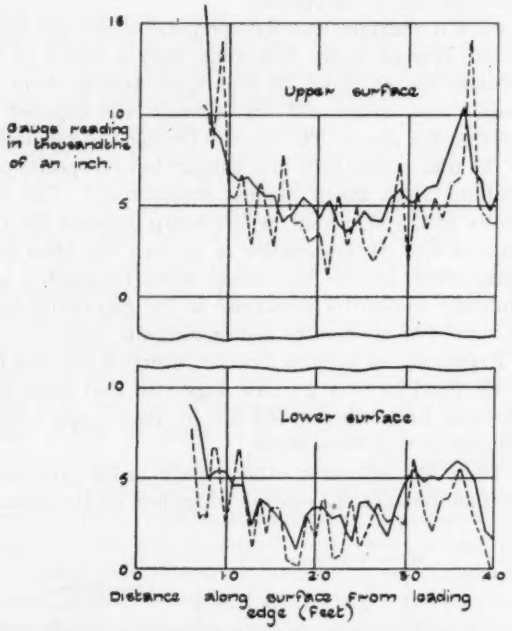

FIG. 4. Surface waviness measurements with a 2-in. gauge on the test section of the wing of the Hurricane. ----Original condition. ——Final condition.

weathering. It is worth recording, therefore, that the R.A.E. Staff report[3] that efforts to impress the ground crews with the importance of avoiding damage during handling and servicing were completely successful and that "the ground crews became in fact enthusiastic custodians of the surface finish."

The second series of flight tests[4] was on a Hurricane with specially fitted low-drag wings. These wings were designed, by methods described in the next section, to be of moderate low-drag type, with maximum suction at mid-chord, and with a maximum thickness-chord ratio of nearly 18 per cent at the root and nearly 15 per cent at the tip; the test section was just over 17 per cent thick. The lowest drag to be expected on this wing is, of course, greater than on the Kingcobra. Fig. 3 shows the drag measured on the wing as first received from Messrs. Armstrong Whitworth Ltd. and after reduction of waviness by the firm by a technique similar to that described above. The results of measurements of the waviness by a 2-in. gage are shown in Fig. 4. With this moderately low-drag wing fair results are obtained, even with considerable waviness, over a moderate range of lift coefficients and up to Reynolds numbers of about 14 millions. When the deflections are reduced to about $\pm 1/1{,}000$ in. over the front portion of the surface the drag coefficient is about 0.0044 over the whole range of lift coefficients from 0.1 to 0.5, with a slight increase at the lowest lift coefficients and highest Reynolds numbers (which may have been due to the fact that the deflections exceeded $1/1{,}000$ in. at some places on the surface). Otherwise—with regard to both trouble with flies and satisfactory maintenance—the experiences with the Kingcobra were repeated with the Hurricane.

It is now possible to find the position of transition to turbulence in a boundary layer along the whole span of a wing in flight by a chemical technique due to Mr. W. E. Gray.[5] A photograph illustrating the results obtained in this way on the Hurricane is shown in Fig. 5; on the lighter parts of the wing the boundary layer is laminar. Fig. 5 shows part of the upper surface of the Hurricane after a flight at 205 m.p.h. at $C_L = 0.22$ ($R = 14 \times 10^6$); the general transition to turbulence is at

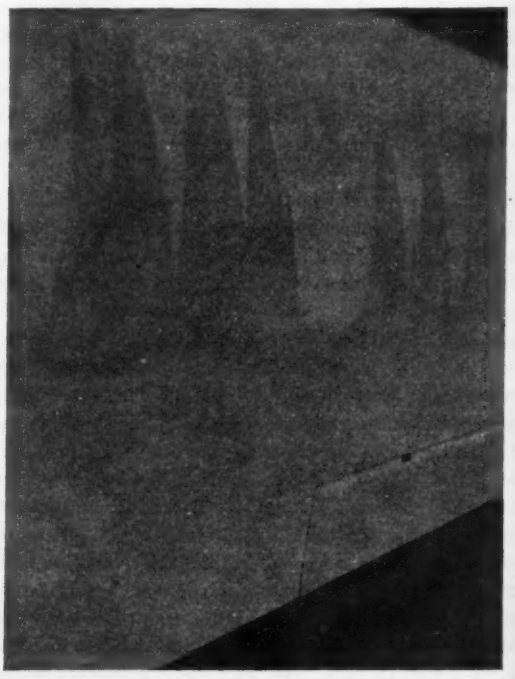

FIG. 5. Transition to turbulence in the boundary layer of a wing of the Hurricane in flight. The boundary layer is laminar on the lighter parts of the wing. The general transition to turbulence is at 55 per cent of the chord from the leading edge, with "wedges" of turbulent flow further forward. ($C_L = 0.22$, $R = 14 \times 10^6$.)

55 per cent of the chord from the leading edge, with "wedges" of turbulent flow further forward.

The conclusions from the flight experiments may be summarized as follows. Low drag may be obtained in flight if an accuracy of the surface over the relevant parts of $\pm 1/1{,}000$ in. on a 2-in. gage can be achieved. Although the best method of obtaining the required accuracy of surface is not yet clear, such an accuracy could be both achieved and maintained without excessive difficulty. Particular attention to joints and rivets is still needed when maintenance problems are considered. The problem presented by the adherence of flies and other insects on the surface near the leading edge is serious, and no practical solution has yet been found.

(4) Mathematical Airfoil Theories

If the boundary layer does not separate, the velocity just outside the boundary layer on an airfoil is, except at and near the trailing edge, very nearly equal to the velocity calculated from the potential flow at the lift experienced by the airfoil. If, on the basis of experimental knowledge, we are prepared to guess at the position of transition to turbulence and the occurrence or nonoccurrence of turbulent separation and at the reduction of the lift from its theoretical value on the Kutta-Joukowski hypothesis, we can forecast many of the aerodynamic properties of an airfoil section when we have calculated values, according to potential theory, of the velocity on the surface. It is also an advantage to be able to design sections of airfoils which will have specified velocity distributions, or velocity distributions of a specified type, on the surface. In this way we can design and choose promising models for experimental tests in wind tunnels and, eventually, for flight tests if the wind-tunnel results are satisfactory. It should be pointed out at once, however, that our ability to guess at all correctly about the occurrence of turbulent separation is very limited, so that, for example, maximum lift cannot be predicted with any confidence. Nevertheless, such theoretical calculations as we can make, and particularly the solution of the inverse problem of designing a section with a specified velocity or pressure distribution, provide a valuable tool in investigating low-drag wings according to the principles discussed in Section 2.

A solution of the first problem, that of computing the velocity distribution on the surface of a given airfoil section, was given a good many years ago by Theodorsen,[6] and by Theodorsen and Garrick.[7] This is a full and complete solution, but careful computation is required, especially for cambered airfoils, if the computed points are to be smooth and accurate; I have seen computed points that looked more like experimental points with a fair amount of scatter. In its original accurate form the theory is not easy to use for the solution of the inverse problem—of designing a wing section with a velocity distribution on the surface of specified type—or for forming rapidly judgments on the probable relations between the geometric and aerodynamic properties of the wing. It is therefore well worth while to approximate Theodorsen and Garrick's results.

For the first, and crudest, approximation we linearize all the formulas completely, retaining only quantities of the first order in the thickness, the camber, and the incidence of the wing; for a symmetrical airfoil at zero incidence this leads to the formula

$$q/U = 1 + g_s$$

where

$$g_s = -(1/\pi)P\int^1 y_s'(\xi)d\xi/(\xi - x)$$

U is the relative velocity of the wing and the undisturbed air, q is the relative velocity at a distance x from the leading edge measured along the chord in fractions of the chord length, and $y_s(x)$ the half-thickness at that position also measured in fractions of the chord length. The integral is an improper integral, and P denotes that the principal value is to be taken. The prime denotes a derivative.

This formula, obtained by linearizing Theodorsen and Garrick's accurate solution, may also be obtained by physical reasoning, since we may suppose that we could allow approximately for the variation in breadth of the wing by supposing sources, of strength $2Uy_s'(x)$ per unit length, placed along the chord; the same formula would be obtained in this way, and was so obtained by Squire. Now the leading edge is a stagnation point, and so is the trailing edge if it is not a cusp; and it is clear that a distribution of sources along the chord that would accurately produce the disturbance flow cannot extend right up to the leading edge or the trailing edge, whereas the approximate distribution does so. For this reason this first approximate expression must be wrong at and near the leading and trailing edges, and in particular will not give stagnation points at those places.

When we find the first, completely linearized, approximation for a cambered airfoil at any lift, the additional terms (found as before by approximating to Theodorsen and Garrick's accurate solution) may be shown to be exactly those found from the vortex-sheet theory of infinitely thin airfoils, as set out, for example, in Glauert's Aerofoil and Airscrew Theory. Let α be the incidence and $-\beta$ the theoretical no-lift angle, and let the lift coefficient be taken as

$$C_L = a_0 \sin(\alpha + \beta)$$

let

$$x = \tfrac{1}{2}(1 - \cos\theta) = \sin^2 \tfrac{1}{2}\theta$$

so that θ is 0 at the leading edge and π at the trailing edge; let $y_c(x)$ be the ordinate of the centerline, measured in fractions of the chord length, and let

$$dy_c/dx = F(\theta) = \sum_{n=0}^{\infty} A_n \cos n\theta \qquad (0 \leq \theta \leq \pi)$$

so that

$$A_0 = (1/\pi)\int_0^\pi F(t)dt,$$

and

$$A_n = (2/\pi)\int^\pi F(t)\cos nt\, dt$$

for $n \geqslant 1$. Also let $C_{L_{opt.}}$ be the lift coefficient defined by

$$[(1/a_0) + (1/2\pi)]C_{L_{opt.}} = A_1$$

$C_{L_{opt.}}$ may be shown to be the only lift coefficient for which, on a linear theory, there is no infinity at the leading edge in the velocity distribution for an infinitely thin airfoil of the shape of the given centerline; it is also approximately equal to the lift coefficient at which the forward stagnation point is at the leading edge.

Then the first approximation is

$$q/U = 1 + g_s \pm \left[g_t + \frac{1}{2}\left(\frac{1}{a_0} + \frac{1}{2\pi}\right)\left(C_L - C_{L_{opt.}}\right) \times \cot\frac{1}{2}\theta - \frac{1}{2}\left(\frac{1}{a_0} - \frac{1}{2\pi}\right)C_L \tan\frac{1}{2}\theta\right]$$

where g_s was given above and

$$g_t = -\left(\frac{1}{2\pi}\right)P\int_{-\pi}^{\pi} F(t)\cot\frac{1}{2}(t-\theta)dt = \sum_{n=1}^{\infty} A_n \sin n\theta$$

When $C_L = C_{L_{opt.}}$ and $a_0 = 2\pi$, q/U is $1 + g_s \pm g_t$, simply. The positive signs refer to the upper surface and the negative signs to the lower surface.

The no-lift angle is given by $\beta = {}^1/_2A_1 - A_0$, and the moment coefficient at zero lift by $(C_M)_0 = \pi(A_2 - A_1) \div 4$.

We have assumed that the theoretical no-lift angle is sufficiently accurate; the formulas may be adjusted to allow for any discrepancy.

The first approximation will, as we have seen, be wrong near the nose and perhaps also near the tail; the second approximation consists merely of inserting a factor, obvious from the accurate solution, to remedy this. Approximation II is

$$\frac{q}{U} = \frac{(1 + {}^1/_2C_0^2)|\sin\theta|}{(\psi^2 + \sin^2\theta)^{1/2}}\left[1 + g_s \pm g_t\right] \pm \frac{1 + {}^1/_2C_0^2}{(\psi^2 + \sin^2\theta)^{1/2}}\left[\frac{C_L}{2\pi} + \frac{C_L}{a_0}\cos\theta - \frac{1}{2}\left(\frac{1}{a_0} + \frac{1}{2\pi}\right)C_{L_{opt.}} \times (1 + \cos\theta)\right]$$

where

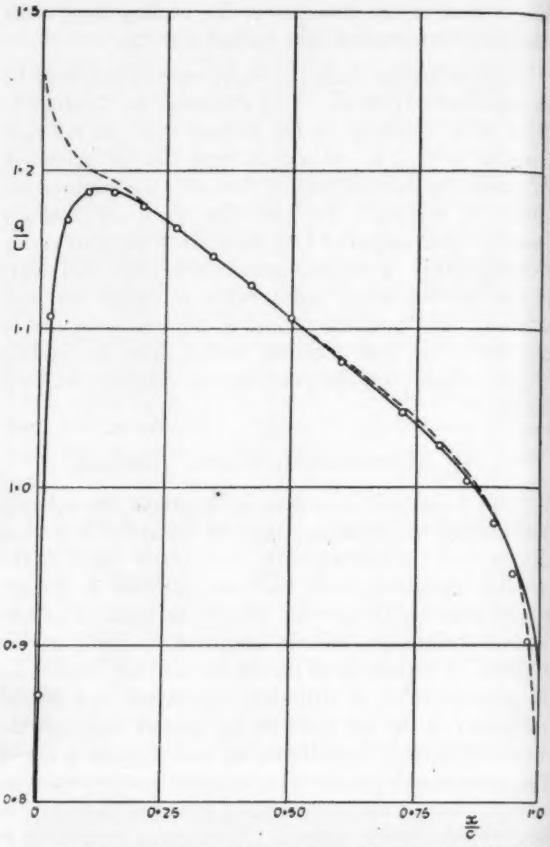

FIG. 6. Computed velocities on the surface of an NACA 0012 airfoil section at zero incidence. ——Accurate computation. ⊙ Approximation III. - - - - -Approximation I.

$$\psi = \psi_s \pm \psi_c$$
$$\psi_s = 2y_s/\sin\theta$$
$$\psi_c = 2y_c/\sin\theta$$
$$C_0 = \frac{1}{\pi}\int_0^\pi \psi_s(t)dt = \frac{1}{\pi}\int_0^1 \frac{y_s(\xi)d\xi}{\xi(1-\xi)}$$

For the third approximation we attempt to come as near as we can to the accurate solution while still keeping the computations simple. With the upper signs referring to the upper surface, and the lower signs to the lower surface, Approximation III is

$$q/U = |AF\sin(\theta \pm \epsilon \mp \beta) \pm BF\cos(\theta \pm \epsilon \mp \beta) \pm CF|$$

where

$$F = e^{C_0}(1 + \epsilon')/(\psi^2 + \sin^2\theta)^{1/2}$$
$$\epsilon = \epsilon_c(\theta) \pm \epsilon_s(\theta)$$
$$\epsilon' = \epsilon_s'(\theta) \pm \epsilon_c'(\theta)$$

the prime denoting a derivative,

$$\epsilon_s(\theta) = -(1/2\pi)P\int_{-\pi}^{\pi}\psi_s(t)\cot{}^1/_2(t-\theta)dt$$
$$\epsilon_c(\theta) = -(1/2\pi)P\int_{-\pi}^{\pi}\psi_c(t)\cot{}^1/_2(t-\theta)dt$$

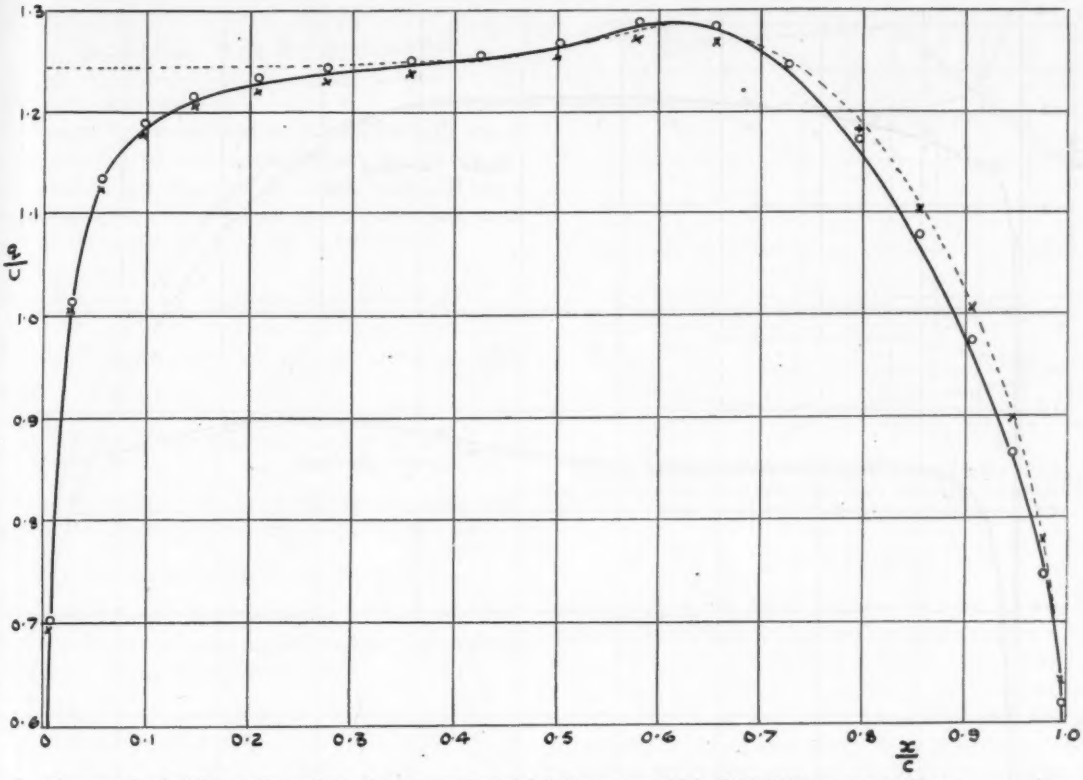

FIG. 7. Computed velocities on the surface of a symmetrical airfoil 24 per cent thick, EQH 2450, at zero incidence. ——Accurate computation. ⊙ Approximation II. x: Approximation II. ------ Approximation I.

note that $\psi_s(\theta)$ is to be taken as an even function and $\psi_c(\theta)$ as an odd function of θ, and

$$A = \cos(\alpha + \beta) = [1 - (C_L^2/a_0^2)]^{1/2}$$

$$B = \sin(\alpha + \beta) = C_L/a_0$$

$$C = C_L/(2\pi e^{C_0})$$

Thus on Approximation III the calculation of all the subsidiary quantities, ψ, ϵ, C_0, is still linear, and the results of the computations of these quantities can all be scaled and added to allow for variations of thickness and camber. The final formula is not linear, but of the three coefficients A, B, C, only A is not linear in the lift coefficient, and results at other lift coefficients are rapidly found from results at any two. We may note that slightly more accurate values for q/U are usually found if the factor e^{C_0} in F (but not in C) is replaced by $\exp(C_0 + [\epsilon'\psi])$, where

$$\left[\epsilon'\psi\right] = \frac{1}{\pi}\int_0^\pi \epsilon_s'(\theta)\psi_s(\theta)d\theta + \frac{1}{\pi}\int_0^\pi \epsilon_c'(\theta)\psi_c(\theta)d\theta,$$

and for a routine procedure the use of this factor is recommended.

For ease of reference, the original nomenclature of Theodorsen and Garrick has been largely retained. Mr. W. Chester, a research student at Manchester, has however recently extended these approximations to the calculation of the streamlines and the velocity at points not on the surface, and we have had to change the notation, since ψ is required for the stream-function.

It is of interest that for nearly all airfoils for which algebraic formulas have ever been suggested, the quantities g_s, g_t, ϵ_s, ϵ_c can be found in closed form in terms of simple functions. Examples are given in the original reports.[3]

In Approximation III the restriction to small incidences has completely disappeared. It is still to be expected, however, that the results would not apply very well for large thicknesses and cambers. A number of very careful exact computations have been carried out for comparison, and the results are rather surprisingly good at large thicknesses; the effects of large camber are somewhat more marked. Some comparisons are given in Figs. 6, 7, and 8. In Fig. 6 the results (other than Approximation II) are shown on a large scale for NACA 0012 at zero incidence; Fig. 7 shows results at zero incidence for a symmetrical 24 per cent thick airfoil with its maximum thickness at mid-chord; and Fig. 8 the results for the upper and lower surfaces, separately, for a 12 per cent thick airfoil with 4 per cent camber, maximum thickness and maximum camber being both at mid-chord; $C_L = 4.8 \sin(\alpha + \beta)$ has been assumed, and the results are shown for $C_L =$

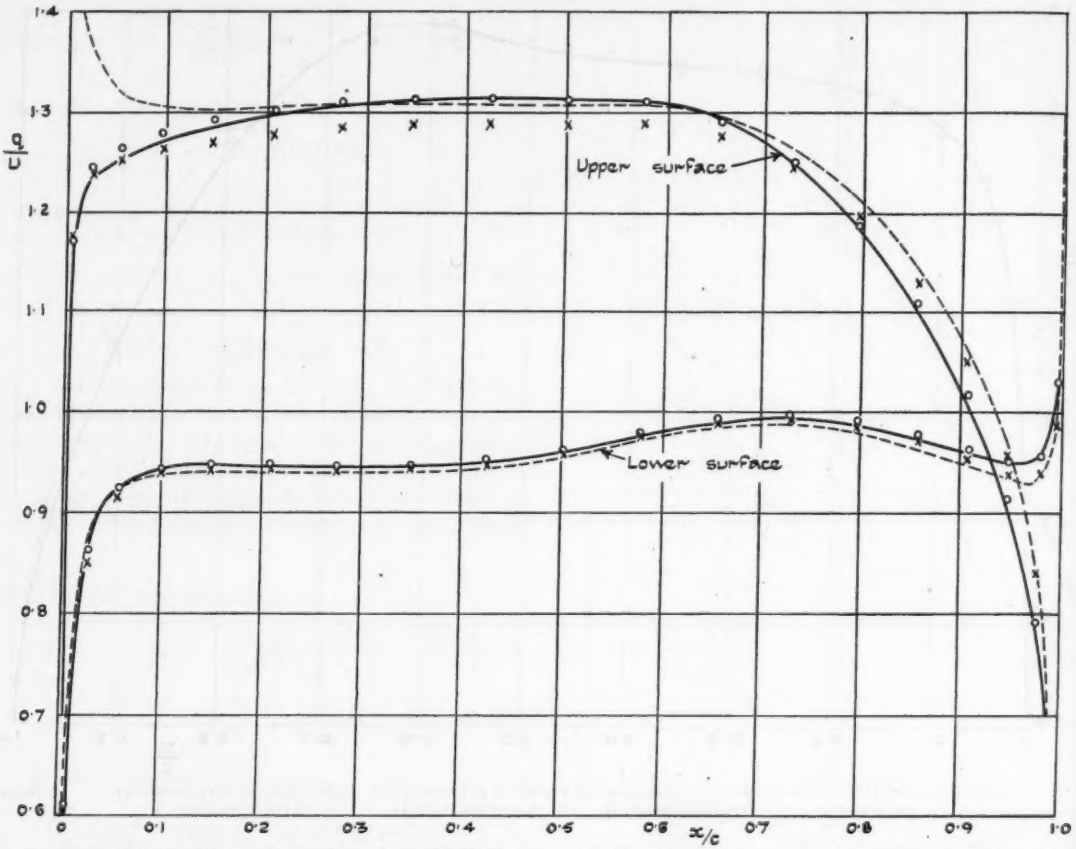

FIG. 8. Computed velocities on the surface of an airfoil 12 per cent thick with a 4 per cent camber, EQH 1250/4050, at $C_L = 0.6$. $C_L/\sin(\alpha + \beta)$ has been assumed equal to 4.8. ——Accurate computation. ⊙ Approximation III. x: Approximation II. -·-·-·-·-Approximation I.

0.6. In all cases, the comparisons at other lift coefficients are rather similar.

Before we leave this branch of the subject, we may remark that, in terms of θ, $g_s \sin\theta$, ϵ_s, and g_t have Fourier sine series that are conjugate to the cosine series for $2dy_s/d\theta$, ψ_s, and dy_c/dx, respectively, and ϵ_c has a cosine series conjugate to the sine series for ψ_c, the integral results previously written being alternative expressions of these facts; but the series should not be used for computation unless they terminate after a small number of terms. [The series conjugate to $\sum_{n=0}^{\infty}(A_n \cos n\theta + B_n \sin n\theta)$ is, by definition, $\sum_{n=1}^{\infty}(A_n \sin n\theta - B_n \cos n\theta$.]

When we turn to the inverse problem—of designing an airfoil section with a specified type of velocity or pressure distribution on its surface—it is found that the best procedure is to design the airfoil section, and at the same time to find Approximation III to the velocity, from an assumed knowledge of Approximation I. In fact a symmetrical airfoil, or the fairing for a cambered one, can easily be designed from a knowledge of the quantity g_s defined above, and centerlines may be designed from a knowledge of the quantity g_t. With some practice, however, it is not too difficult to make a moderately good guess (which may in any case be improved later, if required) at rough values of the factor by which Approximation I is multiplied to yield Approximation II, at any rate in those regions, particularly near the nose, where Approximation I is known to be considerably in error. If the given velocity distribution is regarded as Approximation II, Approximation I may therefore be at any rate roughly found. Moreover C_L is known from the pressure distribution; theoretically $C_{L_{opt.}}$ may be determined directly, if a_0 is assumed specified, from a knowledge of the velocity at the leading edge; but in practice this approach is difficult, and it is better, having estimated the first approximation to q/U on the top and bottom surfaces, to add to find g_s and subtract to find

$$g_t + \frac{1}{2}\left(\frac{1}{a_0} + \frac{1}{2\pi}\right)\left(C_L - C_{L_{opt.}}\right)\cot\frac{1}{2}\theta - \frac{1}{2}\left(\frac{1}{a_0} - \frac{1}{2\pi}\right)C_L \tan\frac{1}{2}\theta$$

and then to use the equation

$$\left(\frac{1}{a_0}+\frac{1}{2\pi}\right)C_{L_{opt.}} = A_1 = \frac{2}{\pi}\int_0^\pi g_t \sin\theta\, d\theta$$

to find $C_{L_{opt.}}$, and hence g_t.

To design a symmetrical airfoil or fairing from a knowledge of g_s we may either use the knowledge, directly, that if y_s is the half-thickness, $-2dy_s/d\theta$ has a cosine Fourier series, without a constant term, conjugate to the sine series for $g_s \sin\theta$, so that

$$2\frac{dy_s}{d\theta} = \frac{1}{2\pi}P\int g_s(t)\sin t \cot\frac{1}{2}(t-\theta)dt$$

and then integrate for y_s, or we may integrate first, writing

$$G(\theta) = \int_0^\theta g_s(\theta)\sin\theta\, d\theta = 2\int_0^x g_s\, dx$$

and then prove that $-2y_s$ has a Fourier sine series conjugate to the Fourier cosine series for $G(\theta)$, so that

$$2y_s = (1/2\pi)P\int_{-\pi}^{\pi} G(t)\cot {}^1\!/_2(t-\theta)dt$$

G being taken as an even function of θ.

If the radii of curvature at the leading and trailing edges are ρ_L and ρ_T, respectively, then

$$(2\rho_L)^{1/2} = (1/\pi)\int_0^\pi g_s(t)\,(1+\cos t)dt$$
$$(2\rho_T)^{1/2} = (1/\pi)\int^\pi g_s(t)\,(1-\cos t)dt$$

There must be certain restrictions on g_s so that the airfoil contour does not cross itself; the most important are that the above expressions for $(2\rho_L)^{1/2}$ and $(2\rho_T)^{1/2}$ should be positive, with the proviso that for a sharp trailing edge $\rho_T = 0$; it may be shown that if g_s is finite at the trailing edge, then a sharp trailing edge must be a cusp.

To calculate Approximation III to the velocity at the surface of the airfoil so designed we use the formula above; ψ_s is found from y_s in the usual way, but C_0, ϵ_s, ϵ_s' are more easily found from g_s and G. In fact,

$$C_0 = {}^1\!/_2 G(\pi)$$

and

$$\epsilon_s = G(\theta)\operatorname{cosec}\theta - C_0\tan {}^1\!/_2\theta$$

If g_s is finite at the leading and trailing edges, $\epsilon_s = 0$ there; ϵ_s' is found by differentiation, and a limiting process shows that, at the leading and trailing edges,

$$\epsilon_s'(0) = {}^1\!/_2[g_s(0) - C_0]$$
$$\epsilon_s'(\pi) = {}^1\!/_2[g_s(\pi) - C_0]$$

It is shown in the original report that y_s may be found in closed form in terms of simple functions for a large class of assumed values of g_s. A particularly simple case is that of the so-called "roof-top" airfoils (of which an example is shown in Fig. 9), where g_s increases linearly from a value a at $x = 0$ to a value b at $x = X_1$, and then decreases linearly to a value c at $x = 1$; then

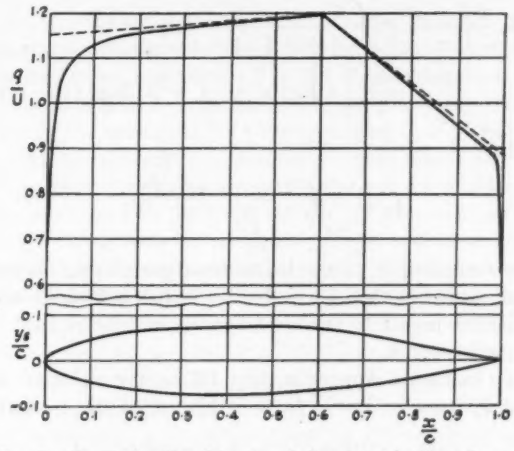

FIG. 9. Example of 'roof-top type' of symmetrical low-drag airfoil, and the theoretical velocities on its surface at zero incidence. ----- Approximation I. ——Approximation III.

$$y_s = af_0 + bf_1 + cf_2$$

where f_0, f_1, f_2 are fixed functions of θ for a given X_1, and may be tabulated once and for all for a set of values of X_1. The radii of curvature at the leading and trailing edges may be found in terms of a, b, c, X_1 before any other work is done, and it may be verified that suitable values of a, b, c have been chosen from this point of view. Of course, the values of a, b, c, X_1 also tell us about the velocity gradients we have chosen in the accelerating and decelerating regions. Although it is possible to design better airfoils, a preliminary study of these rather simple cases helped us to get our ideas clear.

When we turn to problems of designing centerlines from a knowledge of g_t, and of calculating Approximation III to the velocity at the surface and other properties of a cambered airfoil designed in this way, we first note that the Fourier cosine series in θ for $dy_c/dx - A_0$, where y_c is the ordinate of the centerline and A_0 the constant term in the Fourier cosine series in θ for $dy_c \div dx$, is conjugate to the sine series for $-g_t$; so if $g_t(x)$ is given as a function of x, and $g_t(\sin^2 {}^1\!/_2\theta)$ is taken as an odd function of θ,

$$\frac{dy_c}{dx} - A_0 = \frac{1}{2\pi}P\int_{-\pi}^{\pi} g_t(\sin^2 {}^1\!/_2 t)\cot {}^1\!/_2(t-\theta)dt = \frac{1}{\pi}P\int_0^1 \frac{g_t(\xi)}{\xi - x}\,d\xi$$

$y_c - A_0 x$ may be found by integration, and A_0 from the condition that $y_c = 0$ at $x = 1$.

However, y_c and A_0 may also be obtained explicitly, since it may be proved that if

$$G_t(x) = \int_0^x g_t(\xi)d\xi$$

and

$$A_1 = (2/\pi)\int_0^\pi g_t \sin\theta\, d\theta = (4/\pi)G_t(1)$$

then

$$y_c = \frac{x(1-x)}{\pi} P \int_0^1 \frac{G_i(\ ) - \xi G_i(1)}{\xi(1-\xi)(\xi - x)} d\xi - \frac{1}{4} A \left[x \log_e x + (1-x) \log_e (1-x) \right]$$

and

$$A_0 = \frac{1}{\pi} \int \frac{G_i(\xi) - \xi G_i(1)}{\xi(1-\xi)} d\xi$$

The formula for y_c is a transformation of the integral that expresses that $\psi_c (= 2y_c/\sin\theta)$ has a Fourier sine series conjugate to the cosine series in θ for $[{}^1/_2 A_1\theta - 2G_i(x)]$ cosec θ.

To calculate Approximation III to the velocity we find ψ_c from y_c, but ϵ_c from g_i by use of the formula

$$\epsilon_c(\theta) = 2[G_i(x) - {}^1/_4 A_1 \theta] \text{ cosec } \theta - A_0$$

The no-lift angle is given by

$$\beta = \epsilon_c(\pi) = {}^1/_2 A_1 - A_0$$

and the moment coefficient at zero lift is

$$(C_M)_0 = -\int_0^1 (4x - 1) g_i(x) dx$$

also

$$\epsilon_c(0) = -{}^1/_2 A_1 - A_0$$

ψ_s, ϵ_s, and C_0 are found from the design of the fairing, so all relevant quantities are known for the use of the formulas written previously. The formulas for the radii of curvature at the leading and trailing edges are the same for a cambered as for a symmetrical airfoil.

It may be noted that g_i must be zero at the leading and trailing edges if dy_c/dx is to be free from singularities and $\epsilon_c'(\theta)$ is not to be discontinuous at $\theta = 0$ and π.

In the calculation of y_c formulas may be found in closed form in terms of simple functions for a wide variety of assumed forms for g_i; the results for special cases have, in fact, been given by a number of authors. The remark made in considering the direct problem, that the Fourier series should themselves be used if they terminate after a few terms, holds for the inverse problem also.

A large part of the work in either the direct or the inverse problem consists in finding the sum of the Fourier series conjugate to the series for a given function. Although in many useful cases formulas may be found for the sums in finite terms, the best use cannot be made of the theory unless the given functions may be varied arbitrarily, and the conjugates must then be found numerically. The same kind of computation has to be made in the exact theory, and a computational formula was given by Theodorsen and Garrick. All suggested methods have this in common, that they suppose the given function known numerically at a number of equally spaced points in the interval $(-\pi, \pi)$. Theodorsen merely took the function as constant in each subinterval; this is definitely too crude, and we worked out formulas in which the given function was approximated by a quadratic expression (i.e., its graph was approximated by a parabola) in each subinterval. The results were, of course, much more accurate, but the formulas have been superseded by others derived by a method due to Germain,[9] who approximates the given function by a trigonometrical polynomial, or finite Fourier series, coinciding with the given function at the points where its value is known numerically. Watson[10] has shown that general formulas may be found for the constants occurring in the resulting formulas; moreover, formulas may be found for computing the derivative and the integral of the conjugate in terms of the values of the given function, without its derivative or integral having to be found, and also for the integral of the conjugate multiplied by sin θ, i.e. for its integral with respect to x instead of θ.[11] The results are not without mathematical interest, but from the aerodynamic point of view the main point of interest is that such useful formulas are now known.

The formulas for the velocity at the surface of an airfoil, especially Approximation II for airfoils designed from a knowledge of g_s and g_i, may be used to estimate rapidly the positions and magnitudes of the velocity maxima on the surface at any lift coefficient, and also to find the theoretical C_L-ranges for low-drag airfoils, defined as the range of lift coefficients for which, on both the upper and lower surfaces, the nearest velocity maxima to the leading edge still occur at their designed positions at the design lift coefficient. As an example, we have the result that, with $a_0 = 2\pi$, the C_L-range of any one of the "roof-top" airfoils of the type previously described is $9.27(2\rho_L)^{3/4} s^{1/4}$, where, as before, ρ_L is the radius of curvature at the leading edge, and s is the slope of the nondimensional velocity (i.e., $s = dg_s/dx$) over the front of the airfoil. (Divide by $\pi/a_0 + {}^1/_2$ for other values of a_0.) For a given radius of curvature at the trailing edge, given position of maximum velocity, and given value of the maximum velocity or maximum thickness, there is a value of s which makes the C_L-range a maximum; for example, for a cusped airfoil of given maximum thickness, with maximum suction at mid-chord, this value is $s = 0.982t$, where t is the maximum thickness (not the half-thickness) as a fraction of the chord. When the trailing edge becomes blunter (i.e., when ρ_T increases) the most favorable value of the slope (from this point of view) decreases, and the maximum C_L-range also decreases slightly. For cusped airfoils the C_L-range is nearly proportional to $t^{7/4}$.

I have ventured to summarize some of the results of the new approximate airfoil theory for two reasons: no account of the theory has yet been published, and the formulas form a basis for judgments, and subsequent calculations, in designing, for test, airfoils of a new and unorthodox type. But the theory, like all mathematical theories, must be used in conjunction with good engineering judgment, controlled experiment, and,

eventually, full-scale trials. The need for judgment makes itself felt at once. Knowledge of the position of maximum velocity on an airfoil, for example, may be considered to provide information on the probable position of transition to turbulence in the boundary layer, since transition takes place soon in an adverse gradient. But because of our lack of knowledge of the processes leading to transition, care is needed in using this information. Certainly other factors in addition to the velocity distribution—waviness and roughness of the surface, turbulence in the air, Reynolds number—affect the position of transition even on a flat or convex surface; and the effect of the velocity distribution, and its interaction with other factors, do not depend solely on the position of the maximum velocity. If the velocity falls off steadily and not too slowly after the maximum, then in practice, at high Reynolds numbers, transition will not be delayed to any appreciable extent beyond the maximum. But whether transition occurs before the maximum will depend on the velocity gradient and the other factors mentioned; and moreover transition may occur well after the velocity maximum in certain circumstances—for example, with a good surface and low turbulence in the air, if the maximum is followed by a small fall in velocity and the velocity then begins to rise again, or even if the fall in velocity after the maximum is slow enough. The former state of affairs applies near to the nose of a good many airfoils, including some N.A.C.A. airfoils, at certain lift coefficients. So for a judgment of the position of transition, knowledge of the position of the velocity maximum can be only of restricted use for a preliminary "sorting out."

All this has, of course, a bearing on the definition of the C_L-range for low-drag airfoils. A definition of the "theoretical" range has been given. A second possible definition is the range of lift coefficients over which the drag stays low and practically constant when measured on models made as carefully as possible and tested in a low-turbulence wind tunnel at a given Reynolds number, say 30×10^6; this "wind-tunnel" definition is useful to those to whom a suitable tunnel and model-making facilities are available, but we had in Great Britain—and still have—no such tunnel. A third definition—the "practical" definition—is the most probable range of lift coefficients for low and nearly constant drag under practical conditions of manufacture, flight, and maintenance; in the words of the original report, "values according to this definition are the values we should all like to be able to give but none of us can." The information in Section 3, however, has taken us some way since the report was written.

One other remark should be made in connection with transition. Experimental evidence of the effect of velocity gradient on the tolerance that can be allowed for waviness of the surface is still scanty and not at all systematic; such evidence as we have indicates that, once a fair value of the gradient has been reached, any further increase needs to be very large to make any practical difference to the tolerance. Thus, once the nondimensional gradient s is 0.1, for example, it is doubtful whether it would make any practical difference to the tolerance if s were increased to 0.2; but if it is made very much bigger, for example multiplied by 10, so that it becomes 1.0 instead of 0.1, then it seems that the tolerance on waviness may be increased, so we expect to be able to tolerate a larger waviness very near an airfoil nose than further back. Also if s is much decreased the tolerance on waviness becomes less; but exact knowledge is still lacking. It is of some interest that the values of s for maximum theoretical C_L-range are reasonable values from the point of view of tolerance on waviness.

It is not only knowledge about the transition to turbulence in the boundary layer that we lack; the influence of compressibility, when part of the flow field is supersonic, is also still imperfectly understood. For those transport aircraft for which it is still hoped to avoid compressibility effects, however, we still believe that it is a good thing to keep the maximum velocity low enough, if possible, to ensure that the whole flow field is subsonic at top speed; if that is impossible, the best method of design is still a matter of doubt and controversy, and I do not propose to enter on it here, contenting myself with the remark that once we have decided what we want, the formulas found help us to design to get it. One thing we often do want is thin wings with as good a maximum lift as possible, and there is some evidence, though not conclusive, that a large radius of curvature at the leading edge is beneficial.

The formulas of approximate airfoil theory help us to design airfoil sections with required properties, once the requirements have been translated effectively into conditions on the velocity distribution at the surface and on the geometry of the section. We can design for a low maximum velocity for a given thickness, a large theoretical C_L-range, a large leading-edge radius of curvature, a low moment coefficient at zero lift, and so on; we can see what is physically possible and are helped to make judgments about the inevitable compromises between different desirable characteristics; and we can design for a mixture of aerodynamic and geometrical properties, as structural and manufacturing questions and control characteristics may require. A few reports by Thwaites[11–13] and Miss Douglas[14] have been issued on these aspects from the Aerodynamics Division of the National Physical Laboratory.

Finally, we remark that the formulas written are, after all, only approximate; they are flexible and general and very useful for helping us to get our ideas straight and to decide what is possible, and are accurate enough for most airfoils of small camber and not too great a thickness; but our mathematical apparatus is not complete unless we have, not only an exact method for determining the velocity on a given airfoil, but also some more exact theory for designing an airfoil with a

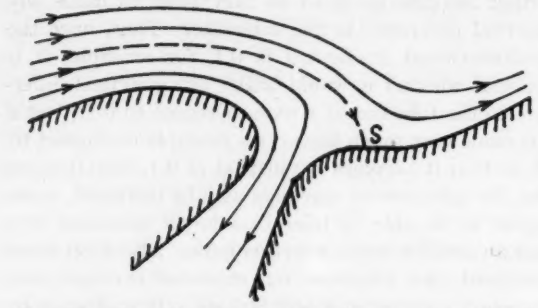

FIG. 10. Streamlines in a boundary layer near a suction slot. ----- Dividing streamline. S: Stagnation point.

given velocity distribution. This gap has been filled by Lighthill.[16] Let us suppose the airfoil section conformally transformed into a circle, with the same undisturbed relative air velocity, and all lengths represented as multiples of the radius of the circle. The airfoil plane is taken as the z-plane, with $z = x + iy$, and the circle plane as the ζ-plane, the circle itself being $\zeta = e^{i\theta}$, with $\theta = 0$ corresponding to the trailing edge of the airfoil section (note that the meaning of θ is different from that in the approximate theory); the Kutta-Joukowski condition is assumed satisfied at the trailing edge. If q_α is the ratio, at incidence α measured from zero lift, of the relative air velocity at the point on the airfoil surface corresponding to the point θ on the circle to the undisturbed relative air velocity, and q_0 the corresponding quantity at zero incidence,

$$q_\alpha = q_0[\cos(\tfrac{1}{2}\theta - \alpha)/\cos\tfrac{1}{2}\theta]$$

so that q_0 is known as a function of θ if q_α is assumed. For symmetrical airfoils q_α must be assumed on one surface only, since q_0 is the same on both surfaces; for cambered airfoils, q_α may be assumed at two different incidences for the two surfaces, subject to conditions of continuity on q_0. The resulting airfoil may then be designed from the formulas

$$x = \int (2/q_0)\cos\chi\, d(\cos\theta)$$

$$y = \int (2/q_0)\sin\chi\, d(\cos\theta)$$

for the coordinates, where χ is the sum of the Fourier series in θ conjugate to the series for $\log q_0$, so that

$$\chi(\theta) = -(1/2\pi)P\int_{-\pi}^{\pi} \log q_0(t)\cot\tfrac{1}{2}(t-\theta)dt$$

and may be found by methods previously described. Thus the airfoil is designed from a knowledge of $q_0(\theta)$, which is found if required from a knowledge of the velocity distribution at incidence in terms of θ; since x varies rather like $\cos\theta$, we can make a good guess at the velocity distribution in terms of x. But in order to obtain the correct undisturbed relative air velocity, and to ensure that the airfoil section shall be a closed curve, $q_0(\theta)$ must be chosen so that

$$\int_{-\pi}^{\pi}\log q_0\, d\theta = 0$$

$$\int_{-\pi}^{\pi}\log q_0\cos\theta\, d\theta = 0$$

$$\int_{-\pi}^{\pi}\log q_0\sin\theta\, d\theta = 0$$

The chord c, as a multiple of the radius of the circle, is rather less than 4, and with a little experience can be guessed fairly accurately, so the formula for the moment coefficient at zero lift,

$$(C_M)_0 = -(4/c^2)\int_{-\pi}^{\pi}\log q_0\sin 2\theta\, d\theta$$

may also be used to design from the beginning with the value of $(C_M)_0$ in mind.

This completes the present summary of the mathematical methods used. We use all our judgment, knowledge of experimental results, and experience to decide what we should like to design an airfoil section for in terms of its geometry and the velocity distribution on its surface; we use the approximate theory to sort out what is possible and what are the best compromises to make, and for trial designs; and we use the exact theory to finalize the design, particularly for airfoils that are thick or highly cambered.

(5) The Design of Suction Airfoils

In considering the principles of the design of low-drag airfoils, we saw that we should like the velocity outside the boundary layer to rise to a position as far back along the wing as possible, but that we are hindered by the danger of turbulent separation if the rate of velocity decrease at the back of the airfoil is too great; the danger increases, roughly, when the thickness of the airfoil increases and when the position of maximum suction is moved further back. If, however the whole, of the pressure recovery, or velocity decrease, is concentrated over a very narrow interval along the chord, over, which the boundary layer, or as much of it as necessary, is sucked away to stop separation, all danger of separation is avoided, and we can have, if we wish, a favorable velocity gradient over the whole of the rest of the chord. More specifically, if the upstream boundary layer, or part of it, is sucked in through a slot, there must be a streamline that divides the air crossing the slot from that entering it, and that streamline must meet the surface at a stagnation point (Fig. 10). With the stagnation point behind the slot the flow in the boundary layer along the surface is reversed in direction between the stagnation point and the slot, and all danger of separation is avoided with a well-designed slot if the design of the airfoil is such that the pressure recovery takes place wholly between the upstream lip of the slot and the stagnation point. Up to now suction airfoils have actually been designed with a discontinuous drop in velocity; the velocity rises to a given position on the chord, drops discontinuously, and thereafter rises, stays constant, or at any rate does not decrease rapidly enough to produce any danger of separation, to the trailing edge; the velocity distribution has this character on both the top and bottom surfaces.

When Dr. Griffith suggested that airfoil surfaces should be designed specially for suction, the mathematical apparatus of the approximate theory was ready and was at once applied; the exact theory of design followed later. On the approximate theory the simplest thing to do is to take the first, linear, approximation to q/U for a symmetrical airfoil to rise linearly from $1 + a$ at $x = 0$ to $1 + b$ at $x = X_1$, where it drops discontinuously to $1 + c$, and thence proceeds linearly to $1 + d$ at $x = 1$ (Fig. 11); the ordinates of the airfoil are given by

$$y = af_0 + bf_1 + df_2 + (b - c)f_3$$

where f_0, f_1, and f_2 are the same functions as occurred in the design of "roof-top" airfoils, and f_3 is easily calculated.

The first suction airfoil, designed in this way and tested by Mr. Richards at the National Physical Laboratory, was about 16 per cent thick and had the velocity discontinuity and suction slot on each surface at seven-tenths of the chord from the leading edge. The shape of the airfoil section, and Approximations I and III to the velocity distribution at zero lift, are shown in Fig. 11. Transition to turbulence and boundary-layer separation were observed both by filaments of smoke introduced into the boundary layer and by fine silk threads, about $^1/_2$ in. long, attached to the surface. The model as made and tested did not, in fact, reproduce accurately the computed shape, but Mr. Richards soon found several interesting results, among which we may mention here that the method of design was satisfactory, that separation could be avoided by sucking away less than half the air in the boundary layer, and that, in spite of the favorable velocity gradient behind the slot, the flow in the boundary layer became turbulent soon after the slot except at low Reynolds numbers. The airfoil surface is concave to the flow aft of the slot (Fig. 11), and there is no doubt that the transition to turbulence is caused by the instability of flow in a boundary layer over a concave surface; this instability had been studied theoretically by Görtler,[16] and transition on a concave surface of constant curvature was studied experimentally by Liepmann,[17] of whose results we were informed just as the possibility of several other causes for the transition after the slot had been eliminated by special experiments. Liepmann's results fitted ours as well as could be judged in view of the variable curvature of the surface of our airfoil. It is not possible to design an airfoil of this type without a concavity aft of the slot, but the concavity can be reduced by increasing the velocity over the tail and the radius of curvature at the trailing edge; Richards and I soon convinced ourselves, however, that at Reynolds numbers of 20 millions or more it would be impossible to design an airfoil for which the gain due to increasing the length of the laminar portion of the boundary layer would not be more than counterbalanced by the increase of form drag. We therefore decided to accept turbulent flow in the boundary layer aft of the slot, and the next airfoil designed had the velocity discontinuity and the slot further back, at eight-tenths of the chord from the leading edge; and, since theoretically the idea should work equally well for very thick airfoils, the next airfoil, which was still symmetrical, was 30 per cent thick. It was still designed by the approximate theory, and the shape of the section, together with Approximations I and III to the velocity distribution at zero lift, is shown in Fig. 12. It should be stated at once that Approximation III agrees quite well with experiment, so there is no reason to believe that it is insufficiently accurate for a symmetrical airfoil even 30 per cent thick. A comparison of Approximations I and III in Fig. 12, however, shows that the favorable velocity gradient of Approximation I has been replaced for

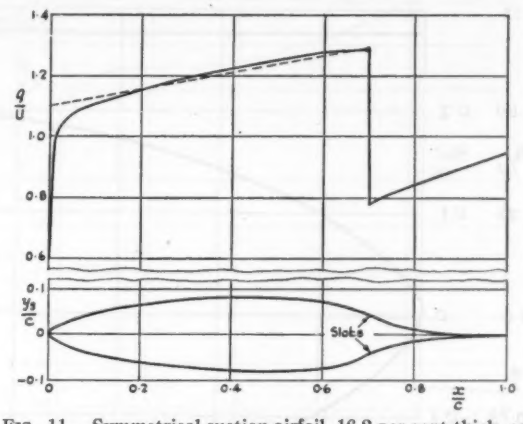

FIG. 11. Symmetrical suction airfoil, 16.2 per cent thick, and the theoretical velocities on its surface at zero incidence. ----- Approximation I. ——Approximation III.

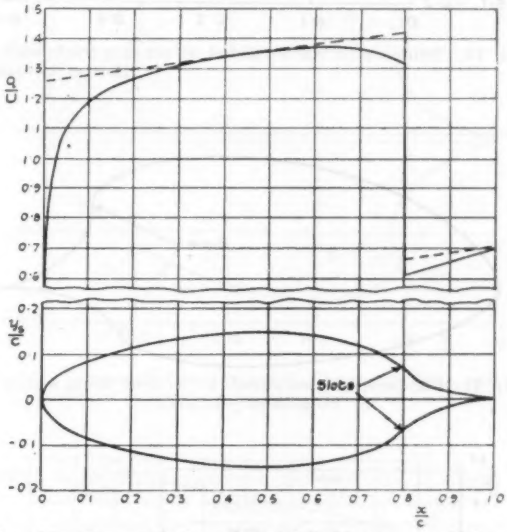

FIG. 12. Symmetrical suction airfoil, 30 per cent thick, and the theoretical velocities on its surface at zero incidence. ----- Approximation I. ——Approximation III.

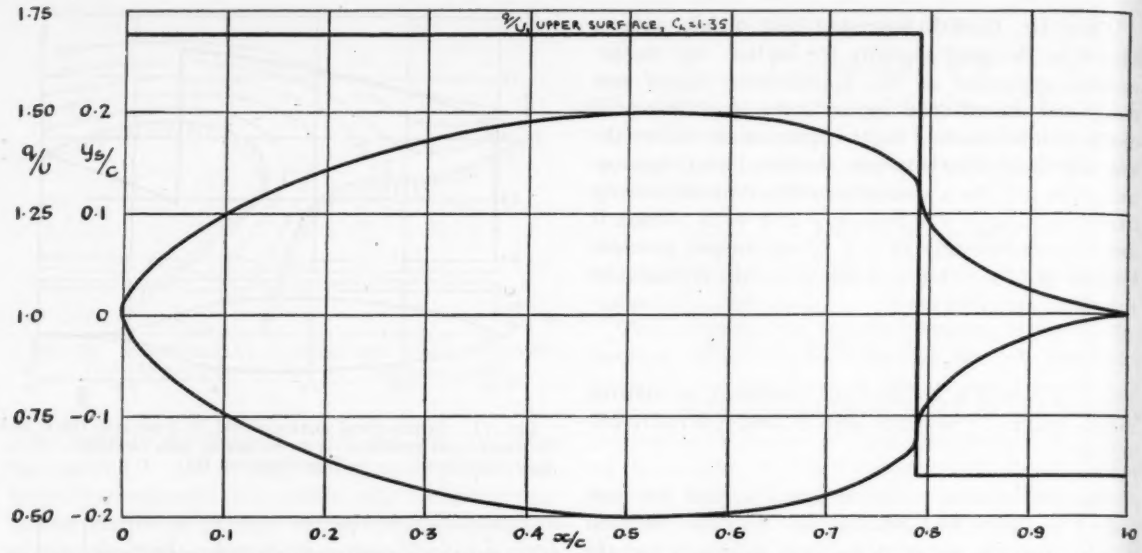

FIG. 13. Symmetrical suction airfoil, 40 per cent thick, with a C_L-range from -1.35 to $+1.35$, and the theoretical velocity distribution on its upper surface at $C_L = 1.35$.

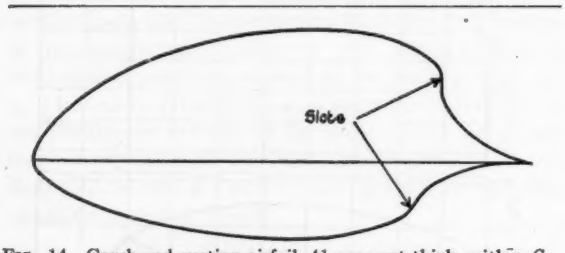

FIG. 14. Cambered suction airfoil, 41 per cent thick, with a C_L-range from 0 to 2.85.

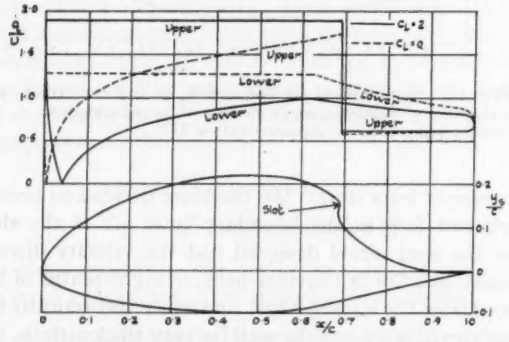

FIG. 15. Cambered suction airfoil, 31½ per cent thick, with a velocity discontinuity on the upper surface only and a C_L-range from 0 to 2, and the theoretical velocities on its surface at $C_L = 0$ and at $C_L = 2$.

some distance forward of the discontinuity by an adverse gradient according to the more accurate Approximation III, and the design criteria have to this extent not been fulfilled; this adverse gradient could lead to laminar separation at low Reynolds numbers and premature transition to turbulence at higher Reynolds numbers. This defect in the design could be removed by an alteration in the first approximation, $1 + g_u$ to q/U, but thick suction airfoils have, in fact, lately been designed by use of Lighthill's exact theory. Some specimens are shown in Figs. 13–17, of which Fig. 15 is due to Mr. M. B. Glauert,[18] and the rest to Mr. Lighthill.[15]

The original 30 per cent thick airfoil had a C_L-range from -0.6 to 0.6, and it is evident that much larger C_L-ranges may be obtained. Fig. 13, for example, shows a 40 per cent thick symmetrical section with a C_L-range from -1.35 to 1.35, the velocity distribution on the upper surface at $C_L = 1.35$ being flat both in front of and behind the slot, as shown. In Figs. 14, 15, and 16 three cambered airfoil sections are exhibited; cambered sections have not previously been mentioned. No cambered suction airfoils were, in fact, designed by the approximate theory, although formulas are known for the design of centerlines with discontinuities in g_i; it is clear from the approximate theory that not only may cambered suction airfoils be designed, but by introducing discontinuities in both g_s and g_i the discontinuities in the velocity on the top and bottom surfaces may be treated independently, and an airfoil may be designed with a discontinuity on one surface but not on the other. Fig. 14 shows a 41 per cent thick cambered airfoil, with a velocity discontinuity on each surface, and a C_L-range from 0 to 2.85; Fig. 15 a 31½ per cent thick cambered airfoil, with a velocity discontinuity on the upper surface only, and a C_L-range from 0 to 2; in this case the theoretical velocity distributions at the ends of the C_L-range are also shown. The theoretical value of $(C_M)_0$ for this airfoil is zero. Figs. 16 and 17 illustrate, by a couple of rather extreme designs, some of the curious shapes that can theoretically be designed. Fig. 16 shows a

cambered 30 per cent thick section with a C_L-range from 0 to 2.69; the velocity discontinuity on the lower surface is rather far forward, and there would presumably be a rather long turbulent boundary layer on the concave surface behind it; but the C_L-range is remarkable for a 30 per cent thick section. Fig. 17 shows a theoretical symmetrical section 70 per cent thick, together with the velocity distribution on the upper surface at a lift coefficient of 3.

Of all the sections shown in Figs. 13 to 17, only that in Fig. 15 has been made and tested in a wind tunnel at the National Physical Laboratory, and the tests so far carried out are preliminary. It is still impossible to say whether the design is satisfactory or not. Certain troubles were encountered, but the shape of the slot entry was not entirely satisfactory since an attempt was made to design a slot suitable for blowing as well as for suction, and it now appears that that is not really possible, at any rate on this shape. When flow without separation was established, good agreement was obtained with the properties forecast in the theoretical design. Further tests will be carried out with a new and improved slot. An airfoil of this shape has also been tested in Australia, where fairly satisfactory results were obtained by using more than one slot and rounding off the surface near the design position of the discontinuity in velocity. Final judgment must await further experiment.

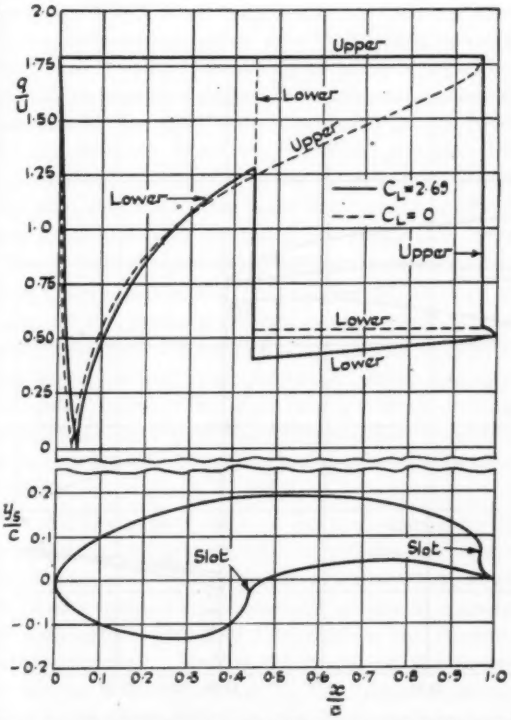

FIG. 16. Cambered suction airfoil, 30 per cent thick, with a C_L-range from 0 to 2.69, and the theoretical velocities on its surface at C_L = 2.69 and at C_L = 0.

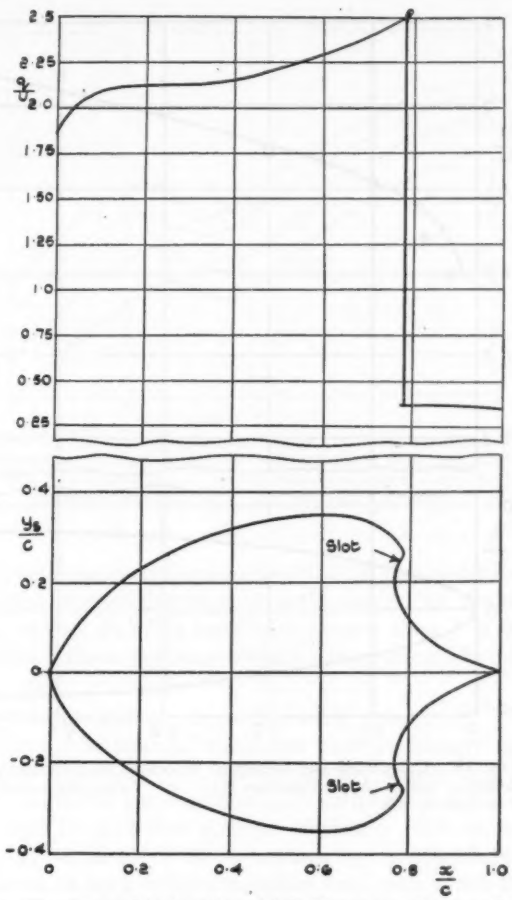

FIG. 17. Symmetrical suction airfoil, 70 per cent thick, and the theoretical velocities on its upper surface at C_L = 3.

(6) SOME EXPERIMENTAL RESULTS ON SUCTION AIRFOILS

Although the shape of the model of the first suction airfoil designed, 16 per cent thick with the slot at seven-tenths of the chord from the leading edge, did not accurately agree with the computed shape, it is of interest to reproduce at least one set of experimental results—namely, the measured velocity distribution at zero lift with and without suction.[19] These are shown, and compared with the theoretical distribution, in Fig. 18. The discrepancies between theory and experiment are largely due to the errors in shape. The results without suction are of considerable interest, and were closer to the theoretical values than we had expected. The boundary layer, which separates from the surface, is shown by these results to rejoin the surface at about 0.85 of the chord from the leading edge, and this accounts for the high effectiveness found for control without suction in wind-tunnel experiments, both in two-dimensional tests at the National Physical Laboratory and in tests in a wind tunnel at the Royal Aircraft Esfablishment on a model of a complete aircraft fitted

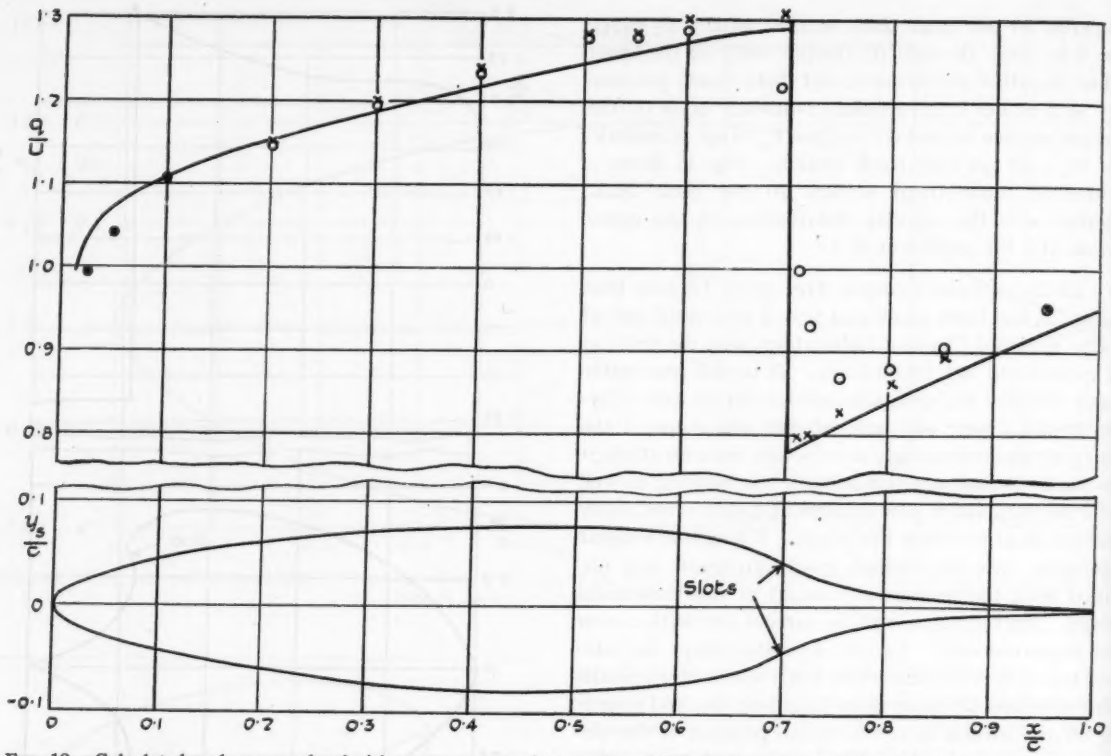

FIG. 18. Calculated and measured velocities on a symmetrical suction airfoil, 16.2 per cent thick (Fig. 11), at zero lift. —— Calculated values (Approximation III). x: Values measured with suction. ⊙ Values measured without suction. Reynolds number = 3.85×10^6.

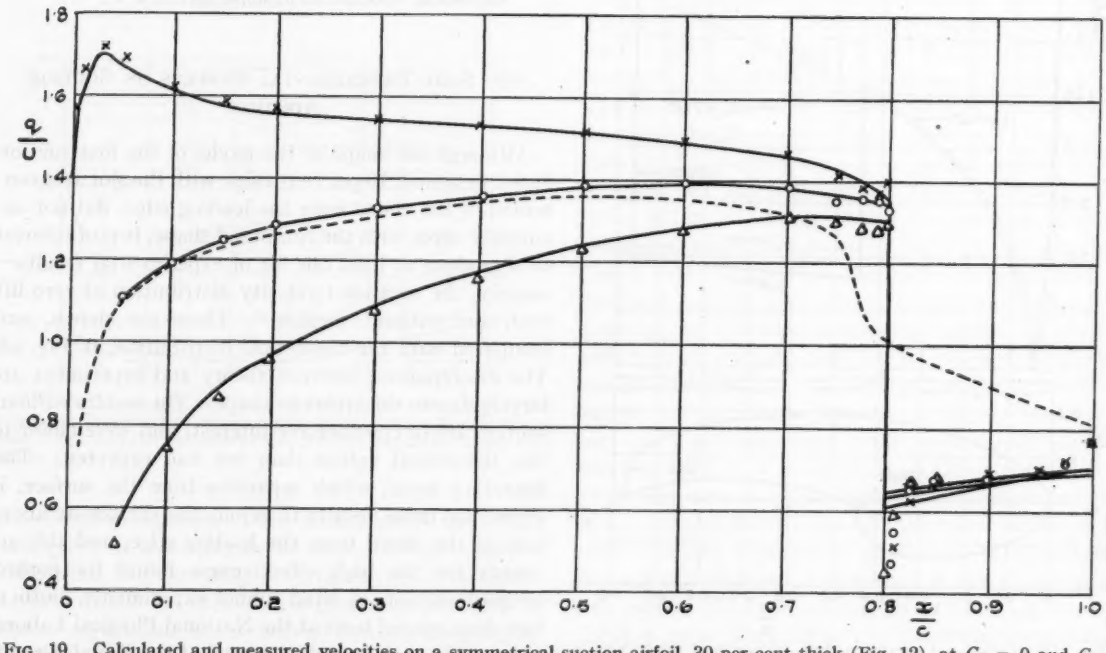

FIG. 19. Calculated and measured velocities on a symmetrical suction airfoil, 30 per cent thick (Fig. 12), at $C_L = 0$ and $C_L = 0.883$. ——Calculated values (Approximation III). x, △, ⊙ Values measured with suction. x: $C_L = 0.883$, upper surface; △ $C_L = 0.883$, lower surface; ⊙ $C_L = 0$. ------Values measured without suction ($C_L = 0$). Reynolds number = 0.96×10^6.

with wings of the shape shown in Fig. 11. The maximum lift and aileron effectiveness were, in fact, larger with these wings without suction than with high-speed wings of a more orthodox shape which tapered from 12 to 10 per cent thick. It should be remarked that results without suction are liable to a large, and, on the whole, probably favorable, scale effect.

The "measured" velocities were obtained, from pressures measured at the surface, by assuming the pressure constant across any section of the boundary layer and using Bernoulli's equation, so that normally the velocity should be that just outside the boundary layer. In the regions of separated boundary-layer flow, however, the results should perhaps be regarded purely as a measure of the pressure on the surface.

Some of the experimental velocities[20, 21] measured at the surface of the 30 per cent thick symmetrical airfoil of Fig. 12 are compared with theoretical results in Fig. 19, where the full lines are again the theoretical results and the points the experimental results at lift coefficients zero (actually the mean of results on the upper and lower surface at $C_L = -0.02$) and 0.883; the dotted curve refers to the results without suction at zero lift.

The theoretical slope of the curve of lift coefficient against incidence for this airfoil is 7.9; experimentally, with sufficient suction to prevent separation, a straight line was obtained up to the highest lift coefficient, 2.3, measured, and the slope was 7.3; there was no sign of a stall. Thus these thick suction airfoils have large lift-incidence slopes, rather near the theoretical values; if sufficient suction is available to prevent separation, the stall is at such a high lift and incidence that the maximum lift for these airfoils probably has no practical significance. Moreover parallel straight lines were obtained for the (C_L, α) curves with a 20 per cent plain flap deflected, the increment in lift coefficient being about 0.045 per degree of flap deflection; measurements were made with deflections up to 14°.

With sufficient suction to prevent separation, the graphs of the moment coefficient and hinge-moment coefficient against lift coefficient are also all represented fairly well by straight lines, and are in reasonable agreement with theory. The large rate of change of hinge-moment coefficient with flap deflection may necessitate some special system of control balance, even with power operation.

The lift coefficients without suction, shown in Fig. 20 for a Reynolds number of 2.88 millions, are of considerable interest. It should be remembered, however, that results without suction are all subject to considerable scale effect, probably favorable as the Reynolds number increases. This is illustrated in the present case by the dotted curve in Fig. 20, which represents results at zero flap deflection at a Reynolds number of 0.96 millions; there is no reason to believe that scale effect will be absent above 3 millions, and tests at higher

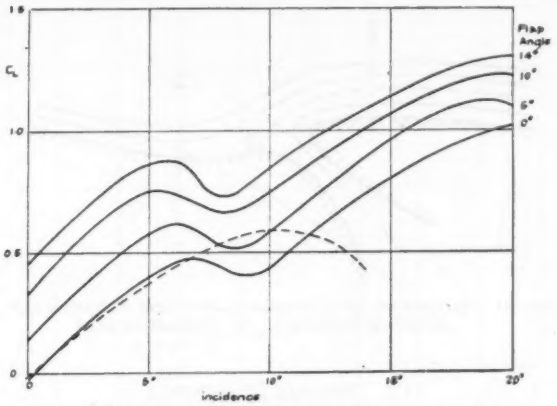

FIG. 20.* Measured lift coefficients, without suction, of a symmetrical suction airfoil, 30 per cent thick (Fig. 12), with a 20 per cent plain flap. ——Reynolds number 2.88 × 10^6. - - - - - Reynolds number 0.96 × 10^6, zero flap deflection.

Reynolds numbers are required. The lift curves without suction also certainly depend on the design; for the airfoil of Fig. 15 a lift coefficient greater than 1 is obtained without any bends in the curve or traces of a partial stall.

Without suction, at a Reynolds number of 2.88 millions, the moment coefficient changes linearly and agrees reasonably well with theoretical values derived for completely potential flow up to an incidence between 6° and 7°, and then changes violently; this change appears to be due to the replacement of a gentle laminar separation by a violent turbulent one, with which the dips in the curves in Fig. 23 are also associated. The measured values of the hinge moments at a Reynolds number of 2.88 millions indicate overbalance following the response to control movement. However, scale effect on results without suction makes it impossible to draw firm conclusions.

One other rather curious result without suction should be mentioned: at a Reynolds number of 2.88 millions the drag coefficient at small incidences and small flap deflections is only about 0.010, which is a very low value for such a thick airfoil with such an unorthodox shape.

We may sum up our results so far by saying that with sufficient suction to prevent separation, the behavior in the wind tunnel is in accordance with theoretical ideas; without suction the results are better than might have been expected. I might perhaps add that as a result of wind-tunnel tests on the 31½ per cent thick airfoil with a single slot, shown in Fig. 15, the Australians believe that in the event of suction failure lateral control, although poor, will be tolerable and an emergency landing should be possible.

In this summary of experimental results no mention has yet been made of the quantity of air that must be sucked to prevent separation or of the effective drag; some discussion is advisable before we start to look at experimental results on quantity and drag.

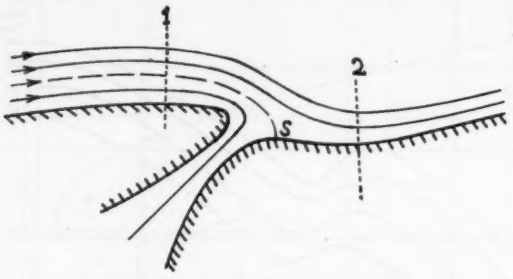

FIG. 21. Streamlines in a boundary layer near a suction slot. ----- Dividing streamline. S: Stagnation point.

(7) SUCTION QUANTITIES

We have already remarked that separation was avoided on the first suction airfoil tested by sucking less than half the air in the boundary layer just upstream of the slot; this result was explained, and a means suggested for computing the minimum quantity necessary, by a simple calculation due to Sir Geoffrey Taylor. Let us assume that the total head does not change appreciably along a streamline in the boundary layer as it crosses the slot from section 1 to section 2 in Fig. 21. If u_1, u_2 are the velocities and p_1, p_2 the pressures at those sections on the same streamline in the boundary layer, then

$$\tfrac{1}{2}\rho(u_1^2 - u_2^2) = p_2 - p_1$$

If we now further assume that the static pressure is constant across each of the sections 1 and 2 of the boundary layer,

$$p_2 - p_1 = \tfrac{1}{2}\rho(U_1^2 - U_2^2)$$

where U_1, U_2 are the velocities just outside the layer, so

$$u_1^2 - u_2^2 = U_1^2 - U_2^2$$

and if the fluid in a streamtube is to have sufficient total head to cross the pressure discontinuity, u_1^2 must be greater than $U_1^2 - U_2^2$. Hence the portion of the upstream boundary layer extending from the surface to the streamline where

$$u_1/U_1 = (1 - U_2^2/U_1^2)^{1/2}$$

must be sucked away. If we assume that U_2/U_1 has the theoretical value in a potential flow, and that the velocity distribution in the boundary layer upstream of the discontinuity can be found sufficiently accurately, the minimum quantity that must be sucked can be calculated. Moreover, by using the equation of continuity for a streamtube we may compute, downstream of the discontinuity, the distance from the surface of any streamline that has crossed the slot, and since the velocity, u_2, on it is given by

$$u_2^2 = u_1^2 - (U_1^2 - U_2^2)$$

we can find the distribution of velocity in the boundary layer downstream of the slot, the momentum thickness there, and any other property of the boundary layer that we require.[22,23]

Gregory[22] has tested the assumptions of the theory by boundary-layer explorations. He finds that the change of total head along a streamline in the boundary layer crossing the slot is small compared with the changes normal to the streamline, so Taylor's assumption is justified. Near a slot, however, the surface of a suction airfoil and the streamlines in the boundary layer have a large curvature, which, for some of the streamlines, is enhanced by the sink effect; this curvature produces a large pressure gradient across a section of the boundary layer. Consequently if the sections 1 and 2 of Fig. 21 are taken just upstream and just downstream of the slot, corrections must be applied to the simple theory above to allow for the effects of curvature. One such effect is that on any particular streamline u_2 will be less than the value given above, and on this account the minimum suction quantity would be greater than calculated. Another effect is that U_1 is less and U_2 is greater than the values that would be calculated from Bernoulli's equation and the measured pressures on the surface with the assumption that the pressure is constant across a section of the boundary layer; these latter values are the "experimental velocities at the surface" with which theoretical results from potential theory were in good agreement. Hence the second effect makes U_1 less and U_2 greater than the theoretical values, and on this account the minimum suction quantity would be less than calculated. The two corrections nearly cancel, leaving the simple calculation nearly right—as we should expect since the large curvatures are localized near the slot.

Note also that the curvature of the streamlines in the boundary layer explains why the "measured" discontinuity, is so near the theoretical one, instead of being softer, as we might have expected.

When Taylor's theory is applied, calculations are necessary of the velocity distribution in the boundary layer; for laminar layers these are not difficult, but for turbulent layers are still estimates rather than satisfactory calculations, but are probably sufficiently nearly correct for our purposes. For laminar layers the calculated minimum quantities agree with experiment, but for turbulent layers separation can be avoided with rather less suction than the theoretical minimum, probably because of turbulent mixing. A few results are shown in Fig. 22, where the nondimensional coefficient C_Q, equal to the quantity sucked per unit time per unit span on one surface divided by the product of the chord and the undisturbed relative air velocity, is plotted against the position of transition to turbulence in the boundary layer. The results refer to the airfoil of Fig. 12 at zero incidence. The increase of C_Q as transition moves forward is not the same for all airfoils; it depends particularly on the ratio, U_2/U_1, of the veloc-

ities outside the boundary layer at the discontinuity, being less rapid for larger values of this ratio, as, for example, on the 16 per cent thick airfoil of Fig. 11.

The necessary C_Q is found in experiment to vary very little with C_L when the lift is obtained by deflection of a flap; when the incidence is altered, the necessary C_Q with a largely laminar boundary layer does not alter within the low-drag C_L-range, but at higher lifts the value for the upper surface increases because transition moves forward, and, in addition, increasingly adverse velocity gradients produce a thickening of the turbulent boundary layer. However, airfoils may be designed with very large C_L-ranges; moreover in flight the speed falls as the lift coefficient increases, and the total quantity that must be sucked does not alter so rapidly, and is reasonable even at the largest incidences that are likely to be required.

The quantities considered so far are those needed to prevent boundary-layer separation; if separation has taken place, larger quantities—which it is difficult to specify exactly, but which may in certain circumstances be as much as double—are required to make the boundary layer return to the surface.

There is some evidence that, with slot widths greater than the boundary-layer thickness, the necessary C_Q increases gradually with increase in width; the losses in the duct entries decrease, however.

Finally we remark that though it is certainly necessary to have as clear an idea as possible of the minimum quantity that must be removed to prevent separation, it does not follow that that quantity will be used in practice. As we shall see, that quantity may not even necessarily give the least effective drag; the quantity that does that will depend on the losses in the ducts. Even that, however, does not settle the matter. We must consider what we are going to do with the air sucked away from the boundary layer. We may either use a separate pump, somewhat in the nature of a ducted fan, to remove the boundary-layer air, or take the air through the wing slots to the intake of a turbojet engine; and the arrangement to be preferred must be decided separately for each airplane design. Certainly with the latter arrangement the amount of air to be withdrawn will be settled by the requirements of the engine, rather than by purely aerodynamic considerations, so long as the losses in the ducting with that amount of air are not prohibitively large compared with those in other intakes.

(8) Effective Drags

Drags of suction airfoils are measured in wind tunnels by the pitot-traverse method; when we consider what is measured in that way we see that it is nearly the drag of the tail of the airfoil aft of the slots. For essentially what we measure is the loss of momentum in the wake, and the parts of the boundary layers that have lost most momentum before the slots are drawn into the slots and do not appear in the wake with this loss of momentum.

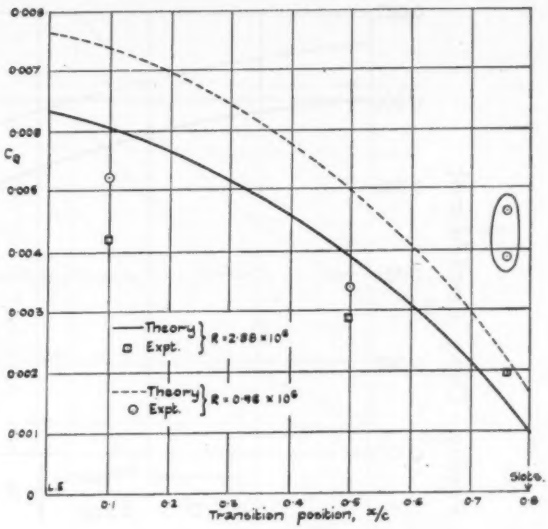

Fig. 22. Minimum suction quantities to prevent separation on a symmetrical suction airfoil, 30 per cent thick (Fig. 12), at zero lift: theoretical and experimental values at two Reynolds numbers. C_Q, equal to the quantity sucked per unit time per unit span on one surface, divided by the product of the chord length and the undisturbed air velocity, is plotted against the position of transition to turbulence in the boundary layer, measured along the chord. For the points ringed the values are high because of the tendency to laminar separation at the lower Reynolds number produced by the adverse velocity gradient in front of the slot (Figs. 12 and 19).

As we have seen, the momentum thickness of a boundary layer just aft of a slot may be estimated, and thence the value of the momentum thickness at the trailing edge and the profile drag may be computed in the usual way.[23] Gregory finds that when the theoretical minimum quantity is sucked, the momentum thickness of a laminar boundary layer is increased by only about a quarter across the slot; the increase across the slot of the momentum thickness of a turbulent boundary layer varies appreciably with the ratio, U_2/U_1, of the velocities outside the boundary layer on the two sides of the discontinuity; for the airfoil of Fig. 12 the momentum thickness of a turbulent boundary layer may be multiplied by a factor varying from 4.5 to 6 for Reynolds numbers between 10^6 and 10^8. The increase of momentum thickness falls rapidly as the quantity sucked is increased.

In the calculations of profile drag the boundary layer was assumed to be turbulent along the whole of the surface of the airfoil behind the slots. In the experiments on the airfoil of Fig. 12 (at Reynolds numbers of 2.88×10^6 and 0.96×10^6) there were some lengths of laminar layer behind the slots before the transitions to turbulence. We must expect the computed values of the profile drag to be higher than the measured values on this account. The comparisons of theory and experiment for the profile-drag coefficients of this airfoil are shown in Fig. 23.

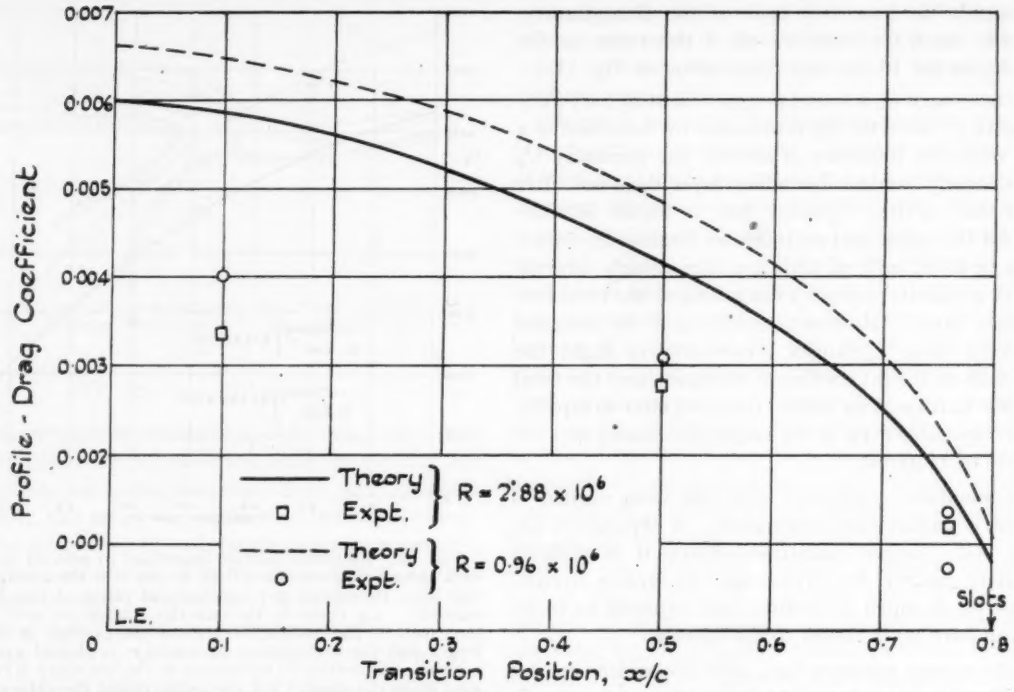

FIG. 23. Profile-drag coefficients of a symmetrical suction airfoil, 30 per cent thick (Fig. 12), at zero lift: theoretical and experimental values at two Reynolds numbers.

Some theory is necessary for extrapolation to other Reynolds numbers; calculated values of the profile drag of this airfoil (for the theoretical minimum suction quantities) are plotted against the position of transition at Reynolds numbers of 1, 10, and 100 millions as the dotted curves in Fig. 24; increasing the quantity sucked would produce a rapid decrease of the profile drag when transition is far forward.

To obtain the "effective" drag of the wing we have to take into consideration the power input to the pump, but one remark may be made before considering the equivalent "pump" drag. With sufficient suction the profile drag is much less than that of a normal wing, and the total drag that has to be balanced by a jet reaction (profile drag, induced drag, and parasitic drag) will also be considerably less; the requisite jet momentum is correspondingly reduced, and a turbojet may be profitably used at lower speeds.

For a calculation of the equivalent pump drag we may suppose that the air taken in is discharged with the undisturbed relative air velocity and static pressure; the pump must then restore the loss of total head suffered by the air removed from the boundary layer at the slot, and must also make good the losses of head in the slot entry and the ducting. These losses, in any practical case, are still unknown. The ideal pump drag is found by neglecting them. For a rough calculation we may be content to neglect the effect on the static pressure of the curvature of the streamlines in the boundary layer; then if the boundary layer to a distance Y from the surface is sucked into the slot, the loss of head per unit time per unit span which has to be made good by the pump is ideally

$$\rho U_1^3 \int_0^Y \frac{1}{2}\frac{u_1}{U_1}\left[1 - \left(\frac{u_1}{U_1}\right)^2\right]dy$$

and if η_1 is the efficiency of an assumed propulsive unit, η_2 the efficiency of the pump, U_0 the undisturbed air velocity, and c the chord, the ideal equivalent "pump-drag" coefficient is

$$(C_D)_p = \frac{\eta_1}{\eta_2}\left(\frac{U_1}{U_0}\right)^3 \frac{1}{c}\int_0^Y \frac{u_1}{U_1}\left[1 - \left(\frac{u_1}{U_1}\right)^2\right]dy$$

η_1/η_2 is unknown; it may, in practice, easily be greater than 1. If we assume that it is equal to 1, and add the profile drag to the ideal "pump" drag, we obtain the "ideal" effective drag shown by the full-line curves in Fig. 24 and cross-plotted in Fig. 25. It should be emphasized that these curves refer to the theoretical minimum quantity to prevent separation, and not to the quantity to give minimum ideal effective drag, which would be rather meaningless in the absence of knowledge of duct losses.

We can say nothing definite yet about losses in practical ducting systems; the losses will, however, depend on the quantity to be sucked and we do know some-

thing about that. We may therefore carry out hypothetical calculations with reasonable assumptions about quantity and various assumptions about the efficiency of the slot and ducting system, and arrive at the following rather general conclusions. With transition far forward and an inefficient ducting system the effective drags are too large for the scheme to be attractive; with transition far forward and an efficient ducting system, a suction airfoil 30 per cent thick may probably be designed whose drag is about the same as that of an 18 per cent thick airfoil with transition in the same place. If laminar layers can be maintained to the slots, at $0.8c$, the drag with an efficient ducting system is exceedingly low, and even with an inefficient ducting system the quantity could be kept so low (and we should clearly keep the quantity low if we could not have an efficient ducting system) that the effective drag would still be less than that of a thin low-drag wing with

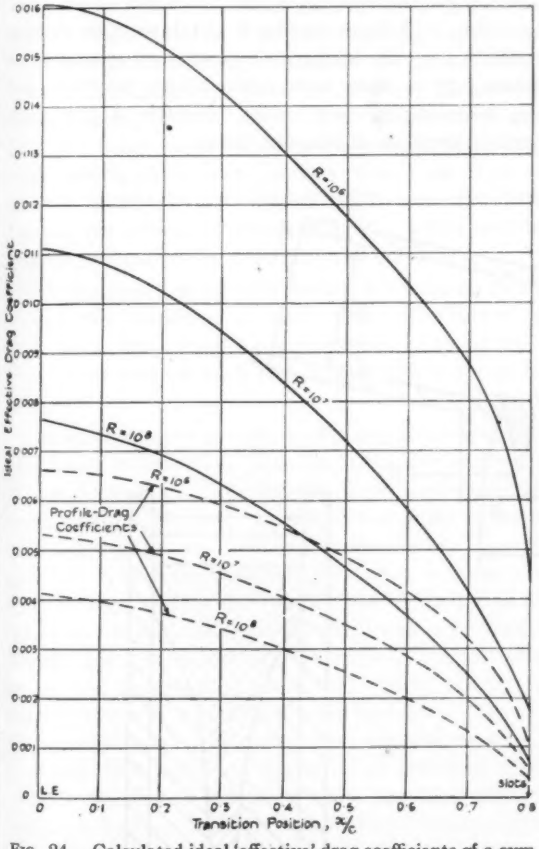

FIG. 24. Calculated ideal 'effective' drag coefficients of a symmetrical suction airfoil, 30 per cent thick (Fig. 12), at zero lift. -----Profile-drag coefficients. ——Ideal 'effective' drag coefficients, equal to the sum of the profile-drag and ideal pump-drag coefficients, with losses in the slots and ducting not included. The coefficients are section coefficients, with no allowance for induced drag; they are calculated for the theoretical minimum quantity to prevent separation, and not for the lowest drag, and for an assumed propulsive unit with an efficiency equal to that of the pump.

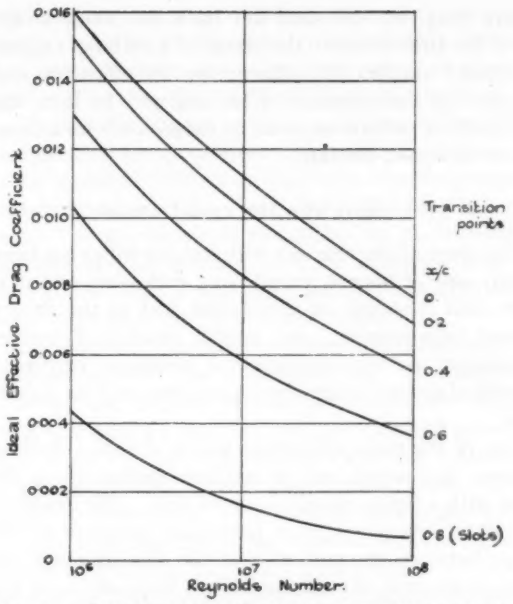

FIG. 25. Calculated ideal 'effective' drag coefficients of a symmetrical airfoil, 30 per cent thick (Fig. 12), at zero lift. The results shown in Fig. 24 are cross-plotted against Reynolds number.

maximum suction at $0.6c$, say. It is now apparent how important it is to keep as long a length of laminar layer as possible; the efficiency of the ducting system is important if we fail to maintain a sufficient length of laminar layer or if we wish to take a large amount of air for an engine through the wing slots.

Two more remarks may be made about drag, one theoretical and the other practical. Although the main purpose of the scheme is to allow a maximum suction far back without danger of separation, we may note that ideally there is always some gain, independently of the prevention of separation, if the loss of head in a boundary layer is restored by a pump instead of appearing as a loss of momentum in a wake. In the simplified case when the pump sucks the whole boundary layer from the trailing edge of a flat plate, it may be shown[23] that the ratio of the ideal drags, with equal efficiencies for the pump and propulsive system, is ϑ/θ, where ϑ is the energy thickness of the boundary layer,

$$\vartheta = \int {}^1/_2(u/U)[1 - (u/U)^2]dy$$

and θ the momentum thickness,

$$\theta = \int (u/U)[1 - (u/U)]dy$$

the integrals being taken across the boundary layer. Since $u/U < 1$, $\vartheta < \theta$. For a laminar boundary layer this saving is 21 per cent; for a turbulent one, at a Reynolds number of 10 millions, only about 8 per cent.

We should notice also that even when we know the duct losses, and include them in the calculation of ef-

fective drag, we still shall not have the whole story. For if the air is taken to the intake of a turbojet engine, we should consider the influence on the efficiency and specific fuel consumption of the engine. In fact, the full effect on performance can be judged only for a completely designed aircraft.

(9) Slot and Ducting Design

The story of the research with suction wings has been largely one of honest, painstaking endeavor, and it is right that it should be noted that just as the theory needed improvement, and is still capable of further refinement, so the experimental technique originally employed needed improvement, and may still be elaborated.

One of the main difficulties was to design a ducting system that would lead to uniform suction along the span with a pump attached to one end. The design of the slots themselves, with particular reference to the angle between the surface and the slot axis and the ratio of the radii of curvature of the front and back lips to the width of the slot, had been studied by Fage and Sargent.[24] A glance at Fig. 12, however, will show that the direction of the slot relative to the surface is largely dictated by the airfoil shape and the need to accommodate the ducting and collector without sharp bends in the slots; in the airfoil of Fig. 12 the slot was, in fact, cut starting backwards towards the leading edge nearly parallel to the chord. Moreover, the slots used are at least as wide as the boundary layer, and preferably wider, to keep down losses.

Ducting design has been studied by Rawcliffe,[25] and two views (on different scales) of a recent ducting system are shown in Fig. 26. The air enters at AB, which is along the span, and is drawn off through EF. In the other view CD is along the boundary of a section of the airfoil through the chord. There should first be an entry carefully designed to avoid separation of the flow from the wall;[26] this is followed by a two-dimensional diffuser with straight walls at a slope of 1 in 12 until the arrow P is reached, where the partitions start which are shown in the first view. The straight-walled diffuser is continued until an expansion ratio of $2^1/_2$ has been reached, and the walls are then curved to preserve a constant area. The trailing edges of the partitions should be sharp, cusped, and extended in a straight line a short way downstream—about the width of one bend if possible. Uniform suction is obtained with ducting of this type; the losses in it have been measured at present only in static tests, with still air drawn in, and were found to be just under one-fifth of the mean dynamic pressure at the slot throat.

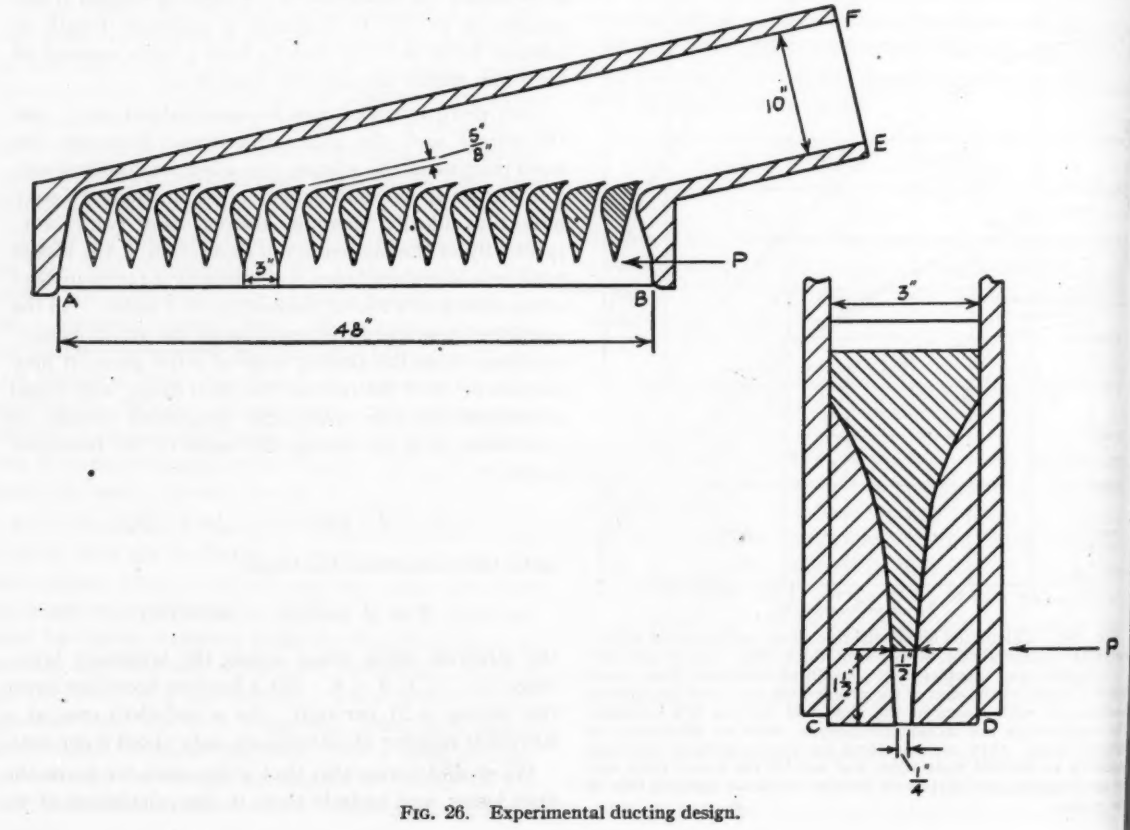

Fig. 26. Experimental ducting design.

(10) THICK SUCTION WINGS. CONCLUDING REMARKS

In spite of the work that has been done, it is clear that much is yet unknown about suction wings. Most consideration has been given to thick wings, and though it is important to realize that suction wings may be designed of any thickness required, certainly including thicknesses less than 30 per cent, it seems likely that something like this thickness may be the first to be used, so as to take advantage of the greatly increased stowage that will be possible in the wing and the possibility of burying the power plant in it. The greatest gains will be obtained by applications to flying wings, and it becomes feasible to design a much smaller flying wing than would otherwise be the case. Moreover the possibility of designing for a very small or zero $(C_M)_0$ and a very large C_L-range, with a maximum C_L which may be regarded as practically unlimited in relation to present requirements, should ease the trim problem on flying wings, though suction failure still needs further thought.

The large thickness must necessarily lead to a low critical Mach number, and the main application must be to transport aircraft; a straight 30 per cent thick wing at a lift coefficient of 0.5 would have a (theoretical) critical speed of 350 m.p.h. at stratospheric heights. But the wings would certainly be used with sweepback, which might increase this critical speed to 450 m.p.h.; it may be that suction will to some extent delay serious effects of compressibility; and somewhat thinner wings may be used on large craft.

Our ignorance is now apparent. We have no experimental information at all about the application of the principle to finite wings with sweepback, or about the effects of suction on such wings when shock waves are present.

Our knowledge of the effects of compressibility on suction wings is limited to the case when the whole field of flow is subsonic. The theoretical principles are then experimentally verified, but the suction quantity necessary to prevent separation, which remains less than the quantity of air in the boundary layer, may increase with speed. This effect may, however, have been due to the fact that on the airfoil tested there was a decreasing velocity for a short distance upstream of the slot similar to, but less marked than, that shown in Fig. 12; the airfoil tested was 22 per cent thick, with the slot at three-quarters of the chord from the leading edge.[27] It is true that tests[28] on an airfoil of orthodox shape (NACA 0020) had indicated that, provided efficient slots and ducting could be installed and extrapolation to higher Reynolds numbers was justified—in particular, provided that boundary-layer separation was still associated with a shock wave at the Reynolds numbers of flight—then with suction the drag coefficient becomes equal to its value without suction and at the critical Mach number, M_D, for a rise of drag at a Mach number 0.1 higher than M_D, and this would be attained with an economical use of power at such Reynolds numbers. But this information is not sufficient for us to feel any certainty about the behavior of a specially designed suction wing at speeds above the critical.

There will be many practical questions to be settled, and the field for speculation still appears boundless. It is an interesting reflection how every improvement in aerodynamic efficiency produces difficulties in other ways. In this case it is exemplified by the increase in severity of gust stresses, and the increased need for gust alleviation for passenger comfort, arising from the large increase in the lift-incidence slope.

There are still unsolved problems associated with the aerodynamics of even a straight wing. The design of practical and efficient ducting and the correct design of wing tips and of a junction with any fuselage or nacelle that might be fitted are obvious examples. Although some excellent systematic experimental work on slot design has been done,[24, 29, 30] further work is needed, especially with the curvatures of the surface encountered on these airfoils at the slots. Theoretically, it may be possible to extend the calculation of suitable shapes for slot walls—e.g. to design walls with constant pressure[26]—so as to take some account of the vorticity in the entering flow; and in the theoretical designs of the more extreme shapes it may be possible to take account not only of the sink effect (which is easy) but also of the shape of the slot entry (which is much harder). Above all, it must be remembered how much there is to be gained if the boundary layer can be kept laminar to the slot; when no account is taken of duct losses, this is clear from Fig. 23; with duct losses included the values of the drag coefficient would fall even more sharply with backward movement of transition. The problem of maintaining laminar flow on these airfoils is much the same as on ordinary low-drag airfoils, which we have already discussed, except that we are now becoming even more ambitious and seeking to maintain laminar flow over greater stretches of the surface. What shall we do about the insect problem—about the turbulence caused by portions of flies' bodies stuck on the surface near the leading edge? We must remember that the turbulence from any one protuberance spreads spanwise, and that one spanwise stretch of turbulent flow will require a largely increased suction quantity, not only along that stretch, but also (if we have taken pains to achieve uniform suction, as we must) all along the span; if we do not suck enough to prevent separation at the stretch of turbulent flow, the spanwise length of separated flow will spread enormously as it passes through the designed discontinuous increase of pressure. Shall we be able to devise chemical or other means of keeping the surface clean and free from flies, or must we be prepared to suck away a turbulent boundary layer through a slot not too far behind the leading edge? Shall we arrange to suck similarly behind access doors and the like? If it is too ambitious to seek to keep laminar flow right up to a single slot on each sur-

face, shall we not put in several slots along the chord? If we do that, could we not save even more by locating the rear slot nearer to the trailing edge than the 20 per cent of the chord shown in Fig. 12, for example? If we are to use several slots on each surface, shall we use a surface designed with a single velocity discontinuity, as heretofore, or a more orthodox surface, or shall we not rather divide the velocity discontinuity into the same number of parts as there are to be slots, placing one at each? Perhaps in this way we can design an airfoil with large favorable velocity gradients everywhere except at the slots and at the extreme tail; but we have still to see whether we can avoid concavity of the surface upstream of the last slot, and to consider what the economy of the system will be with the divided velocity discontinuity; to these last questions we should soon have at least theoretical answers.

Finally we note that the purpose of the original scheme, as shown in the designs of Figs. 11 and 12, may be considered achieved if we have a rising velocity gradient over most of the chord and some means of preventing separation over the rear portion of the airfoil, and that separation may be prevented by blowing air with sufficient momentum into the boundary layer through a slot in the surface. Some preliminary experiments[31, 32] with air blown into the boundary layer have been made with the airfoils of both Figs. 11 and 12, and indicate that the quantities required to prevent separation are larger with blowing than with suction, and that when separation is just prevented the form drag is larger with blowing; on the other hand, the form drag with blowing decreases continuously as the quantity increases, and with sufficiently large quantities becomes equal to and then less than that with suction. The actual recorded values, for what they are worth, for the ratios of the quantities required to prevent separation were 5:2 and 5:3 for the airfoils of Figs. 11 and 12 respectively; the ratios of the quantities to give the same form drag were 7:1 and 3:1, respectively. The power required for blowing has not been estimated, but was probably greater than that required for suction. The effect of blowing, however, depends not only on the quantity of air ejected, but also, on the velocity and pressure with which it leaves the slot; neither these nor the width of the slot have been systematically varied in experiments. Moreover, the experiments mentioned were made with ducting, slot shapes, and airfoil shapes, all specially designed for suction. There is nothing like the same background of theory and systematic experiment for blowing as there is for suction; and it seems unlikely, for instance, that the airfoil surface itself should have the same shape in the two cases, at any rate behind the slot. Therefore blowing cannot be condemned on the strength of these experiments alone, especially since, on the face of it, it looks an easier job to provide ducting for blowing than for suction. In view of all these considerations it does not seem worth while to consider further the recorded experimental results, except perhaps to mention that at incidence the lifts were all just a little greater with blowing than with suction, as was to be expected.

(11) Thin Suction Airfoils Designed for High Maximum Lifts

Another application of the same basic idea—to design the shape of the contour of an airfoil section specially for suction at a few points, where the design velocity on the surface decreases discontinuously, or at any rate very, very rapidly—is to attempt to design a thin airfoil, suitable for high speeds, with the principle applied to increase the maximum lift. Generally speaking, a theoretical velocity distribution on the upper surface of a thin airfoil at a high lift coefficient has a high peak near the leading edge, a sharp fall immediately behind the peak, and a more gradual decline over the rest of the surface; the sharp fall behind the peak leads to separation and stalling. If this sharp fall is replaced by a discontinuity, with the boundary layer sucked away there, and if the adverse velocity gradient over the rest of the surface is reasonable, separation and stalling may perhaps be postponed to higher lift coefficients without any adverse effects on the other qualities of the airfoil section.

It is not obvious, *a priori*, how successful the application of these ideas will be in practice. When separation occurs at a high lift on a thin airfoil we expect only a partial stall, with the boundary layer rejoining the surface, so it is not clear how much gain is to be expected. There is, of course, a subsidiary favorable effect of suction, in that the sink effect itself produces a favorable alteration in the theoretical velocity distribution; but we should not expect this effect to be large, because, especially in view of the thinness of the wings and the difficulty of fitting ducting, the quantity sucked must be kept small.

Since the airfoil is thin, it may be thought at first that the approximate theory may be used for design. The discontinuity, however, must be located near the leading edge, where the first, linear approximation fails completely, so Approximation II must be used. The most elementary theory of design must therefore be more difficult for these airfoils than for thicker airfoils with the discontinuity far back. Actually Approximation II has not yet been used to explore the possibilities of design of these airfoils; it would be instructive if this were done. So far, several airfoils have been designed by Lighthill[15, 33] and one by Glauert[34] by the use of Lighthill's exact theory; Lighthill takes the sink effect into consideration and relies upon it to some extent to achieve the required results; Glauert does not.

Small-scale models of Glauert's design and of one of Lighthill's designs have been tested[34, 35] at the National Physical Laboratory at Reynolds numbers of

about half a million. Both designs were about the same thickness (8.65 and 8.6 per cent thick, respectively). Without suction both airfoils had a maximum normal-force coefficient C_N of 1.08. On Glauert's design a normal-force coefficient of 1.25 is obtained with a small suction quantity, the suction coefficient C_Q being not greater than 0.003, and increase of C_Q has only little effect on $(C_N)_{max.}$ On Lighthill's design, $(C_N)_{max.}$ seems to increase almost linearly with C_Q, up to the largest value used, 0.019 (much too large to be practical); interpolation in the results shows that a $(C_N)_{max.}$ of 1.25 should be obtained for a C_Q of 0.005.

I have discussed these results only briefly because we do not know that the airfoils tested approach at all closely to the best that could be designed. No thorough attempt has yet been made to explore the theoretical possibilities and limits of design.

(12) Distributed Suction

No discussion of suction airfoils would be complete without some mention of distributed suction through porous surfaces, though the experiments on this aspect are still in a rudimentary state. Theoretical considerations[36, 37] point to the need of very small quantities to prevent boundary-layer separation under adverse pressure gradients, and if the practical difficulties of the mechanical weakness of porous sheet, of shaping the sheet, and of the danger of clogging by rain and dirt, can be overcome, the applications seem very promising, particularly to increasing the maximum lifts of thin airfoils by distributed suction through porous noses fitted to them.[38]

The size and spacing of the pores in the surface must be small compared with the thickness of the boundary layer, and the distribution of the pores should preferably be a random one. The aim is that the concept of a velocity through the surface and continuous all over it—not spotty—should be realized as closely as possible. This velocity, even if small, produces a marked decrease in the rate of growth of the boundary layer in an adverse pressure gradient and marked changes in the distribution of the forward velocity across it; and it is this effect that delays separation.

Here, too, the nose may be shaped to give the best results, a large radius of curvature at the leading edge being desirable, but the shapes are much more orthodox than those designed for suction at a single slot.

The basic idea of distributed suction is not new, but it is only lately, since suitable materials[39]—sintered metals, e.g. sintered bronze—became available, that systematic calculations have been made, and experiments became possible.

Theoretically, distributed suction should also help considerably to stabilize the boundary layer and preserve laminar flow. (For the case of zero pressure gradient see reference 40.) Experimental confirmation is still lacking, and it is still, in particular, an open question whether a porous material can be produced with a surface sufficiently smooth for this purpose.

In some ways the use of a large number of slots on an airfoil of orthodox section, as in Pfenninger's experiments,[29] may be considered to be a half-way stage between the use of a few slots and the use of distributed suction. But the underlying principles are so different in the three cases that this view should not be pressed too far. It seems that distributed suction, which works in quite a different way, requires a smaller quantity than suction through separate slots. The final decision on the merits of the various schemes must be left to aeronautical scientists, designers, and time.

(13) Conclusion

This lecture is in the nature of an interim report on work still in progress, and, without any conscious direction on my part, the descriptions became less and less detailed and satisfactory as we moved on. Looking back, I believe that is as it should be, since the subjects mentioned became progressively less and less explored, the ideas—or the possibility of their application—newer and newer, until we reached a stage when we were considering matters on which experiments have only just begun.

I believe that the work on suction airfoils is as neat an example as we could wish to find of the amount of work to which a comparatively simple new idea can give rise, and of how the problems that arise should be tackled by all the methods—theoretical and experimental—at our command. Mathematical theories can be used to design both the models for test and the experiments themselves, and to help to interpret the results; the laboratory results must themselves be checked by full-scale trials.

One final word: the shapes of suction airfoils doubtless appear strange and novel to designers. I venture to prophesy that if future experiments show that considerable savings may be obtained with safety by their use, the time will come when they will "look right" to designers, whose intuition, based on a deep scientific background used without conscious effort, will then lead them to choose such shapes for the purposes for which they were produced.

References

[1] Richards, E. J., *Note on the Limiting Thickness-Chord Ratios allowable on Low Drag Wings*, A.R.C. Report No. 7813, June, 1944; Addendum, A.R.C. Report No. 8139, October, 1944.

[2] Smith, F., and Higton, D. J., *Flight Tests on "King Cobra" F.Z.440 to Investigate the Practical Requirements for the Achievements of Low Profile Drag Coefficients on a "Low Drag" Aerofoil*, A.R.C. Report No. 9043, August, 1945.

[3] Gray, W. E., and Davies, H., *Note on the Maintenance of Laminar Flow Wings*, A.R.C. Report No. 10518, February, 1947.

[4] Plascott, R. H., *Profile Drag Measurements on Hurricane II Z.3687 fitted With "Low Drag" Section Wings*, A.R.C. Report No. 10106, September, 1946.

[5] Gray, W. E., *Interim note on boundary layer transition tests in flight by the chemical method*, A.R.C. Report No. 10233, January, 1947.

[6] Theodorsen, T., *Theory of Wing Sections of Arbitrary Shape*, N.A.C.A. Report No. 411, 1931.

[7] Theodorsen, T., and Garrick, I. E., *General Potential Theory of Arbitrary Wing Sections*, N.A.C.A. Report No. 452, 1933.

[8] Goldstein, S., *Approximate Two-Dimensional Aerofoil Theory. Part I. Velocity Distributions for Symmetrical Aerofoils*, A.R.C. Report No. 5804, May, 1942; *Part II. Velocity Distributions for Cambered Aerofoils*, A.R.C. Report No. 6156, September, 1942; *Part III.* (with Richards, E. J.) *Approximate Designs of Symmetrical Aerofoils for Specified Pressure Distributions*, A.R.C. Report No. 6225, October, 1942; *Part IV. The Design of Centre Lines*, A.R.C. Report No. 8548, March, 1945; *Part V. The Positions of Maximum Velocity and Theoretical C_L-Ranges*, A.R.C. Report No: 8549, March, 1945; *Part VI.* (with Preston, J. H.) *Aerofoils with Hinged Flaps*, A.R.C. Report No. 8877, August, 1945.

[9] Germain, Paul, *The Computation of certain Functions Occurring in Profile Theory*, A.R.C. Report No. 8692, May, 1945. See also Thwaites, B., *A Method by P. Germain for the Practical, Evaluation of the Integral* $\epsilon(\theta) = -(1/2\pi)\int_0^{2\pi} \psi(\phi) \cdot \cot(1/2) \times (\phi - \theta)d\phi$, A.R.C. Report No. 8660, May, 1945.

[10] Watson, E. J., *Formulae for the Computation of the Functions Employed for Calculating the Velocity Distribution About a Given Aerofoil*, A.R.C. R. & M. No. 2176, May, 1945.

[11] Thwaites, B., *A New Family of Low Drag Wings with Improved C_L-Ranges*, A.R.C. Report No. 8532, March, 1945.

[12] Thwaites, B., *A Method of Aerofoil Design. Part I. Symmetrical Aerofoils*, A.R.C. R. & M. No. 2166, May, 1945; *Part II. Cambered Aerofoils*, A.R.C. R. & M. No. 2167, September, 1945.

[13] Thwaites, B., *On the Design of Aerofoil Sections for High Speed Aircraft*, A.R.C. Report No. 9076, October, 1945.

[14] Douglas, Ola, *A Series of Low Drag Aerofoils Embodying a New Camber-line*, A.R.C. Report No. 10620, May, 1945.

[15] Lighthill, M. J., *A New Method of Two-Dimensional Aerodynamic Design*, A.R.C. R. & M. No. 2112, April, 1945.

[16] Görtler, H., *Über eine dreidimensionale Instabilität laminarer Grenzschichten an konkaven Wänden*, Göttinger Nachrichten, Math. Phys. Kl., Neue Folge, 2, pp. 1–26, 1940.

[17] Liepmann, H. W., *Investigations on Laminar Boundary-Layer Stability and Transition on Curved Boundaries*, N.A.C.A. A.C.R. No. 3H30 (Wartime Report No. W107), August, 1943; *Investigation of Boundary-Layer Transition on Concave Walls*, N.A.C.A. A.C.R. No. 4J28 (Wartime Report No. W87), February, 1945.

[18] Glauert, M. B., *The Design of Suction Aerofoils with a Very Large C_L-Range*, A.R.C. R. & M. No. 2111, November, 1945.

[19] Richards, E. J., Walker, W. S., and Greening, J. R., *Tests of a Griffith Aerofoil in the 13 ft. by 9 ft. Wind Tunnel*, A.R.C. R. & M. No. 2148, March, 1944.

[20] Richards, E. J., Walker, W. S., and Taylor, C. R., *Wind-tunnel Tests on a 30 per cent Suction Wing*, A.R.C. R. & M. No. 2149, July, 1945.

[21] Gregory, N., and Walker, W. S., *Further Wind-Tunnel Tests on a 30% Symmetrical Suction Aerofoil with a Movable Flap*, A.R.C. Report No. 9810, July, 1946.

[22] Gregory, N., *Note on Sir Geoffrey Taylor's Criterion for the Rate of Boundary-layer Suction at a Velocity Discontinuity*, A.R.C. Report No. 10630, May, 1947.

[23] Preston, J. H., Gregory, N., and Rawcliffe, A. G., *The Boundary-layer Theory of Suction Aerofoils, together with Calculations of Quantity, Profile Drag and "Pump" Drag for Two Typical Thick Griffith-Type Suction Aerofoils*, A.R.C. Report No. 10280, January, 1947.

[24] Fage, A., and Sargent, R. F., *Design of Suction Slots*, A.R.C. R. & M. No. 2127, February, 1944.

[25] Rawcliffe, A. G., *Suction-Slot Ducting Design*, A.R.C. Reports Nos. 9487, March, 1946, and 10522, April, 1947.

[26] Watson, E. J., *Free Streamline Suction Slots*, A.R.C. Report No. 9411.

[27] Pearcey, H. H., and Rogers, E. W., *The Effect of Compressibility on the Performance of a Griffith Aerofoil*, A.R.C. Report No. 10096, November, 1946.

[28] Fage, A., and Sargent, R. F., *Effect on Aerofoil Drag of Boundary Layer Suction Behind a Shock Wave*, A.R.C. Reports Nos. 7153, October, 1943, and 7365, January, 1944.

[29] Pfenninger, W., *Untersuchungen über Reibungsverminderungen an Tragflügeln, insbesondere mit Hilfe von Grenzschichtabsaugung*, Mitteilungen a. d. Inst. f. Aerodynamik, E.T.H., Zürich, No. 13, 1946.

[30] Pierpont, P. K., *Investigation of Suction Slot Shapes for Controlling a Turbulent Boundary Layer*, N.A.C.A. T.N. No. 1292, June, 1947.

[31] Preston, J. H., Walker, W. S., and Taylor, C. R., *The Effect on Drag of the Ejection of Air from Backward-facing Slots on a 16.2 per cent. Griffith Aerofoil*, A.R.C. R. & M. No. 2108, January, 1946.

[32] Gregory, N., Walker, W. S., and Raymer, W. G., *Wind Tunnel Tests on the 30 per cent symmetrical Griffith Aerofoil with Ejection of Air at the Slots*, A.R.C. Report No. 10097, November, 1946.

[33] Lighthill, M. J., *A Theoretical Discussion of Wings with Leading-edge Suction*, A.R.C. Reports and Memoranda No. 2162, May, 1945.

[34] Cheers, F., and Douglas, Ola, *Tests on a "Glauert" Nose Suction Aerofoil in the N.P.L. 4 ft. No. 2 Wind Tunnel*, A.R.C. Report No. 10507, April, 1947.

[35] Cheers, F., Raymer, W. G., and Douglas, Ola, *Tests on a "Lighthill" Nose-Suction Aerofoil in the N.P.L. 4 ft. No. 2 Wind Tunnel*, A.R.C. Report No. 10506, April, 1947.

[36] Preston, J. H., *The Boundary Layer Flow Over a Permeable Surface through which Suction Is Applied*, A.R.C. Report No. 9364, February, 1946.

[37] Thwaites, B., *Investigation into the Effect of Continuous Suction on Laminar Boundary-Layer Flow Under Adverse Pressure Gradients*, A.R.C. Report No. 9555, April, 1946.

[38] Thwaites, B., *A Theoretical Discussion of High-Lift Aerofoils with Leading-edge Porous Suction*, A.R.C. Report No. 9809, July, 1946.

[39] Preston, J. H., and Rawcliffe, A. G., *Note on Sintered Metal with a View to its Use as a Porous Surface in Distributed Suction Experiments*, A.R.C. Report No. 9383, February, 1946.

[40] Pretsch, J., *Umschlagbeginn und Absaugung*, Jahrbuch der Deutschen Luftfahrtforschung, I, pp. 1–7, 1942.

Discussions of the Lecture

Ira H. Abbott, Aeronautical Consultant, N.A.C.A.: It is a privilege to congratuate Dr. Goldstein on his excellent presentation of the research being done in Great Britain on low-drag and suction airfoils. The subject of today's lecture appears particularly appropriate to me because today is the tenth anniversary of the first Wright Brothers Lecture, delivered by B. Melville Jones on the subject, "Flight Experiments on the Boundary Layer." The results presented 10 years ago were heartening to those of us in the N.A.C.A. who were then just getting started on the problem of extending the laminar layer on wings. Much has been accomplished in the past 10 years, but, as pointed out by Dr. Goldstein, much remains to be done. The problem of improving the efficiency of wings offers a continuous challenge that cannot be met adequately at subsonic speeds until answers are obtained to the questions raised by Dr. Goldstein. Even at supersonic speeds, it may safely be predicted that optimum wing efficiency will require that more attention be directed to the boundary layer.

It is difficult to discuss this lecture because I am so thoroughly in agreement with the basic ideas presented. However, it appears appropriate to point out the parallel between the work in Great Britain and that of the N.A.C.A. in this country. In both instances, the research has been directed toward the broad objective of improving the efficiency of wings by increasing the extent of the laminar boundary layer. Although the emphasis has been different, this objective has been sought, in both instances, through the design of low-drag airfoils and the use of boundary-layer control. To a large extent, the results of the different approaches to the objective have supplemented each other and illustrate the advantages of separate attacks on an objective by independent research teams. It is easy to overemphasize the differences in the two approaches, but at the risk of doing so, I wish to discuss some of them briefly.

The most notable difference in the two approaches is the emphasis placed on theoretical and experimental work. Dr. Goldstein and his associates have tended to rely mainly on theoretical results with spot checks in flight or in the wind tunnel. When rigorous theory was lacking, they devised approximate or empirical relations to fill the gap. The success of this approach is well shown by today's lecture.

We, in this country, have been unwilling to rely on calculation when means could be devised for the experimental determination of overall airfoil characteristics. Knowledge of the boundary layer has not progressed sufficiently as yet to permit reliable calculation of all airfoil characteristics over the useful range of angle of attack. The N.A.C.A. two-dimensional low-turbulence wind tunnels were designed and built as the result of an early decision that practical airfoil sections could be obtained in a reasonable length of time only if facilities were available to permit systematic testing under conditions closely approximating those of flight. Initial exploratory investigations of a wide variety of airfoil sections served to outline the possibilities. The objective was then established of a series of sections that would exhibit low-drag characteristics with smooth surfaces without appreciable sacrifice of any of the good characteristics of the more conventional sections when compared under conditions of equal thickness ratios, camber, and surface condition. The N.A.C.A. 6-series airfoils are the result of our attempt to reach this objective.

The solution presented by Dr. Goldstein to the so-called inverse problem of designing airfoil sections to have desired types of pressure distribution differs markedly from the method used by the N.A.C.A. It should be noted that there are difficulties in an adequate mathematical formulation of the problem. The designer is faced, nevertheless, with the real problem of accurately associating profile shapes with desired types of pressure distribution. The difficulty of this problem presented a serious obstacle to the design of low-drag airfoils. The N.A.C.A. 1-series airfoils were obtained through empirical methods. The N.A.C.A. 2- through 5-series airfoils were designed by various approximate methods. Our experiences with these approximate methods were so unpromising that we abandoned this line of attack before a satisfactory method was developed and concentrated on the development of an exact method based on the Theodorsen solution.

The remarks of Dr. Goldstein with regard to the difficulties involved in accurate computation of the Theodorsen solution are well justified. Even though the method is theoretically exact, an accurate numerical solution by usual methods may require the use of 80 points and not less than two approximations. It was found, however, that the epsilon-curve could be modified to produce changes of the desired type in the pressure distribution and that the resulting profile shapes and pressure distributions could be accurately related without undue difficulty in the computations. Contributions to this method were made by Theodorsen, Garrick, Jacobs, von Doenhoff, Pinkerton, and Naiman. This method has been used successfully in a routine manner for the design of the N.A.C.A. 6-series airfoils.

It would be presumptious to compare the Goldstein and N.A.C.A. methods without experience in the detailed use of both of them. However, some general comments may be offered. The N.A.C.A. method, in practice, has been applied to the design of symmetrical sections or thickness distributions, although it is not limited to this application. These thickness distribu-

tions are then combined with mean lines derived by thin airfoil theory. The pressure distributions of the final sections may be obtained by Theodorsen's solution or, approximately, by superposition of velocities using tabulated characteristics. This method has many advantages because the pressure distributions of a large variety of sections may be obtained quickly from a modest number of basic characteristics tabulated by the N.A.C.A.

Although the N.A.C.A. method is sufficiently accurate for most engineering purposes, no great claim for accuracy can be made for the first approximation pressure distributions of the cambered sections. This situation is satisfactory for sections of small and moderate thickness ratios, but we are finding it necessary to design thick sections directly as cambered airfoils. The Goldstein method has been applied directly to the cambered sections and contains within it an approximation of high order for the effect of camber changes. It is thus apparent that both methods have certain advantages. It is hoped that a way may be found to combine the advantages of both methods without introducing undue complication.

The research reported by Dr. Goldstein on specially designed suction wings is of considerable fundamental importance. Such wings avoid the difficulty of producing long favorable pressure gradients without excessive pressure recoveries in the limited region between the point of minimum pressure and the trailing edge. It is well known that the highest values of the lift-drag ratio are obtained with the largest extent of laminar flow and the largest amounts of camber consistent with prevention of turbulent separation. With ordinary airfoils, turbulent separation imposes limits on these design variables and on the thickness ratio. With suction airfoils, these limitations are avoided, making it possible to design thick sections that should have extremely high lift-drag ratios if extensive laminar layers can be realized.

As indicated by Dr. Goldstein, the advantages of the suction airfoils are dependent to a great extent on actually achieving the design extent of the laminar flow. This problem is not solved, as is apparent from the cited difficulties with insects in flight. Large numbers of airplanes are using low-drag wings. Special efforts have been made on some of these airplanes to obtain sufficiently smooth and fair surfaces to permit reasonably extensive laminar flow. So far as I know, none of these airplanes are obtaining extensive laminar flow under actual conditions of field maintenance and service operation. It must be concluded that the important problem is to stabilize the laminar boundary layer to prevent transition resulting from the types of surface roughness and irregularities that cannot be avoided without unreasonable maintenance or impractical restriction of operating conditions.

The N.A.C.A. is now concentrating its efforts in this field on the problem of obtaining a stable laminar boundary layer by means of boundary-layer control. Research conducted just before the war indicated that the use of suction slots would permit a greater extent of laminar layer to be realized. The results did not indicate that the use of slots stabilized the layer in the sense of preventing transition resulting from roughness. This research was discontinued during the war in favor of the development of airfoil sections of immediate practical value.

In resuming this research we have been aided by the result of German and Swiss investigations. It appears that the use of porous surfaces is of particular interest. Preliminary N.A.C.A. results indicate qualitatively that suction through porous surfaces can stabilize the boundary layer, to some extent at least, to the effects of roughness. This result is believed to be significant, although the studies have not progressed as yet to any practical surface or to flight values of the Reynolds Number. It thus appears premature to discuss the practical problems of using sections of the type presented today. If it proves possible to stabilize the laminar boundary layer, we shall be forced to revise our concepts of what is and is not practical.

Major General L. C. Craigie, U.S.A.F., Director of Research and Development: Professor Goldstein is to be congratulated on his masterly presentation of this important subject. The paper is timely, since it comes during a period when increased interest and activity in boundary-layer control are being evidenced with a view toward *increasing the performance* of military aircraft.

Boundary-layer control has always shown great *potential* promise but has not, in general, come up to expectations because of the fact that it has been largely used as a so-called "aerodynamic crutch." In other words, *it has been used as an aid* in overcoming boundary-layer difficulties on aerodynamic surfaces that were designed primarily for operation *without* boundary-layer control.

Professor Goldstein has presented a constructive new approach in *designing the basic airfoil for operation with boundary-layer suction.*

It is believed that this new concept will have promising applications in military aviation. Continued research along the lines suggested by Professor Goldstein *should lead* to wing designs which would considerably increase the *range* of high-speed jet aircraft, since it should decrease the wing drag and make use of the large amount of surplus air required by thermal jet propulsive systems. It should be emphasized that the advent of jet propulsion provides a built-in pumping system that eliminates the previous handicap of having to provide an extra pump for the purpose.

Some of the unexplored applications that Professor Goldstein has mentioned appear especially promising for the future; for instance, the possibility of using, for high-speed flight, thin small wings that still have

adequate lift for take-off and landing under conditions that might be encountered in service.

It is believed that boundary-layer suction will help diminish losses in the *supersonic régime*. In supersonic flow, the shock waves occurring around the surface of an airfoil are associated with a rapid rise of pressure through the shock. At the surface of the wing this strong adverse pressure gradient causes an essential increase in the boundary-layer thickness with strong tendencies toward separation. It is believed that systematic exploitation of Professor Goldstein's methods will lead to considerable aerodynamic improvements in both the external and internal flow systems of supersonic aircraft and missiles.

In conclusion, Professor Goldstein's paper shows clearly the great number of *theoretical* and *experimental* investigations which must be carried on and *integrated* to make progress on a *single new concept*. This emphasizes the complexity of a research and development program leading to improvements in air materiel.

As a representative of the United States Air Force, I wish to thank Professor Goldstein for his stimulating paper. I am happy to see this continued cooperation between Great Britain and the United States, which, I am sure we all agree, is to our mutual advantage.

Captain Walter S. Diehl, U.S.N., R. & D. Group, Bureau of Aeronautics, Navy Department: Dr. Goldstein is an outstanding authority on mathematics in the fields of fluid mechanics and theoretical aerodynamics. The Institute is most fortunate in having such a distinguished guest speaker for the Eleventh Wright Brothers Lecture. Anything that Dr. Goldstein might say regarding the work that he has been doing is certain to be of great interest to our members. It is particularly pleasing to find that he has chosen to give us a complete explanation of one of the most interesting applications of mathematical analysis to a specific problem.

One of the most striking of the broad aspects of Dr. Goldstein's paper is the revelation of the extent to which modern mathematical analysis can enter into the detail design of airplane wings. This is not a matter of accident, but rather it is the result of many years of thought and hard work on the part of those concerned. Our N.A.C.A. can point with pride to its efforts in this field. The development of highly satisfactory approximations for the exact theory as outlined in the lecture appears to have been a major achievement. For one thing it shows that the mathematician is a normal human being and that he does not always insist on doing a thing the hard way. It is significant to note the close coordination of the theoretical studies with the experimental work. This, as many of us firmly believe, holds the key to rapid progress. In it, the theoretical analysis is always being crowded by the experimental data—which may not always agree with the predicted values. One well-known professor is reported to have told his class that, "When theory and facts do not agree, it is just too bad for the facts." That was many years ago. The modern mathematician is not satisfied until it has been fully demonstrated that the theory accurately predicts the facts.

The lecture really consists of two parts. The first part is concerned with Dr. Goldstein's research work on laminar-flow wings, covering ground generally similar to previous N.A.C.A. research. Most of our members will find this an interesting account, and especially so in the sections devoted to flight evaluation of the practical difficulties encountered in the attempts to obtain and then to maintain laminar flow.

The second section is concerned with suction wings and boundary-layer control. This section presents new material that requires some detailed technical comment. The comments that follow represent my personal appraisal and do not necessarily reflect the views of the U.S. Navy.

Suction wings and boundary-layer control schemes have been with us for many years. The Bureau of Aeronautics sponsored an N.A.C.A. flight investigation of the Katzmayr wing more than 20 years ago. There have been numerous attempts made subsequently, with varying results, but boundary-layer control must still be classed by the designer as an incompletely demonstrated device. One finds three broad points of view among those who are familiar with the subject:

(1) It is the most promising method we have for getting real improvement in airplane performance.

(2) It shows some promise in special applications, but, in general, it is ruled out by considerations of the overall effects on the airplane.

(3) It is just another "boot-strap" proposition.

Most engineers hold to the middle ground point of view and probably will continue to do so until the matter is settled for them in a convincing manner.

Although Dr. Goldstein predicts cautiously that the time may come when suction airfoils will "look right" to designers, his paper is to be considered as a report on what has been done theoretically and experimentally rather than as a proposal to jump immediately into a practical application. Before this can be done there is another job for mathematical analysis—and it is an important job. An airplane consists of wings, power plant, and controls. Any practicable combination must have reasonably acceptable stability, control, and performance characteristics. There can be no doubt that these characteristics will be affected by the use of suction wings. The mathematician must now determine the boundaries for the design parameters giving at least some promise for a practical application of the suction wings.

I should like to compliment Dr. Goldstein on his masterly presentation of a highly technical paper. By all ordinary standards the complex technical ground

covered would seem to limit rather severely the size of audience that could appreciate the details involved. Dr. Goldstein has been able to surmount the barriers with ease and give us, not a technical broadside, but a most entertaining lecture. I am sure that all of those who were fortunate enough to hear the lecture join with me in thanking Dr. Goldstein for his contributions to our knowledge of boundary-layer flow.

Professor William R. Sears, Director, Graduate School of Aeronautical Engineering, Cornell University: First I must express my share of appreciation to Professor Goldstein for this masterful lecture. It is particularly fortunate when the Wright Brothers Lecture, as has been the case today, can be devoted to the unveiling of an engineering invention. Dr. Griffith's ingenious idea, based on designing an airfoil contour for a discontinuous velocity distribution, could hardly have been conceived by anyone unfamiliar with the theory of aerodynamics. We have here a refutation of the popular fallacy that ingenuity and scientific learning are for some reason incompatible and that, therefore, inventions can be made only by untrained geniuses—diamonds in the rough—whose imaginations are not stifled by familiarity with the laws of physics or their mathematical expressions! In this respect today's lecture is especially fitting to honor the Wright Brothers; they were certainly inventors of a more scientific character than is permissible according to the popular legend!

I am sure that the suction wings will be studied with great interest by the designers of flying-wing airplanes, as Dr. Goldstein has predicted. The combination of low drag, high lift, small pitching moment, and increased volume will be extremely attractive. On the other hand, in recent years we have seen a greater demand for thick profiles for conventional airplanes than for flying wings. This has been because of the requirements of spar depth. Perhaps we shall see this trend carried on to produce conventional airplanes of very great aspect ratio and very thick profiles. If sweepback up to about 40° is used—as one of Dr. Goldstein's figures indicates—we shall be thankful for the large values of $dC_L/d\alpha$.

One of the most startling results we have seen this afternoon is the reasonable behavior of the suction wings without suction. It seems possible that they can be designed to be safely usable without suction. This would certainly increase the attractiveness of the sections. But here again we would be faced with our ignorance regarding transition and turbulent separation.

Certainly Professor Goldstein's remarks on this subject and his whole lecture, for that matter, should inspire us to further research on transition and the turbulent boundary layer. And since it is doubtful whether we shall ever understand the turbulent boundary layer before we fully understand simpler turbulent flows, we may take this as an incentive also to attack the turbulence problem in general.

In this connection, I am interested in the speaker's rather deflationary remarks on the subject of transition. I think that in this country we have felt a bit more optimistic, believing that the amplified laminar-boundary-layer oscillations do represent the essential phenomenon leading to transition. But if Dr. Goldstein means that we cannot, at present, predict the transition point on the surface of an airfoil, and could not even if we knew the Reynolds Number of laminar instability, then we cannot refute him. Admittedly, we still have a lot to learn!

One of the other discussers has already mentioned certain parallel American work, especially on low-drag wings. On one essential point there seems to be agreement between Teddington and Langley Field—that is, the question, how smooth is a smooth surface? Eastman Jacobs, the father of low-drag airfoils, whose influence is certainly present in these low-drag and suction airfoils, used to say that a wing was smooth when its finish resembled that of a new automobile. This put the criterion in terms of a product mass-produced and sold for a profit! The British experience seems to have been similar, and Dr. Goldstein's remarks about the effects of weather and service are also encouraging. One might question his opinion that larger waviness is permissible near the leading edge because of the favorable gradient there; probably this means "larger" only in relation to the boundary-layer thickness there and, therefore, very small permissible waviness indeed.

The Lighthill theory for calculation of an airfoil to fit a prescribed pressure distribution also has its counterparts in certain researches in this country. I think there is general agreement that this "inverse" problem has no solution in general. Lighthill's theory might appear to contradict this, until we notice that Lighthill specified the velocity distribution in the transformed "circle" plane, not on the airfoil. This can always be done, but it does not strictly constitute a solution of the inverse problem, since the exact variation of pressure along the airfoil remains unknown until the profile is calculated.

I am not sure that in this country we have had any analog of Sir Geoffrey Taylor's ingenious approximate calculation of the suction quantity. It is inevitable that Professor Taylor's name should appear in a lecture like this. They say he has a whole desk drawer full of unpublished calculations similar to the one I refer to, and he gets them out when baffled engineers come to Cambridge for help, as they apparently often do.

Finally, I cannot resist adding a word about this surprising aerodynamic-entomological problem. As I understand it, Professor Goldstein has told us this: that low-drag and suction wings are not different from most aeronautical inventions. They show great promise, but they still have a few bugs!

The discussions that follow were prepared for the West Coast presentation of the Wright Brothers Lecture.

Philip A. Colman, Chief Aerodynamics Engineer, Lockheed Aircraft Corporation: One of the significant points brought out in Dr. Goldstein's paper is the importance of airfoil smoothness. Many people believe that, with boundary-layer control, the drag of a wing could be materially reduced, while, at the same time, the degree of accuracy of maintaining airfoil contour and the surface smoothness requirements could be relaxed. This is just the opposite to what is required according to this paper. If an extended region of laminar boundary-layer flow is not obtained, the drag reduction is small, and the ducting problems and internal power requirements are excessive.

Lockheed has at various times experimented with boundary-layer control. The last investigation included wind-tunnel tests of a laminar-flow-type airfoil section of the kind used on the Constitution airplane. In the wind tunnel, slots were developed to obtain optimum shape for uniform suction and low intake losses. These tests showed a drag reduction, and therefore a flight-test program was initiated. A P-38 airplane was equipped with a "glove," which had sufficient width to obtain representative flow conditions. This "glove" had the same airfoil section tested in the wind tunnel and included the optimum slot. The source of suction was from the turbosupercharger. These tests showed first the importance and the difficulty in obtaining true aerodynamic smoothness. With a smooth airfoil and boundary-layer control, the drag was reduced, but the net gain was not of sufficient magnitude to encourage further test work. Since this occurred at the time that the laminar-flow-type airfoil was first coming into use, the decision was that the development of this new-type airfoil reduced materially the amount to be gained from boundary-layer control.

Now Dr. Goldstein shows us that to gain the ultimate in drag reduction, the airfoil shape should be designed to fit with the boundary-layer removal principle. This now appears to be obviously correct. I hope to see rapid development under the principle he has presented. This is a tedious job but should be attacked vigorously today so that the benefits can be realized in actual airplane design in the near future.

A. M. O. Smith, El Segundo Plant, Douglas Aircraft Company, Inc.: For many years, boundary-layer control, especially stall control, in an indefinite sort of way has appeared to promise improvement in aerodynamic design. However, until recently, no one had indicated a method of full utilization of the effects that can be obtained by suction. Thanks to the recent progress in laminar-boundary-layer stability theory, the German porous plate theoretical studies, and Dr. Griffith's idea of a velocity discontinuity at a slot, we are beginning to obtain promising methods and theory for use in further attacks on the drag problem. Dr. Goldstein is to be congratulated for his work on this problem and for his excellent report on the British efforts.

During the past few years great strides in aircraft high speed have been made, but range capabilities have hardly progressed. Jet and gas-turbine aircraft at the present have less range than the best reciprocating engine types of recent years. Hence, a paper stimulating thought toward improving the intrinsic efficiency of aircraft seems timely.

I am pleased also to learn about the recent developments in airfoil theory. Since the methods were developed to be timesavers, we intend to study them carefully.

The thought of the very thick wings considered by Dr. Goldstein, especially ahead of the control surfaces, is disturbing to the industrial aerodynamicist, whose most difficult problem is to produce satisfactory flying qualities for the various critical conditions of flight. For a suction wing it is control suction power off. However, no evaluation can be made until more test data are available.

Some additional information on the overall problem of the boundary-layer control aircraft may be of interest at this time. The significance of drag reductions by suction can only be determined by study of the overall performance of such an aircraft, including allowance for the deleterious effects on engine performance. When the work of Dr. Pfenninger[1] on control of the laminar layer was received, such a study was made of the performance of a large, tailless, six-engined jet airplane. Three cases were studied, (a) operating conventionally on ramming inlet jet engines; (b) using the jet engines to suck off the boundary layer and applying the data of reference 1 to all surface area to estimate the drag coefficient C_{D_P} [the induced drag was unchanged from case (a)]; (c) the same as case (b) except that the drag data of reference 1 were corrected to full scale by extrapolation along the $10^3 C_Q = 0.2$ line of Fig. 24[2] (full-scale cruising Reynolds Number varied from 60×10^6 to 10^8 depending on speed and altitude).

An additional 15 per cent parasite drag increase over case (a) was added for cases (b) and (c) to account for inefficiencies of boundary-layer control on a complete airplane. Based on reference 1, N.A.C.A. tests, and some of our own test data, the total head into the engines was assumed to be static pressure minus $0.4q$; $0.25q$ corresponds to the peak negative pressure on the wing at cruising and the other $0.15q$ represents ducting losses. It appears that this value is somewhat conservative. For case (a) 100 per cent ram was used. The engines used were late production engines. The study was made possible because the engine data were in a form suitable for calculation of thrust and fuel flow at

TABLE I
Range Comparison

Condition	a	b	c
	100% ram	Per reference 1 Ram = Static $-0.4q$	Per reference 1 extrapolated to full scale Reynolds Number Ram = Static $-0.4q$
Absolute range, miles	5,290	5,500	13,600
Average cruise speed, m.p.h.	541	522	591
Initial speed and altitude	541 at 35,000 ft.	589 at 25,000 ft.	600 at 15,000 ft.
Final cruise altitude, ft.	45,000	35,000	35,000
Power-plant operation	All engines operating	6 engines at start, 4 halfway out, 3 at finish Normal r.p.m. never exceeded	Engines on Suction / Engines on Ram Start 1.7 / 0.11 Halfway 1.6 / .14 Finish 1.5 / .15 Normal r.p.m. never exceeded

negative rams. The engine data made it possible to adjust the tailpipe area to obtain optimum performance. Consequently, except for doubt about the total head at the engine, the power-plant calculations are straightforward, using manufacturers' data, and should be considered as valid as for any ramming system.

In Table I are the results of this study. The same fraction fuel was used in all cases; hence, cases (b) and (c) are optimistic by whatever added structural weight becomes necessary to accommodate slots.

Calculation of performance for this type of operation is tremendously difficult because drag loses its independence of power. In case (a) the altitude was adjusted at all times so that all the engines were operating at good efficiency. In cases (b) and (c) partial engine operation was permitted if better economy resulted. In case (b) no engines operated on ramming air. In case (c) operation was at a specified C_Q of 0.0002 based on wetted area. Based on airflow considerations only, the minimum number of engines required is then determined by the engine airflow at maximum cruising r.p.m. As thus determined, slightly more thrust was needed than could be given by the engines when they consumed this amount of air. The needed extra thrust is indicated by the fractional number of ramming engines. Since so little extra thrust over that given by the suction engines is needed, it is apparent that the aerodynamic and power-plant airflow requirements are nearly equal. Of course, it should not be forgotten that the air requirements for case (c) basically come from porous plate calculations, although the airflow and drag relations check rather well with the Swiss test using discrete slots.

Two means for obtaining the necessary extensive laminar layers appear possible—porous surfaces or single or multiple slots. Examination of Dr. Goldstein's data shows that his values are little different from those assumed in the above study and so it can be considered as a rough guide to the possible overall effects of boundary-layer control with any of the suction systems. From the study the following tentative conclusions can be made:

(1) It may be possible to increase the range of jet aircraft two and one-half to three times the present-day values.

(2) Cruising speeds may be somewhat higher than for the ramming-jet airplane because optimum operation is at lower lift coefficients, and, if there are Mach Number limitations, optimum altitude becomes lower where the velocity of sound is higher.

(3) Because the optimum altitude is lower, fears of combustion difficulties due to abnormally low pressure in the burners seem unfounded.

(4) There is a satisfactory correspondence between boundary-layer control and engine air requirements.

(5) In the aircraft studied, there was sufficient space for the necessary ducting.

(6) Because of the change from ramming to pumping operation, very large drag reductions must be made before a boundary-layer control system begins to be an improvement in overall economy.

As previously mentioned, the above study appears applicable to the British work whether for jet or gas-turbine operation. The single-slot system appears to be the most desirable from a practical point of view. Consequently, since it shows possibilities of such very large range increases, it is hoped that the above information will serve as further encouragement to Dr. Goldstein in his work.

REFERENCES

[1] Pfenninger, Werner, *Investigations on Reductions of Friction on Wings, in Particular by Means of Boundary Layer Suction*, N.A.C.A. T.M. No. 1181, August, 1947.

[2] Ulrich, A., *Theoretical Investigation of Drag Reduction in Maintaining the Laminar Boundary Layer by Suction*, N.A.C.A. T.M. No. 1121, June, 1947.

Warping and Shear Lag in Closed Cylindrical Shells

LEON BESKIN*

Consolidated Vultee Aircraft Corporation

ABSTRACT

The state of stress in thin-walled closed cylindrical shells is determined hereafter in the neighborhood of sections with concentrated loads or of sections corresponding to discontinuities of section properties, such as fixed ends. A method of successive approximations is developed, using the conventional beam formulas as the first approximation. The second approximation, considered as a correction to the first, is determined and examined in some detail in the cases of torsion and bending. This correction may be regarded as a type of stress distribution having the property of producing no section warping to a greater degree of accuracy than the conventional solution. Superposition of the two solutions gives the possibility of writing arbitrary warping conditions at given sections. For instance, at a fully restrained section (built-in cantilever), the nonwarping solution replaces the conventional one, but, along the beam, the nonwarping solution damps out, following an exponential law, and is replaced by the conventional solution. In the case of a section with a concentrated load, it is possible to write that the mean warping due to the conventional distribution is the same on the two sides of the loaded section, thus defining the portions of the loads taken by each distribution on each side. A similar method applies to the case of a change of section properties in shear, if the rigidities in shear change in the same ratio at all points of the section. The validity of the method, in the case of structures stiffened by frames, is limited by the fact that the frame spacing is often of the order of, or even larger than, the characteristic length along which the nonwarping solution damps out, while it is assumed that the frames are infinitely closely spaced. However, the fundamental aspects of the phenomenon remain unchanged, and a more complete analysis could be made along the same lines.

PRINCIPAL NOTATIONS

a_0	= total area of a section
a_1, a_2	= flange areas
da	= elementary area ($= h\,ds$)
A, A'	= polar areas from twist centers
A_0	= total area inside section contour
B	= bimoment
b, c	= dimensions of a rectangular section
C_x, C_y, C_{xy}	= constants [Eq. (67)]
E, G	= moduli of elasticity and rigidity
h	= thickness resisting axial loads
I_x, I_y	= principal moments of inertia of a section
I_0	= torsion bending constant
J	= coefficient of rigidity in twist
J_1	= secondary coefficient of rigidity in twist [Eq. (54)]
K	= constant [Eq. (47)]
K_{z1}, ...	= constants [Eqs. (69)]
L, L_1, L_2	= characteristic perturbation lengths [Eqs. (50) and (70)]
$\bar{M}$	= applied torque (about twist center)
M	= torque distributed according to conventional formulas
ΔM	= complementary torque ($= \bar{M} - M$), perturbation
$\bar{M}_x$, $\bar{M}_y$, $\bar{M}_z$	= components of the applied moment (bending moments and torque)
M_x, M_y, M_z	= components of the applied moment distributed according to conventional formulas
ΔM_x, ΔM_y	= perturbations to the bending moments
p	= normal stress flow ($= h\sigma$)
P	= constant [Eq. (32)]
q	= shear flow ($= t\tau$)
Q_x, Q_y	= static moments ($= \int x\,da$ and $\int y\,da$)
r	= distance between the tangent to a contour and the center of twist
s	= arc along the section contour
t, t_1, t_2	= thicknesses resisting to shears
u, $\bar{u}$	= functions defining secondary stress distributions [Eqs. (28) and (38)]
u_0	= constant [Eqs. (39) and (45)]
w, Δw	= warping and secondary warping
$\Delta\bar{w}_0$, $\Delta\bar{w}$	= unit secondary warpings [Eqs. (38)]
x, y	= principal coordinates of a section
x_0, y_0	= principal coordinates of a specific point
x_T, y_T	= principal coordinates of the twist center
x_T', y_T'	= principal coordinates of the secondary twist center
$\bar{X}$, $\bar{Y}$	= applied shearing forces
X, Y	= shearing forces distributed according to conventional formulas
ΔX, ΔY	= complementary shearing forces (perturbations)
α	= polar areas from centroid
$\Delta\alpha$, $\Delta\alpha'$	= additional constants to polar areas
γ	= shear strain
$d\epsilon$	= ds/t
ϵ, ϵ_0	= function [Eq. (24)], and additional constant [Eq. (18)]
θ	= angle of twist
λ_1, λ_2	= constants [Eqs. (69)]
μ	= constant [Eq. (78)]
ξ_x, ξ_y	= functions [Eqs. (24)]
σ	= normal stress
τ	= shear stress

Received October 1, 1947.

* Design Specialist. Now with Design and Research Division, Bureau of Aeronautics, Navy Department, Washington, D.C.

FUNDAMENTAL ASSUMPTIONS AND METHODS

THE CONVENTIONAL BEAM THEORY is valid under restrictive assumptions, which, essentially, are the following:

(1) The structure is a prism or a cylinder with constant section properties.

(2) The sections are free to deform in their planes.

(3) The sections are free to warp out of their planes.

(4) The loads are applied only at the two ends of the structure or are uniformly distributed over the length (surface and volume forces).

(5) Applied loads are distributed in a section according to definite formulas, which result from the assumptions of the beam theory.

Under these conditions, the beam theory can be applied to closed cylindrical shells—i.e., structures that have sufficient local stiffness to be stable under the applied loads as opposed to membranes that have no determined shape and can coincide with all the surfaces which are applicable on one another. The stabilizing structures required in the case of membranes prevent condition (2) to be fulfilled and, to some degree, condition (3).

However, the limit case of membranes with closely spaced rigid frames does not differ essentially from the case of shells if the following simplifications are introduced:

(1) The influence of lateral contraction (Poisson's ratio) is disregarded, since this contraction is locally prevented by frames.

(2) The material constituting the shell is considered as concentrated along its mean surface.

(3) All plane sections are considered as indeformable in their planes.

Two methods of analysis can be developed from these assumptions; both have been presented by the author in a condensed form:[1]

(1) Representation of the stresses by trigonometric series or trigonometric integrals of the coordinate z, parallel to the generators of the beam. This method has also been developed by von Kármán[2] in a somewhat different manner. The author wishes to acknowledge that a previous work of von Kármán on shear lag theory[5] is at the origin of his research work in this field.[4]

(2) Representation of the stresses by successive approximations, using the conventional beam theory as the first approximation. This second method is the object of this paper.

Section I—Theory

(1) *General Equations*

When the cross sections of a cylindrical membrane are rigid in their planes but can warp out of plane, a deformed state of the membrane is defined by two quantities: the angle of rotation θ between a section defined by its coordinate z along the generators of the cylinders, and the section $z = 0$, and the warping (displacement) w along the generators, function of z and of the coordinate s along a directrix (cross section) of the membrane. The center C of the infinitesimal rotation $d\theta$ between two sections may have a constant location or may be variable. It is defined by its coordinates (x_0, y_0) with respect to the principal axes (x, y) in each section.

The shearing strain being designated by γ, the following well-known relation exists between w, γ, and θ,

$$\partial w/\partial s = \gamma - 2(d\theta/dz)(dA/ds) \tag{1}$$

where $2dA/ds = r$ is the distance from the center of rotation C to the tangent to the directrix of the section (Fig. 1), while A is the corresponding polar area, taken with an arbitrary origin radius. The shearing strain is a function of the shear flow q,

$$\gamma = q/Gt \tag{2}$$

where t is the effective thickness of the membrane resisting to shear and G is the modulus of rigidity.

The warping is a function of the normal stress flow p along the generators,

$$\partial w/\partial z = \sigma/E = p/Eh \tag{3}$$

where σ is the normal stress along the generators and h is the effective thickness of the membrane resisting to normal stress. Thicknesses h and t are often unequal because longitudinal members (stringers) are included only in h and because buckling may affect differently the rigidities under axial loads and under shear.

Eliminating γ and w between Eqs. (1) to (3), it is found

$$\frac{1}{E}\frac{\partial}{\partial s}\left(\frac{p}{h}\right) = \frac{1}{G}\frac{\partial}{\partial z}\left(\frac{q}{t}\right) - 2\frac{dA}{ds}\frac{d^2\theta}{dz^2} \tag{4}$$

while p and q are related by the equation of equilibrium

$$(\partial p/\partial z) + (\partial q/\partial s) = 0 \tag{5}$$

Relations (4) and (5) constitute a system of differential equations in two unknowns, and their solution, with given conditions at the edges, gives the general effect of the interaction between shear and warping.

It should be noted that Eq. (4) is incomplete, since the term representing the displacement of the center of rotation is missing in its right-hand member; this term is

$$-E\frac{d\theta}{dz}\frac{dr}{dz} = -E\frac{d\theta}{dz}\frac{ds_1}{dz}\cos\beta \tag{6}$$

where s_1 is the projected arc defining the motion of C and β is the angle between s_1 and r (Fig. 1). This term is omitted because solutions considered hereafter correspond to a fixed axis of rotation or are obtained by superposition of such solutions.

The conventional beam theory corresponds to the case when the shear flow is independent of z, so that Eq. (4) is simplified, and, after integration, it is found

$$\sigma = \frac{p}{h} = -2AE\frac{d^2\theta}{dz^2} = 2A\frac{B}{I_0} \tag{7}$$

with a proper choice of the origin radius of the areas A.

Since q is independent of z, Eq. (5) shows that the normal stress σ is a linear function of z, and Eq. (7) shows the normal stress in a section is proportional to

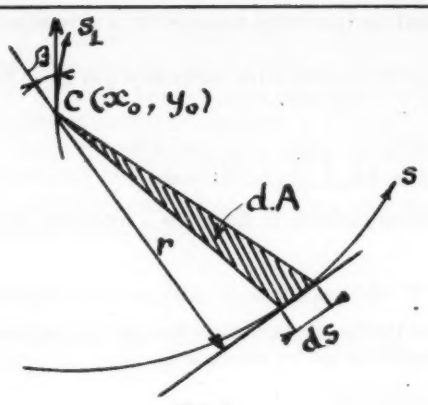

FIG. 1.

the area A. This is the general case of torsion-bending of open sections, where B is the bimoment about the pole and I_0 is the torsion-bending constant.[3] In the case of conventional bending, the center of rotation is at infinity.

The beam theory gives a first approximation of the solution of the system of differential Eqs. (4) and (5). In a second approximation, the value of q calculated from Eq. (5) is introduced into Eq. (4), giving, for p and θ, corrections Δp and $\Delta\theta$ related by

$$\frac{\partial \Delta\sigma}{\partial s} = \frac{\partial}{\partial s}\left(\frac{\Delta p}{h}\right) = \frac{E}{Gt}\frac{\partial q}{\partial z} - 2E\frac{dA}{ds}\frac{d^2\Delta\theta}{dz^2} \tag{8}$$

Eq. (5) then defines a correction Δq,

$$(\partial \Delta p/\partial z) + (\partial \Delta q/\partial s) = 0 \tag{9}$$

The process can be repeated with the system of equations

$$\left.\begin{aligned} \frac{\partial}{s}\left(\frac{\Delta^n p}{h}\right) &= \frac{E}{Gt}\frac{\partial \Delta^{n-1} q}{\partial z} - 2E\frac{dA_n}{ds}\frac{d^2\Delta^n\theta}{dz^2} \\ (\partial \Delta^n q/\partial s) + (\partial \Delta^n p/\partial z) &= 0 \end{aligned}\right\} \tag{10}$$

This method is examined here in the case of one term, and appears as a first order correction to the conventional beam theory. It is generally sufficient for practical problems, at least with the physical assumptions made here (see "Introduction"). Correct methods, using trigonometric series or integrals may be warranted if more accurate physical assumptions are made. This has been done by the writer for the problem of shear lag in I-beams,[4] developing a method first presented by von Kármán.[5]

In Section II, a comparison between the correct and the approximate method shows that in many cases, the approximate method gives results that are extremely close to those of the correct method.

(2) *General Relations for Closed Beams*

The conventional beam formulas, with conventional notations (see also "Notations"), are

$$\sigma = -(M_y/I_y)x + (M_x/I_x)y \tag{11}$$

$$q = -\frac{X}{I_y}Q_x - \frac{Y}{I_x}Q_y + \frac{M_z}{2A_0} \tag{12}$$

with

$$X - (dM_y/dz) = 0, \qquad Y + (dM_x/dz) = 0 \tag{13}$$

A_0 is the area inside the contour of the beam section; the torque M_z is taken about a stress center defined by its coordinates about the principal axes

$$\left.\begin{aligned} X_T &= -(1/I_x)\oint 2Q_y\, d\alpha \\ Y_T &= (1/I_y)\oint 2Q_x\, d\alpha \end{aligned}\right\} \tag{14}$$

the polar areas α being measured from the centroid.

It is known that if the static moments satisfy the conditions

$$\oint Q_x(ds/t) = 0, \qquad \oint Q_y(ds/t) = 0 \tag{15}$$

Eqs. (14) define the coordinates of the conventional twist center, sometimes called shear center. With this choice of the reference point for torques M_z, the expression of the angle of twist, given by the general expression

$$d\theta/dz = (1/2A_0)\oint (q\, ds/Gt) \tag{16}$$

becomes

$$d\theta/dz = M/GJ \tag{17}$$

with

$$J = \frac{4A_0^2}{\epsilon_0}, \qquad \epsilon_0 = \oint (ds/t) \tag{18}$$

Expressions (14) of the coordinates of the twist center are generally derived by applying a dummy torque to a section loaded by given transversal forces that can have an arbitrary line of support. The condition of zero rotation of the dummy torque defines the twist center as the point through which must pass all the lines of support. This method is, however, incomplete, since it does not show the necessity of the existence of a fixed end to define a twist center; if there is no fixed end, any lateral displacement can be superimposed to the twist, which displaces the center of twist. Hereafter, the end restraint is explicitly introduced, and the resulting secondary stresses are determined. Then the moments and shearing forces that appear in Eqs. (11) and (12) must be considered as the portions of the total moments and shearing forces that are transmitted by conventional beam distributions, so that it can be written

$$\left.\begin{aligned} \bar{M}_x = M_x + \Delta M_x, \qquad \bar{M}_y = M_y + \Delta M_y, \qquad \bar{M}_z = M_z + \Delta M_z \\ \bar{X} = X + \Delta X, \qquad \bar{Y} = Y + \Delta Y \end{aligned}\right\} \tag{19}$$

where the quantities with a bar represent the total applied loads and the quantities preceded by a Δ represent the portions of the loads transmitted as perturbations.

The secondary normal stress $\Delta\sigma$ is defined by integration of Eq. (8), in which the shear flow q is given by Eq. (12),

$$\Delta\sigma = \frac{E}{G}\left(-\frac{dX}{dz}\frac{1}{I_y}\int\frac{Q_x\,ds}{t} - \frac{dY}{dz}\frac{1}{I_x}\int\frac{Q_y\,ds}{t} + \frac{dM_z}{dz}\frac{1}{2A_0}\int\frac{ds}{t} - 2A_0G\frac{d^2\Delta\theta}{dz^2}\right) \tag{20}$$

where the areas A are measured from the twist center (x_T, y_T) and are related to the areas α measured from the centroid by

$$2A = 2\alpha + y_T x - y x_T + 2\Delta\alpha \tag{21}$$

The stress $\Delta\sigma$ must be a univalued function of the arc s, a condition that is satisfied by the first and second terms of the parentheses in Eq. (20), since Eqs. (16) are satisfied. Defining $d^2\Delta\theta/dz^2$ by the condition

$$2A_0G(d^2\Delta\theta/dz^2) = (\epsilon_0/2A_0)(dM_z/dz) \tag{22}$$

the stress $\Delta\sigma$ becomes entirely a univalued function of s and can be written in the form

$$\Delta\sigma = \frac{E}{G}\left[\frac{dM_z}{dz}\frac{\epsilon_0}{2A_0}\left(\frac{\epsilon}{\epsilon_0} - \frac{A}{A_0}\right) - \frac{dX}{dz}\frac{\xi_x}{I_y} - \frac{dy}{dz}\frac{\xi_y}{I_x}\right] \tag{23}$$

where

$$\left.\begin{aligned}\epsilon &= \int_{s_0}^{s}(ds/t) = \int_{s_0}^{s} d\epsilon, \qquad \xi_x = \int_{s_x}^{s} Q_x\,d\epsilon\\ \xi_y &= \int_{s_y}^{s} Q_y\,d\epsilon\end{aligned}\right\} \tag{24}$$

The unknown constants s_0, s_x, and s_y are defined by the condition that the secondary stresses must have no resultant force, which yields three conditions

$$\left.\begin{aligned}&\oint[(\epsilon/\epsilon_0) - (A/A_0)]h\,ds = 0\\ &\oint\xi_x h\,ds = 0, \qquad \oint\xi_y h\,ds = 0\end{aligned}\right\} \tag{25}$$

These conditions can be written in the form

$$\left.\begin{aligned}&(\epsilon_0/A_0)\oint A\,da = (\epsilon_0/A_0)(a_0\Delta\alpha + \oint\alpha\,da) = \oint da\int_{s_0}^{s} d\epsilon\\ &a_0\int_0^{s_x} Q_x d\epsilon = \oint da\int_0^{s} Q_x\,d\epsilon, \qquad a_0\int^{s_y} Q_y\,d\epsilon = \oint da\int_0^{s} Q_y\,d\epsilon\end{aligned}\right\} \tag{26}$$

where the total area resisting to normal stresses is a_0,

$$a_0 = \oint da, \text{ with } da = h\,ds \tag{27}$$

It can be verified that the normal stresses due to the torque term dM_z/dz have no resulting bending couple, which corresponds to the conditions

$$\oint x\,du = 0, \qquad \oint y\,du = 0, \qquad \text{with } du = [(\epsilon/\epsilon_0) - (A/A_0)]da \tag{28}$$

which can also be written

$$\left.\begin{aligned}x_T &= -(2A_0/I_x)\oint[(\epsilon/\epsilon_0) - (\alpha/A_0)]y\,da\\ y_T &= (2A_0/I_y)\oint[(\epsilon/\epsilon_0) - (\alpha/A_0)]x\,da\end{aligned}\right\} \tag{29}$$

These equations define the twist center, since they can be identified with Eqs. (14). For instance, it can be shown that

$$\oint Q_y\,d\alpha = (A_0/\epsilon_0)\oint\epsilon y\,da - \oint\alpha y\,da$$

if the second condition (15) is satisfied. Since $dQ_y = y\,da$, the relation above can be transformed, introducing condition (15) and integrating by parts,

$$\oint d(Q_y\alpha) = \frac{A_0}{\epsilon_0}\oint\epsilon\,dQ_y = \frac{A_0}{\epsilon_0}\oint d(\epsilon Q_y)$$

which gives the identity

$$Q_y A_0 = (A_0/\epsilon_0)\epsilon_0 Q_y$$

Thus, the two definitions of the twist center are equivalent. The amount of numerical computations required by the two formulas is approximately the same. Eqs. (29) define the twist center by the property that it is the point around which the torsion occurs under the action of a pure torque, without introducing bending stresses; in these equations, the origin for which ϵ and α are simultaneously equal to zero can be arbitrarily chosen on the contour of the shell. The definition (14) of the twist center corresponds to the property that, if a transversal load is applied at that

point, it produces no twist. By application of the principle of reciprocity (Betti-Maxwell), the two definitions are shown to be equivalent, which proves directly the identity of Eqs. (14) and (29).

The use of the twist center as origin for torques M_z due to shearing forces, makes twisting and bending deformations independent of one another, and they can be examined separately.

(3) *Secondary Stresses Under Pure Torque*

(*a*) *Solution of the General Equations.*—Eq. (23) is reduced to [see Eq. (28)]

$$\sigma = \Delta\sigma = \frac{E}{G}\frac{dM}{dz}\frac{\epsilon_0}{2A_0}\frac{du}{da} \tag{30}$$

where the pure torque is represented by M instead of M_z.

On this equation appears the great difference between axial stresses due to torque in open and closed membranes. For open membranes, Eq. (7) shows that these stresses are proportional to the integral of the torque (bimoment); for closed membranes, axial stresses are proportional to the derivative of the torque and, very often, they can be disregarded or considered as secondary stresses.

Stresses σ are equal to zero if there exists a pole, origin of areas, such that $dA/d\epsilon = rt = \text{const.}$ The constant is equal to A_0/ϵ_0 so that r is defined by

$$r = A_0/t\epsilon_0 \tag{31}$$

It is easy to verify for a given section if lines parallel to the tangents to the contour drawn at distances r, Eq. (31), from these tangents pass by a common point. If such point exists, there is no warping under torque. This is the case for a circular cylinder of constant thickness, for a regular polygonal prism of constant thickness, and for a rectangular prism in which the thickness of each side is proportional to its width. In these cases, the center of twist coincides with the geometric center, a property that is hidden when Eqs. (14) are used. In addition, the following property of the twist center results from Eqs. (28): In structures that do not warp under torque ($du/da = 0$), the twist center is independent of the flange material (areas da), since Eqs. (28) are identically satisfied; in structures that warp under torque, the twist center location depends on the distribution of the flange material.

The quantity du/da [Eq. (28)] represents the warping distribution; both ϵ and A contain arbitrary constants but from the first Eq. (26) it results that du/da is entirely defined. Since the normal stress is equal to zero for at least four points of a convex section, one of these neutral points may be used as a common origin for A and ϵ.

The secondary shear flow is obtained by introducing expression (30) for σ in Eq. (9), defining

$$\Delta q = Pu, \qquad \text{with } P = -\frac{E}{G}\frac{d^2M}{dz^2}\frac{\epsilon_0}{2A_0} \tag{32}$$

In this expression, u contains an arbitrary constant of integration, which will be defined by the condition that the secondary warping due to the shear flow be minimum. To write this condition, the quadratic mean is used. The warping should be equal to zero, but this condition is not generally satisfied, except for nonwarping sections for which no correction is required. The secondary warping Δw is determined by an equation similar to Eq. (1), and it can be written

$$\Delta w = (1/G)\int \Delta q\, d\epsilon - 2A'(d\Delta^2\theta/dz) \tag{33}$$

with

$$2A' = 2\alpha_0' - y_T'x - yx_T' \tag{34}$$

The quantity $d\Delta^2\theta/dz$ is determined by the condition that Δw is univalued,

$$\frac{d\Delta^2\theta}{dz} = \frac{\oint \Delta q\, d\epsilon}{2A_0G} = \frac{P}{G}\frac{1}{2A_0}\oint u\, d\epsilon \tag{35}$$

so that

$$\Delta w = (P/G)\left[\int u\, d\epsilon - (A'/A_0)\oint u\, d\epsilon\right] \tag{36}$$

The secondary center of twist (x_T', y_T'), pole of the areas A', and the constant α_0' are determined by the condition that the normal stresses due to secondary warping have zero resultant and zero resulting couple. These stresses being proportional to the derivative of the warping, the corresponding conditions can be written as:

$$\oint \Delta w\, da = 0, \qquad \oint \Delta w\, x\, da = 0, \qquad \oint \Delta w\, y\, da = 0 \tag{37}$$

Special solutions $\bar{u}$ and $\Delta\bar{w}$ are first defined for u and Δw, which satisfy the relations

$$\oint \bar{u}\, d\epsilon = 0, \qquad \Delta\bar{w}_0 = \int \bar{u}\, d\epsilon, \qquad \oint \Delta\bar{w}_0\, da = 0 \tag{38}$$

and the expressions for u and Δw become

$$\left.\begin{aligned} u &= \bar{u} + u_0 \\ \Delta w &= \frac{P}{G}\Delta\bar{w} = \frac{P}{G}\left(\Delta\bar{w}_0 + \epsilon_0 u_0 \frac{du}{da}\right) \end{aligned}\right\} \tag{39}$$

where u_0 is the constant defined by the condition of minimum secondary warping, equivalent to a condition of minimum strain energy due to secondary normal stresses, since these stresses in any given section are proportional to the warping in that section. Thus, the condition can be written

$$\delta\left(\oint \Delta\bar{w}^2\, da\right) = 0 \tag{40}$$

Substituting the value of Δw given by Eq. (39) in Eqs. (37) and noting that the first of these equations is equivalent to the first Eq. (25), because of the last

condition (38), it appears that

$$\alpha_0' = \alpha_0 \tag{41}$$

The coordinates of the secondary twist center differ from those of the principal twist center, and, by comparison with Eqs. (29), it is found

$$\left.\begin{aligned} x_T' &= x_T - \frac{2A_0}{\epsilon_0 u_0 I_x} \oint \Delta\bar{w}_0 y \, da \\ y_T' &= y_T + \frac{2A_0}{\epsilon_0 u_0 I_y} \oint \Delta\bar{w}_0 x \, da \end{aligned}\right\} \tag{42}$$

The developed expression of Δw is thus

$$\Delta\bar{w} = \Delta\bar{w}_0 + \epsilon_0 u_0 (du/da) - (x/I_y) \oint \Delta\bar{w}_0 x \, da - (y/I_x) \oint \Delta\bar{w}_0 y \, da \tag{43}$$

and can be introduced into Eq. (40), thus defining a quadratic function of u_0, the minimum of which corresponds to

$$u_0 = -\frac{\oint [\Delta\bar{w}_0 - (x/I_y) \oint \Delta\bar{w}_0 x \, da - (y/I_x) \oint \Delta\bar{w}_0 y \, da](du/da)da}{\epsilon_0 \oint (du/da)^2 da} \tag{44}$$

Eqs. (28) show that, after integration, the last two terms in the brackets are equal to zero; the first term, after introducing the definition (38) of $\Delta\bar{w}$ and integrating by parts, yields the final expression for u_0

$$u_0 = \frac{\oint \bar{u}^2 \, d\epsilon}{\epsilon_0 \oint (du/da)^2 \, da} \tag{45}$$

The secondary torque ΔM, corresponding to the secondary shear flow Δq, is, from Eq. (32),

$$\Delta M = 2 \oint \Delta q \, d\alpha = -\frac{E}{G} \frac{d^2M}{dz^2} \frac{\epsilon_0}{A_0} \oint u \, dA$$

expression which can be written in the form

$$\Delta M = -(E/G)(d^2M/dz^2)K \tag{46}$$

with

$$K = \frac{\epsilon_0}{A_0} \oint u \, dA = \epsilon_0 u_0 + \frac{\epsilon_0}{A_0} \oint \bar{u} \, dA$$

The second term can be rewritten as

$$-\epsilon_0 \oint \bar{u} \left(\frac{d\epsilon}{\epsilon_0} - \frac{dA}{A_0}\right) = -\epsilon_0 \oint \bar{u} \, d\left(\frac{du}{da}\right) = \epsilon_0 \oint \left(\frac{du}{da}\right)^2 da$$

because the contribution of $\oint u \, d\epsilon$ is zero [Eq. (38)] and because the integration by parts which leads to the last expression is also giving a zero term, since $\bar{u}$ is a univalued function. Thus, replacing u_0 by its value (45), the constant K has the final form

$$K = \epsilon_0 \oint \left(\frac{du}{da}\right)^2 da + \frac{\oint \bar{u}^2 \, d\epsilon}{\oint (du/da)^2 da} \tag{47}$$

(*b*) *Determination of Stress Distributions.*—From Eqs. (19) and (46), it results that the total torque $\bar{M}$ is

$$\bar{M} = M + \Delta M = M - (E/G)K(d^2M/dz^2) \tag{48}$$

When $\bar{M} = M$—the conventional solution—the warping is total. When $\bar{M} = \Delta M$, there is no warping, to the accuracy of the present solution. If $\bar{M}$ is constant, the solution of Eq. (48)—the origin of the axis z being at the fixed end of a cantilever—is

$$M = \bar{M}(1 - e^{-z/L}), \qquad \Delta M = Me^{-z/L} \tag{49}$$

where

$$L = \sqrt{EK/G} \tag{50}$$

At the fixed end, the normal stresses and shear flows are

$$\sigma_0 = (E/G)(\bar{M}/L)(\epsilon_0/2A_0)(du/da) \tag{51}$$

$$q_0 = \Delta q_0 = \frac{\bar{M}\epsilon_0 u}{2A_0 K} = \frac{\bar{M}u}{\oint 2u \, dA} \tag{52}$$

Under shear flows Δq that produce no warping, there is a twist $\Delta\theta$, and the rate of twist, defined by Eq. (35), is

$$d\Delta^2\theta/dz = \Delta M/GJ_1 \tag{53}$$

with

$$J_1 = 4A_0 \oint \Delta q \, dA / \oint \Delta q \, d\epsilon = JK/\epsilon_0 u_0 \tag{54}$$

or

$$J_1/J = 1 + \{\epsilon_0 [\oint (du/da)^2 \, da]^2 / \oint u^2 \, d\epsilon\} \tag{55}$$

The shear flow at any section is

$$q = q + \Delta q = \frac{M}{2A_0} + \frac{\Delta M \epsilon_0 u}{2A_0 K} \tag{56}$$

and the total rate of twist at any section is

$$\frac{d\theta}{dz} = \frac{M}{GJ} + \frac{\Delta M}{GJ_1} = \frac{\bar{M}}{GJ} - \frac{\Delta M}{G}\left(\frac{1}{J} - \frac{1}{J_1}\right) \tag{57}$$

Because of the effect of end fixity, the total angle of twist is decreased by

$$\theta_0 = \int_0^\infty \frac{\Delta M}{G}\left(\frac{1}{J} - \frac{1}{J_1}\right) dz = \frac{\bar{M}L}{GJ} \frac{\epsilon_0 [\oint (du/da)^2 \, da]^2}{\oint \bar{u}^2 \, d\epsilon} \tag{58}$$

If $\bar{M}$ is variable (concentrated or distributed applied torques), Eq. (48) defines the distribution of M in its two components M and ΔM. On the two sides of a

section where a concentrated torque is applied, the distribution is represented on Fig. 2.

(c) *Strain Energy.*—Methods of strain energy can be applied to problems in which secondary stresses due to torque are considered. The strain energy due to normal stresses is, per unit length of beam,

$$W_n = \oint \frac{\sigma^2\, da}{2E} = \frac{E}{2G^2}\left(\frac{dM}{dz}\right)^2 \frac{\epsilon_0^2}{4A_0^2} \oint \left(\frac{du}{da}\right)^2 da$$

or

$$W_n = (1/2)(EC/J^2G^2)(dM/dz)^2 \tag{59}$$

with

$$C = 4A_c^2 \oint (du/da)^2\, da \tag{60}$$

The strain energy due to shear is, per unit length of beam,

$$W_s = (1/2)\oint (q + \Delta q)^2 d\epsilon/G$$

or

$$W_s = (1/2GJ)[M^2 + (\epsilon_0 u_0/K)(\bar{M}^2 - M^2)] \tag{61}$$

(4) *Secondary Stresses Under Pure Shearing Forces*

Eq. (23) is reduced to

$$\Delta\sigma = -\frac{E}{G}\left(\frac{dX}{dz}\frac{\xi_x}{I_y} + \frac{dY}{dz}\frac{\xi_y}{I_x}\right) \tag{62}$$

and the secondary shear flow Δq is

$$\Delta q = \frac{E}{G}\left(\frac{d^2X}{dz^2}\frac{1}{I_y}\int \xi_x\, da + \frac{d^2Y}{dz^2}\frac{1}{I_x}\int \xi_y\, da\right) \tag{63}$$

From Eqs. (26), it results that Δq is univalued. The origins of the integrals in Eq. (63) are defined by the condition that the resulting moment with respect to the twist center (x_T, y_T) is zero,

$$\oint dA \int \xi_x\, da = 0, \qquad \oint dA \int \xi_y\, da = 0 \tag{64}$$

The stresses $\Delta\sigma$ defined by Eq. (62) generally have a resulting moment to which corresponds a shearing force defined by its components

$$\Delta X = -\frac{d}{dz}\oint \Delta\sigma x\, da, \qquad \Delta Y = \frac{d}{dz}\oint \Delta\sigma y\, da \tag{65}$$

Using expression (62) for $\Delta\sigma$ and integrating by parts, it is found

$$\left.\begin{aligned} \Delta X &= -\frac{E}{G}\left(\frac{C_x}{I_y}\frac{d^2X}{dz^2} + \frac{C_{xy}}{I_x}\frac{d^2Y}{dz^2}\right) \\ \Delta y &= -\frac{E}{G}\left(\frac{C_{xy}}{I_y}\frac{d^2X}{dz^2} + \frac{C_y}{I_x}\frac{d^2Y}{dz^2}\right) \end{aligned}\right\} \tag{66}$$

with the notations

$$\left.\begin{aligned} C_x &= \oint Q_x^2\, d\epsilon, \qquad C_y = \oint Q_y^2\, d\epsilon \\ C_{xy} &= \oint Q_x Q_y\, d\epsilon \end{aligned}\right\} \tag{67}$$

Using expressions (19) for ΔX and ΔY, a system of simultaneous differential equations in two unknowns

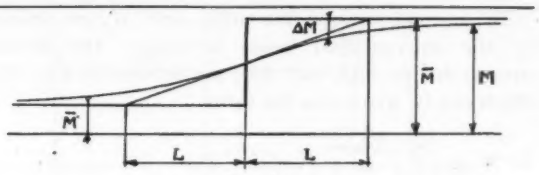

FIG. 2.

X and Y is found

$$\left.\begin{aligned} \bar{X}\frac{G}{E} &= X\frac{G}{E} - \frac{C_x}{I_y}\frac{d^2X}{dz^2} - \frac{C_{xy}}{I_x}\frac{d^2Y}{dz^2} \\ \bar{Y}\frac{G}{E} &= Y\frac{G}{E} - \frac{C_{xy}}{I_y}\frac{d^2X}{dz^2} - \frac{C_y}{I_x}\frac{d^2Y}{dz^2} \end{aligned}\right\} \tag{68}$$

the solution of which gives the second approximation for the stress distribution in closed membranes near a section where the loads or the section properties are discontinuous.

The solutions of Eqs. (68) are of the type

$$\left.\begin{aligned} X &= \bar{X} - (\lambda_1 K_{x1} e^{-z/L_1} + \lambda_2 K_{x2} e^{-z/L_2}) \\ Y &= \bar{Y} - (\lambda_1 K_{y1} e^{-z/L_1} + \lambda_2 K_{y2} e^{-z/L_2}) \end{aligned}\right\} \tag{69}$$

in which the constants L_1 and L_2 are defined by the equation

$$[C_y - L^2(G/E)I_x][C_x - L^2(G/E)I_y] - C_{xy}^2 = 0 \tag{70}$$

The constants K can be chosen as follows:

$$\left.\begin{aligned} K_{x1} &= L_1^2(G/E) - (C_y/I_y) \\ K_{y2} &= L_2^2(G/E) - (C_x/I_x) \\ K_{y1}I_y &= K_{y2}I_x = C_{xy} \end{aligned}\right\} \tag{71}$$

and constants λ_1 and λ_2 are defined by end conditions. For instance, if the warping is equal to zero (fully restrained end), both X and Y must be equal to zero at that end. Then

$$\left.\begin{aligned} \bar{X} &= \lambda_1 K_{x1} + \lambda_2 K_{x2} \\ \bar{Y} &= \lambda_1 K_{y1} + \lambda_1 K_{y2} \end{aligned}\right\} \tag{72}$$

Constants λ_1 and λ_2 being determined, the stress distribution is defined similarly as for torsion: The bending moments are divided into two components, one corresponding to the conventional solution and the other to the corrective terms:

Conventional distribution,

$$\left.\begin{aligned} M_x &= \bar{M}_x - \sum_{i=1}^{2} \lambda_i L_i K_{yi} e^{-z/L_i} \\ M_y &= \bar{M}_y + \sum_{i=1}^{2} \lambda_i L_i K_{xi} e^{-z/L_i} \end{aligned}\right\} \tag{73}$$

Perturbation terms,

$$\left.\begin{aligned} \Delta M_x &= \sum_{i=1}^{2} \lambda_i L_i K_{yi} e^{-z/L_i} \\ \Delta M_y &= -\sum_{i=1}^{2} \lambda_i L_i K_{xi} e^{-z/L_i} \end{aligned}\right\} \tag{74}$$

The normal stresses due to M_x and M_y are defined by the conventional beam formulas; the normal stresses due to ΔM_x and ΔM_y are defined by Eq. (62), which can be written in the form

$$\Delta\sigma = -\frac{E}{G}\left[\frac{\xi_x}{I_y}\sum_{i=}^{3}\frac{\lambda_i}{L_i}K_{xi}e^{-z/L_i} + \frac{\xi_y}{I_x}\sum_{i=1}^{2}\frac{\lambda_i}{L_i}K_{yi}e^{-z/L}\right] \quad (75)$$

Section II—Examples

(1) *Symmetrical Rectangular Section*

The section is defined by its dimensions b and c, the reduced thickness of the webs under shear, t, the reduced thickness h of the webs and stiffeners under normal stresses, and the corner flanges areas a_1. The problem of a tube with a restrained end section under the action of a torque applied at the other end is investigated (Fig. 3). It is assumed that the distance between ends is large as compared with the characteristic length L, so that only decreasing exponentials should be considered.

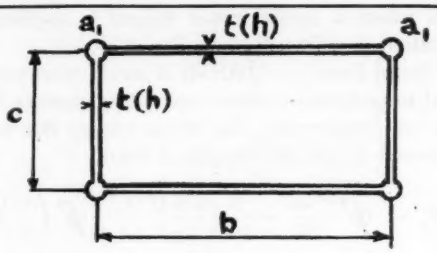

Fig. 3.

The secondary normal stresses at the flanges at the fixed end, calculated by trigonometric integrals,[1] are defined by

$$\frac{\sigma}{\tau} = \frac{4(\beta-\gamma)}{\pi}\sqrt{\frac{Et}{Gh}}\int_0^\infty \frac{d\omega}{\omega(\mu\omega + \coth\beta\omega + \coth\gamma\omega) + 4 - (1/\beta\gamma)} \quad (76)$$

in which the shear stress τ is the conventional stress for a tube under torque,

$$\tau = \bar{M}/2bct \quad (77)$$

and in which the other notations are

$$\beta = b/(b+c), \qquad \gamma = c/(b+c), \qquad \mu = 2a_1/h(b+c) \quad (78)$$

while ω is a variable of integration.

The solution given by Eq. (76) is considered as an "exact" solution, since it satisfies the physical assumptions. The approximate solution developed in this paper can be compared to it, in order to find the order of magnitude of the errors resulting from the consideration of a first order correction.

The constants and functions that appear in the approximate solution have the following values, with the origin of s being in the middle of each face:

$$\epsilon = s/t, \qquad \epsilon_0 = 2(b-c)/t, \qquad A_0 = bc$$

Expression	In Face b	In Face c
dA/ds	$c/4$	$b/4$
du/da	$\dfrac{s(b-c)}{4b(b+c)}$	$-\dfrac{s(b-c)}{4c(b+c)}$
$\dfrac{8\bar{u}(b+c)}{b-c}$	$\dfrac{s^2h}{b} - \dfrac{(b+2c)h}{12} - \dfrac{a_1c}{b+c}$	$-\dfrac{s^2h}{c} + \dfrac{(c+2b)h}{12} + \dfrac{a_1b}{b+c}$

(79)

$$\epsilon_0 \oint (du/da)^2 da = [(b-c)/48t(b+c)][6a_1 + h(b+c)]$$

$$\oint \bar{u}^2 d\epsilon = \frac{1}{32t}\left(\frac{b-c}{b+c}\right)^2\left[a_1bc\left(\frac{a_1}{b+c}+\frac{h}{3}\right) + \frac{h^2(b+c)}{180}(b^2+c^2+4bc)\right]$$

$$K = \frac{b+c}{48t}[6a_1 + h(b+c)] + \frac{h^2}{60t}\frac{b^3+c^3}{6a_1 + h(b+c)}$$

The maximum secondary normal stress at the flanges of the fixed end is defined by

$$\sigma/\tau = \sqrt{E/KG}[(b-c)/4] \quad (80)$$

in which the shear stress τ is given by Eq. (77). Table 1 gives some values of the secondary stresses, calculated by the "exact" Eq. (76) and the approximate Eq. (80), in the case where $h = t$.

TABLE 1
Secondary Stresses in a Rectangular Tube Under Torque, Restrained at One End

$\mu = 2a_1/(b+c)h$	b/c	σ/τ (exact)	σ/τ (approx.)	$L/(b+c)$
1	2	0.49	0.475	0.46
1	4	0.83	0.835	0.47
1/4	2	0.87	0.685	0.32

Comparing the exact and the approximate values, it appears that the error is small when the flange area is relatively important and becomes appreciable for small flange areas. The values with zero flange area obtained by the approximate method are meaningless because the theoretical value is infinite.

When $h = 0$—i.e., when the webs do not transmit normal stresses—the approximate and the exact methods give the same result,

$$\sigma/\tau = (b - c)\sqrt{Et/2G(b + c)a_1} \tag{81}$$

and the length L is given by the relation

$$\frac{L}{b+c} = \sqrt{\frac{Eh}{Gt}\left\{\frac{1+3\mu}{48} + \left[\frac{b^3+c^3}{(b+c)^3}\left(\frac{1}{1+3\mu}\right)\left(\frac{1}{60}\right)\right]\right\}} \tag{82}$$

in which μ is the ratio of the areas concentrated at the flanges, to the distributed areas [see Eq. (78)]. If $h = 0$, $L/(b + c) = 0.4\sqrt{\mu}$. If $\mu = 1$ and $h = t$, $L/(b + c)$ does not vary practically with b/c and is equal to 1/2, while it reaches 1/3 for small values of μ. For a nearly circular tube, assuming that

$$du/da = k \sin (2\pi s/C_1) \tag{83}$$

where k is a small quantity and C_1 is the half circumference,

$$L/C_1 = (1/2\pi)\sqrt{Eh/Gt} \tag{84}$$

and if $h = t$, $L = C_1/4$.

These values show that the length L is a fairly constant fraction of the perimeter of the tube and that the distance between frames may be smaller than L, so that the use of this method, which assumes a continuous distribution of frames, may lead to incorrect results.

Remarks on Some Previous Solutions.—Many authors have previously analyzed the special problem of the rectangular section, examined here as an application of the general theory. The case of the tube without flanges and stiffeners has generally been investigated, and many authors have found that the maximum normal stress σ is given by the simple relation

$$\sigma/\tau = \sqrt{3E/G} = 2.8 \tag{85}$$

In this case, Eq. (78) gives a good approximation of the correct value, while it is apparent that Eq. (85) is basically incorrect, since it indicates the presence of secondary normal stresses in a square tube prevented from warping and subjected to a torque, which is obviously incorrect because a square tube does not warp under torque.

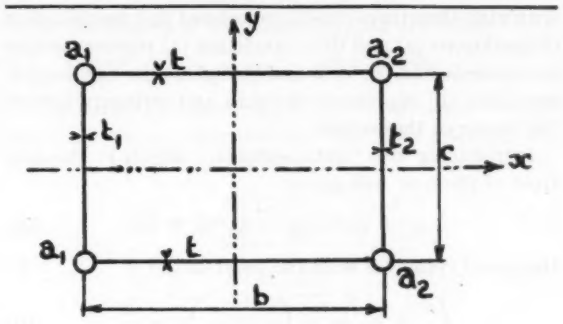

FIG. 4.

This error is generally due to the fact that the secondary warping is defined[2] by the condition $\oint \Delta\tau\, ds = 0$, instead of the condition of minimum warping used here. The error resides in the unjustified extension, to secondary shear, of the relation $\oint \tau\, ds = 0$, valid for the principal shear. As a result, the constant K, defined by Eq. (47), becomes

$$K' = \epsilon_0 \oint (du/da)^2 da \tag{86}$$

This constant K' tends toward zero for a square tube and, if used instead of K in Eq. (80), yields the incorrect result represented by Eq. (85).

In addition, it can be shown that the erroneous basic condition is equivalent to the assumption that the secondary shears produce no general shear deformation. Since the secondary shears replace the primary shears at a fully restrained end, this assumption means that there is no shear deformation at that end, leading to too high values for the normal stresses.

(2) *Unsymmetrical Rectangular Section*

(a) The Webs Have Different Thicknesses and the Flanges Are Unequal.—The web does not transmit axial loads ($h = 0$) (Fig. 4).

The centroid is located at an abscissa x_c from the center of figure,

$$x_c = (b/2)(a_2 - a_1)/(a_2 + a_1) \tag{87}$$

The twist center is at an abscissa x_T from the center of figure,

$$\bar{x}_T = x_c + \left[\left(\frac{a_1}{t_1} - \frac{a_2}{t_2}\right)bc\right] \Big/ \left\{\left[\frac{c}{2}\left(\frac{1}{t_1} + \frac{1}{t_2}\right) + \frac{b}{t}\right](a_1 + a_2)\right\} \tag{88}$$

(b) The Corner Flanges Are Replaced by Flanges on the y Axis.—Then $x_c = 0$ and

$$\bar{x}_T = x_T = \left[\left(\frac{1}{t_1} - \frac{1}{t_2}\right)bc\right] \Big/ \left[c\left(\frac{1}{t_1} + \frac{1}{t_2}\right) + 2\frac{b}{t}\right] \tag{89}$$

(c) Generalization of the Previous Formulas.—An approximately rectangular section such as used in two-

spar wing structures can be considered as a combination of conditions (a) and (b): condition (a) represents spar flange areas and the skin and stringers near the flanges; condition (b) represents the skin and stringers toward the center of the section.

Introducing the "web centroid," which is the centroid of the spar web gages,

$$x_w = (b/2)[(t_2 - t_1)/(t_2 + t_1)] \tag{90}$$

this point coincides with the twist center if

$$\left(\frac{b}{2} + x_w\right)t_1 = \left(\frac{b}{2} - x_w\right)t_2 = \frac{ct}{2} \tag{91}$$

The first relation is satisfied because the definition of the web centroid has been chosen for that purpose; the second relation is satisfied if the constant φ,

$$\varphi = 2bt_1t_2/ct(t_1 + t_2) \tag{92}$$

is equal to unity. In this case, there is no warping, and the twist center is independent of the flange material. In the general case, the location of the twist center is a function of the flange material, and it can be shown that in both problems (a) and (b) the following formula holds:

$$x_T = \bar{x}_T - x_c = [2/(\varphi + 1)](x_w - x_c) \tag{93}$$

In general, for a conventional wing section, φ is greater than unity, so that the twist center is between the web centroid and the flange centroid, and it is generally closer to the web centroid ($\varphi < 3$). The use of the above formulas can be generalized, considering them as approximate expressions for nonrectangular sections. In this case, the quantity designated by x_c is better represented by the abscissa of the centroid of the flange moments of inertia, rather than by the centroid of the flanges.

The centroid of the flange moments of inertia is

$$x_c' = \oint xy^2\,da / \oint y^2\,da \tag{94}$$

and this permits to write an approximate formula for the twist center:

$$x_T = x_c' + [2/(\varphi + 1)](x_w - x_c') \tag{95}$$

General Conclusions

For a structure without end restraint which warps under torque, there is no definite twist center under constant torque, since the direction of a warped end section is not defined. If a section is prevented from warping, it is possible to define a twist center [Eqs. (14) or (29)]. Because these solutions are approximate, a new twist center is found at each successive approximation, except for non-warping structures, such as a circular cylinder of constant thickness. In this case, simple geometric considerations define the twist center.

The effect of an end restraint or of a change of loading or of section properties is to produce a redistribution of shears and of normal stresses, and the deviation from the conventional distribution follows approximately an exponential law, rapidly decreasing on both sides of the section at which the perturbation is caused.

There exists a characteristic length, designated by L, along which the main perturbation damps out; since $e^{-1} = 0.37$, 63 per cent of the perturbation is eliminated along this length L. It has been shown that this length is small as compared with the perimeter of the section and is frequently smaller than the frame spacing. In these cases, the method developed in this paper does not apply, and an analysis that introduces the frame spacing in an explicit manner may be required.

Summary of Formulas

A—Coordinates of the Twist Center About the Principal Axes

There are two equivalent sets of formulas:

$$x_T = -\frac{1}{I_x}\oint 2Q_y\,d\alpha, \qquad y_T = \frac{1}{I_y}\oint 2Q_x\,da \tag{a}$$

with the conditions of definition of Q_x and Q_y,

$$\left.\begin{aligned} &\oint Q_x(ds/t) = 0, \qquad \oint Q_y(ds/t) = 0 \\ &x_T = -\frac{2A_0}{I_x}\oint\left(\frac{\epsilon}{\epsilon_0} - \frac{\alpha}{A_0}\right)y\,da \\ &y_T = \frac{2A}{I_y}\oint\left(\frac{\epsilon}{\epsilon_0} - \frac{\alpha}{A_0}\right)x da \end{aligned}\right\} \tag{b}$$

with an arbitrary common origin for the following integrals,

$$\epsilon = \int_0 ds/t, \qquad 2\alpha = \int_0 2d\alpha = \int_0 r\,ds$$

B—Secondary Stresses in Torsion

The applied torque $\bar{M}_z$ is divided into a warping component M corresponding to the conventional distribution of shear flows q,

$$q = M/2A_0$$

and a nonwarping component ΔM, corresponding to the distribution of shear flows Δq and normal stresses σ,

$$\Delta q = \frac{u\,\Delta M}{\oint 2u\,dA}, \qquad \sigma = \frac{E}{G}\frac{dM}{dz}\frac{\epsilon_0}{2A_0}\frac{du}{da}$$

in which the variable u is defined as follows,

$$\bar{u} = u + u_0$$

with, the areas A being taken from the twist center,

$$\frac{du}{da} = \frac{d\bar{u}}{da} = \frac{\epsilon}{\epsilon_0} - \frac{A}{A_0}, \qquad \oint \bar{u}\,d\epsilon = 0$$

$$\oint (A/A_0)da = \oint (\epsilon/\epsilon_0)da$$

and

$$u_0 = (\oint \bar{u}^2\,d\epsilon)/[\epsilon_0 \oint (du/da)^2 da]$$

The relation between M and ΔM is

$$\Delta M = -(E/G)K(d^2M/dz^2)$$

with

$$K = \frac{\epsilon_0}{A_0}\oint u\,dA = \epsilon_0\left[u_0 + \oint\left(\frac{du}{da}\right)^2 da\right]$$

The differential equation defining M is

$$\bar{M} = M - (E/G)K(d^2M/dz^2)$$

At a fixed end, $M = 0$ and $\Delta M = M$; then, if $\bar{M}$ is constant,

$$M = \bar{M}(1 - e^{-z/L}), \qquad L = \sqrt{(E/G)K}$$

C—Secondary Stresses in Bending

The applied loads $\bar{X}$ and $\bar{Y}$ are divided into warping components X and Y, and nonwarping components ΔX and ΔY. The second components give normal stresses $\Delta\sigma$ and shear flows Δq which, in principal coordinates, are

$$\Delta\sigma = -\frac{E}{G}\left[\frac{dX}{dz}\frac{\xi_x}{I_y} + \frac{dY}{dz}\frac{\xi_y}{I_x}\right]$$

$$\Delta q = \frac{E}{G}\left[\frac{d^2X}{dz^2}\frac{\int\xi_x da}{I_y} + \frac{d^2y}{dz^2}\frac{\int\xi_y\,da}{I_x}\right]$$

with the following definitions of ξ_x, ξ_y

$$\xi_x = \int_{\epsilon_x}^{\epsilon} Q_x\,d\epsilon, \qquad \xi_y = \int_{\epsilon_y}^{\epsilon} Q_y\,d\epsilon$$

and of ϵ_x, ϵ_y

$$\oint\xi_x\,da = 0, \qquad \oint\xi_y\,da = 0$$

while the origins of the integrals in Δq are defined by

$$\oint dA\int\xi_x\,da = 0, \qquad \oint dA\int\xi_y\,da = 0$$

The warping components X and Y correspond to conventional stress distributions, and the relations between the two sets of components are

$$\Delta X = -\frac{E}{G}\left[\frac{C_x}{I_y}\frac{d^2X}{dz^2} + \frac{C_{xy}}{I_x}\frac{d^2Y}{dz^2}\right]$$

$$\Delta Y = -\frac{E}{G}\left[\frac{C_{xy}}{I_y}\frac{d^2X}{dz^2} + \frac{C_y}{I_x}\frac{d^2Y}{dz^2}\right]$$

with

$$C_x = \oint Q_x^2\,d\epsilon, \qquad C_y = \oint Q_y^2\,d\epsilon, \qquad C_{xy} = \oint Q_xQ_y\,d\epsilon$$

For the determination of X, Y and ΔX, ΔY, see Eqs. (68) to (75).

REFERENCES

[1] Beskin, L., *Deformations Due to Shear in Closed Shells*, 6th International Congress of Applied Mechanics, September, 1946, Paris (unpublished—in French).

[2] von Kármán, Th., and Chien, Wei-Zang, *Torsion with Variable Twist*, Journal of the Aeronautical Sciences, Vol. 13, No. 10, pp. 503–510, October, 1946.

[3] Beskin, L., *Stress Analysis of Open Cylindrical Membranes*, Journal of the Aeronautical Sciences, Vol. 11, No. 4, pp. 343–355, October, 1944.

[4] Beskin (Beschkine), L., *Determination of the Effective Width of the Compression Flanges of T-Beams*, publications of the International Association for Bridge and Structural Engineering, Vol. 5, pp. 65–89, 1938.

[5] von Kármán, Th., *Festrischrift August Foppls*, p. 114 & ss., 1923.

Letter to the Editor

Dear Sir:

We must protest against the view of "Supersonic Axial Flow About a Body of Revolution" presented by E. V. Laitone in the November issue of the JOURNAL OF THE AERONAUTICAL SCIENCES. It is true that, if in this problem the linearized solution be substituted in the exact equation of motion, the error is of the order t^2, where t is the thickness ratio of the body. However, in reference 1 it was shown that this does *not* affect the validity of the terms in t^2 in the linearized solution. This is confirmed by the complete discussion in reference 2, where it is shown that, using the exact equations throughout, the pressure coefficient on any body of revolution in an axial supersonic stream can be expressed as a sum of (specified) terms of orders t^2, $t^2\log t$, t^4, $t^4\log t$, and $t^4\log^2 t$, if terms of order $t^6\log^3 t$ be neglected, and that the terms of orders of t^2 and $t^2\log t$ are the linearized solution as given in reference 1. Thus, the linearized solution is correct if terms of order $t^4\log^2 t$ be neglected.

We must stress that, for *every* Mach Number M, the linearized solution is a good approximation for sufficiently small t. Of course, for large M, t would have to be very small and Mr. Laitone's "hypersonic" results are then valuable. We see no reason, however, why doubt should be cast on the linearized solution, *independently* of t, for $M > \sqrt{2}$, a number apparently chosen arbitrarily.

The objections we raise are of practical importance, since the use of a formula not based on sound theory, even if chosen to fit known facts in one special case (here, flow past a cone), may in others give widely wrong results.

REFERENCES

[1] Lighthill, M. J., *Supersonic Flow Past Bodies of Revolution*, ARC, R. & M. No. 2003.

[2] Broderick, J. B., *Supersonic Flow Round Pointed Bodies of Revolution*, to be published in the Quarterly Journal of Applied Mathematics and Mechanics (Oxford University Press).

M. J. LIGHTHILL
J. B. BRODERICK
Department of Mathematics
University of Manchester, England

Low-Speed Flutter and Its Physical Interpretation

M. A. BIOT* AND LEE ARNOLD

Brown University and Aeronautical Consultant

ABSTRACT

The phenomenon of low-speed flutter of an oscillating airfoil is investigated. The problem resolves itself into the study of two phenomena: that of zero air-speed classic flutter and that of an oscillating airfoil with no vortex shed. It is seen that both cases involve oscillation of the airfoil about a nodal line located three-quarters of the chord aft of the leading edge. The study is based on the fundamental theory developed by Theodorsen.

The relationship between the parameters required for zero-speed flutter for the general case is developed, and the physical interpretation of this phenomenon is discussed.

For the latter case, the solution of the equations of motion, based on noncirculatory flow, and the equations resulting from the Kutta condition result in a relationship between the inertia and elastic parameters for which the airfoil will flutter (i.e., maintain oscillations at constant amplitude) for all air speeds. The physical interpretation and the mechanism of this phenomenon are discussed.

Practical implications, such as the importance of nodal-line location and the effect of the physical parameters of the airfoil on nodal line location, are discussed.

The possibility of a new approach to the flutter problem is suggested—that of employing the ground vibration modes of the airplane to study the existence of a low flutter speed and as a design guide to raise the flutter speed.

Conclusions are also drawn regarding the influence of aspect ratio and the relative importance of theoretical aerodynamic coefficients against values of these quantities measured in the wind tunnel.

NOTATION

h = downward displacement of airfoil at elastic axis
α = pitch of airfoil (nose upward)
V = air speed
ω = flutter frequency (rad. per sec.)
I_α = moment of inertia of airfoil about elastic axis
M = mass of airfoil
S_α = static moment of airfoil about the elastic axis
$\bar{I}_\alpha$ = $I_\alpha + \pi\rho b^4(1/8 + a^2)$ = moment of inertia of airfoil including apparent mass effect
$\bar{M}$ = $M + \pi\rho b^2$ = mass of airfoil plus apparent mass
$\bar{S}_\alpha$ = $S_\alpha - a\pi\rho b^3$ = static moment including apparent mass effect
ω_h = natural frequency in h degree of freedom
ω_α = natural frequency in α degree of freedom
b = semichord
ab = elastic axis location aft of mid-chord
k = $\omega b/V$ = reduced frequency
ρ = air density
R_{ac}, I_{ac}, etc. = real and imaginary parts of aerodynamic coefficients, not including apparent mass effects
g = structural damping

Received December 11, 1947.

* Professor of Applied Physical Sciences.

INTRODUCTION

MUCH HAS BEEN DONE to improve the methods of flutter analysis during the last few years, but no tools have been devised which can be applied with reliance during the early stages of design. Various "tricks of the trade" are resorted to (such as the set rule of moving the center of gravity forward), but the reminder that there have been exceptions to these rules compels one to search further for more reliable guides.

With regard to flutter, the only controls the designer has are those that pertain to mass and elasticity distribution. However, the two are interdependent and the influence of the change of one on the other and the joint effect on the flutter characteristics are too complex to allow for the determination of suitable design guides begotten from intuition alone.

By examining the basic two-dimensional flutter theory of Theodorsen,[1] one becomes aware of a feature of the aircraft which incorporates both the inertia and elastic characteristics. This feature, the so-called nodal-line location, is shown to be the primary factor in the occurrence of low-speed flutter. In fact, it is shown that for an idealized airfoil the location of the nodal line at the three-quarter chord results in a zero flutter speed.

NODAL LINE

If an external vibratory load is applied to the wing of an airplane on the ground, at each of certain frequencies of excitation maximum amplitudes of wing response would be induced. It would be seen that at each of these frequencies every point of the system would move in phase with every other point and that the motion of any section, say B of Fig. 1, would be essentially the rotation of the section about a point that remains stationary in space. The locus of these nodal points is the nodal line.

Let us examine the behavior of one of these wing sections (Fig. 2). We assume that the section is free to oscillate in only two degrees of freedom. The first resonant condition will involve oscillations about a nodal point a large distance forward of the airfoil; the second will involve oscillations about a nodal point on

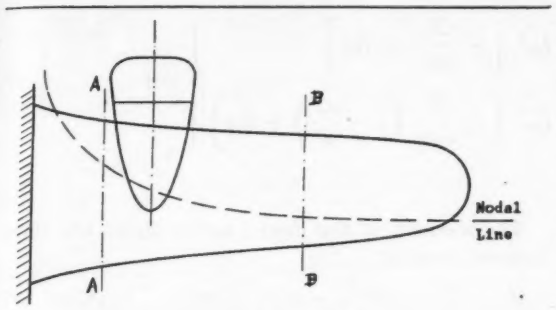

FIG. 1. Plan form of wing and nodal line.

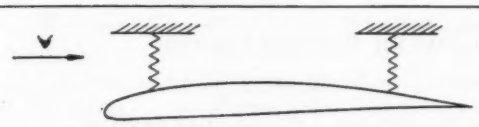

FIG. 2. Isolated section of the wing.

or near the airfoil. It is the latter point that is important in the occurrence of low-speed wing flutter.

ZERO AIR-SPEED FLUTTER

Let us consider the effect of an air stream flowing over the airfoil of Fig. 2. At any air speed below the critical flutter speed, any small disturbance of the airfoil from its static equilibrium position will result in an oscillatory motion that will damp out with time. As the flutter speed is approached, the rate of decay diminishes until at the critical flutter speed there is no decay and the airfoil maintains a constant amplitude oscillation. At this critical speed there is no exchange of energy between the mechanical system and the stream. At any speed above that of flutter, the mechanical system absorbs energy resulting in oscillations whose amplitude builds up with time.

Consider now the airfoil of Fig. 2 in still air. If we neglect the structural and air friction, any displacement from equilibrium will result in constant amplitude oscillations. However, this phenomenon will be a limiting case of flutter for only special distributions of mass and elasticity of the system. It will now be shown that the necessary and sufficient condition for zero air-speed flutter is that the mass and elasticity of the system be such as to result in a node at the three-quarter chord aft of the leading edge.

The equations of motion of an airfoil oscillating in a uniform stream are:

$$-\bar{I}_\alpha(\omega^2 - \omega_\alpha{}^2)\alpha - \omega^2\bar{S}_\alpha h = -\pi\rho b^4\omega^2[(R_{a\alpha} + iI_{a\alpha})\alpha + (R_{ah} + iI_{ah})(h/b)] \tag{1}$$

$$-\omega^2\bar{S}_\alpha\alpha - \bar{M}(\omega^2 - \omega_h{}^2)h = -\pi\rho b^3\omega^2[(R_{c\alpha} + iI_{c\alpha})\alpha + (R_{ch} + iI_{ch})(h/b)] \tag{2}$$

where ω_h and ω_α are the natural frequencies of the system in still air, the former for pure bending and the latter for pure torsion. $\bar{I}_\alpha$, $\bar{S}_\alpha$, and $\bar{M}$ are the moment of inertia and static moment about the elastic axis, and mass, respectively, all including apparent mass contributions. In nondimensional form, Eqs. (1) and (2) become

$$\left[-\frac{\bar{I}_\alpha}{\pi\rho b^4}\left(1 - \frac{\omega_\alpha{}^2}{\omega^2}\right) + (R_{a\alpha} + iI_{a\alpha})\right]\alpha + \left[-\frac{\bar{S}_\alpha}{\pi\rho b^3} + (R_{ah} + iI_{ah})\right]\frac{h}{b} = 0 \tag{3}$$

$$\left[-\frac{\bar{S}_\alpha}{\pi\rho b^3} + (R_{c\alpha} + iI_{c\alpha})\right]\alpha + \left[-\frac{\bar{M}}{\pi\rho b^2}\left(1 - \frac{\omega_h{}^2}{\omega^2}\right) + (R_{ch} + iI_{ch})\right]\frac{h}{b} = 0 \tag{4}$$

The stability determinant becomes

$$\begin{vmatrix} \left[-\frac{\bar{I}_\alpha}{\pi\rho b^4}\left(1 - \frac{\omega_\alpha{}^2}{\omega^2}\right) + R_{a\alpha} + i\frac{1}{k}I_{a\alpha}'\right] & \left[-\frac{\bar{S}_\alpha}{\pi\rho b^3} + R_{ah} + i\frac{1}{k}I_{ah}'\right] \\ \left[-\frac{\bar{S}_\alpha}{\pi\rho b^3} + R_{c\alpha} + i\frac{1}{k}I_{c\alpha}'\right] & \left[-\frac{\bar{M}}{\pi\rho b^2}\left(1 - \frac{\omega_h{}^2}{\omega^2}\right) + R_{ch} + i\frac{1}{k}I_{ch}'\right] \end{vmatrix} = 0 \tag{5}$$

where $I_{a\alpha} = \frac{1}{k}I_{a\alpha}'$, etc.

Separating into real and imaginary parts,

$$\begin{vmatrix} \left[-\frac{\bar{I}_\alpha}{\pi\rho b^4}\left(1 - \frac{\omega_\alpha{}^2}{\omega^2}\right) + R_{a\alpha}\right] & \left[-\frac{\bar{S}_\alpha}{\pi\rho b^3} + R_{ah}\right] \\ \left[-\frac{\bar{S}_\alpha}{\pi\rho b^3} + R_{c\alpha}\right] & \left[-\frac{\bar{M}}{\pi\rho b^2}\left(1 - \frac{\omega_h{}^2}{\omega^2}\right) + R_{ch}\right] \end{vmatrix} - \frac{1}{k^2}\begin{vmatrix} I_{a\alpha}' & I_{ah}' \\ I_{c\alpha}' & I_{ch}' \end{vmatrix} = 0 \tag{6}$$

$$\frac{1}{k}\left\{\begin{vmatrix}\left[-\frac{\bar{I}_\alpha}{\pi\rho b^4}\left(1-\frac{\omega_\alpha^2}{\omega^2}\right)+R_{a\alpha}\right]I_{ah}' \\ \left[-\frac{\bar{S}_\alpha}{\pi\rho b^3}+R_{c\alpha}\right] \qquad I_{ch}'\end{vmatrix}+\begin{vmatrix}I_{a\alpha}'\left[-\frac{\bar{S}_\alpha}{\pi\rho b^3}+R_{ah}\right] \\ I_{c\alpha}'\left[-\frac{\bar{M}}{\pi\rho b^2}\left(1-\frac{\omega_h^2}{\omega^2}\right)+R_{ch}\right]\end{vmatrix}\right\}=0 \tag{7}$$

The factor $1/k$ of Eq. (7), put equal to zero combined with Eq. (6), is the condition for steady-state oscillations at zero air speed but not the condition for flutter. It is the simultaneous vanishing of Eq. (6) and the second factor of Eq. (7) which gives the flutter solution. At zero air speed

$$1/k = R_{a\alpha} = R_{ah} = R_{c\alpha} = R_{ch} = 0$$

and

$$I_{a\alpha}' = (1/2 - a)^2, \qquad I_{ah}' = -(1/2 + a)$$

$$I_{c\alpha}' = 3/2 - a, \qquad I_{ch}' = 1$$

Substituting, Eqs. (6) and (7) become,

$$\begin{vmatrix}\frac{\bar{I}_\alpha}{\pi\rho b^4}\left(1-\frac{\omega_\alpha^2}{\omega^2}\right) & \frac{\bar{S}_\alpha}{\pi\rho b^3} \\ \frac{\bar{S}_\alpha}{\pi\rho b^3} & \frac{\bar{M}}{\pi\rho b^2}\left(1-\frac{\omega_h^2}{\omega^2}\right)\end{vmatrix}=0 \tag{8}$$

and

$$\begin{vmatrix}\frac{\bar{I}_\alpha}{\pi\rho b^4}\left(1-\frac{\omega_\alpha^2}{\omega^2}\right) & (1/2-a) \\ \frac{\bar{S}_\alpha}{\pi\rho b^3} & -1\end{vmatrix}\cdot\begin{vmatrix}(1/2-a)^2 & \frac{\bar{S}_\alpha}{\pi\rho b^3} \\ (3/2-a) & \frac{\bar{M}}{\pi\rho b^2}\left(1-\frac{\omega_h^2}{\omega^2}\right)\end{vmatrix}=0 \tag{9}$$

Eq. (8) is the usual zero air-speed frequency equation. The important equation is Eq. (9). Expanding it, we obtain

$$\left(\frac{1}{2}-a\right)^2 b^2\bar{M}\left(1-\frac{\omega_h^2}{\omega^2}\right)+\bar{I}_\alpha\left(1-\frac{\omega_\alpha^2}{\omega^2}\right)+(2a-1)b\bar{S}_\alpha+\frac{3}{8}\pi\rho b^4=0 \tag{10}$$

which is the equation governing the oscillating motion of an airfoil elastically restrained at the elastic axis but constrained by a node at the three-quarter chord point as shown in Fig. 3.

The total restoring moment for the system of Fig. 3 about the three-quarter chord is

$$M_R = [b^2(1/2 - a)^2\omega_h^2\bar{M} + \omega_\alpha^2\bar{I}_\alpha]\alpha \tag{11}$$

The moment of the inertia forces about the three-quarter chord is

$$M_I = [\bar{I}_\alpha + \bar{M}(1/2 - a)^2b^2 + 2b(a - 1/2)\bar{S}_\alpha]\ddot{\alpha} \tag{12}$$

The aerodynamic moment about the three-quarter chord point when $1/k = 0$ is

$$M_\alpha = -(3/8)\pi\rho b^4 \tag{13}$$

We have the dynamical equation

$$M_R + M_I = M_\alpha$$

For harmonic motion this equation becomes

$$\left(\frac{1}{2}-a\right)^2 b^2\bar{M}\left(1-\frac{\omega_h^2}{\omega^2}\right)+\bar{I}_\alpha\left(1-\frac{\omega_\alpha^2}{\omega^2}\right)+(2a-1)b\bar{S}_\alpha+\frac{3}{8}\pi\rho b^4=0$$

which is identical with Eq. (10), the condition for zero-speed flutter.

We see then that the condition for zero air-speed flutter is that the nodal line is at the three-quarter chord.

The importance of the nodal-line location in flutter is then apparent. One should therefore investigate the variation of flutter speed with nodal-line location as one of the parameters. This has been done for various combinations of parameter values. When the structural damping g is not zero, the flutter speed does not vanish for a node location at the three-quarter chord; however, it reaches a minimum in the vicinity of that location. The variation of flutter speed with nodal-line location is illustrated in Fig. 4 for two values of the structural damping.

Vortex-Free Flutter

There is a case of occurrence of zero air-speed flutter in a two-dimensional airfoil for which flutter occurs also at all other speeds. This type of flutter is as-

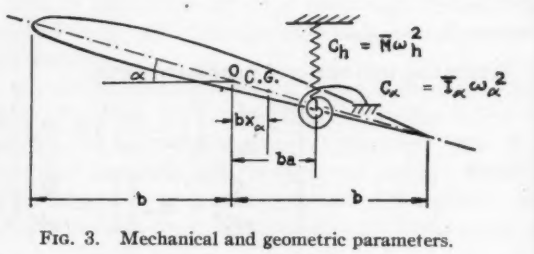

Fig. 3. Mechanical and geometric parameters.

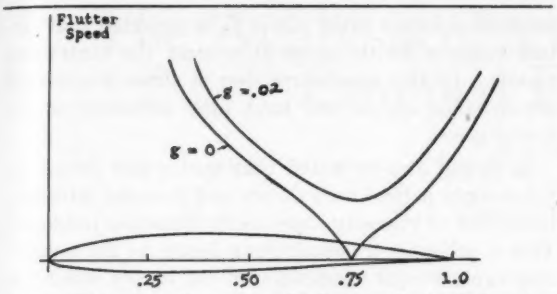

FIG. 4. Flutter speed versus nodal line location (node location in chord lengths).

sociated with the vanishing of the circulation about the airfoil. The aerodynamic force and moment experienced by an oscillating airfoil is made up of two parts—a noncirculatory and a circulatory. If the latter, which also is associated with the shedding of vorticity from the trailing edge of the airfoil, is assumed to vanish, the equations of motion become

$$\ddot{\alpha}\bar{I}_\alpha + \alpha\omega_\alpha^2\bar{I}_\alpha + \bar{S}_\alpha\ddot{h} + \pi\rho b^4\omega^2\left[-\frac{1}{k}\left(\frac{\dot{\alpha}}{k} + \frac{\dot{h}}{\omega b}\right)\right] = 0 \tag{14}$$

$$\ddot{h}\bar{M} + h\omega_h^2\bar{M} + \bar{S}_\alpha\alpha + \pi\rho b^3\omega^2\left[\left(\frac{1}{k}\right)\left(\frac{\dot{\alpha}}{\omega}\right)\right] = 0 \tag{15}$$

For harmonic motion, in nondimensional form, Eqs. (14) and (15) become

$$\left[-\left(1 - \frac{\omega_\alpha^2}{\omega^2}\right)\frac{\bar{I}_\alpha}{\pi\rho b^4} - \frac{1}{k^2}\right] + \left[-\frac{\bar{S}_\alpha}{\pi\rho b^3} - i\left(\frac{1}{k}\right)\left(\frac{h}{b}\right)\right] = 0 \tag{16}$$

$$\left[-\frac{\bar{S}_\alpha}{\pi\rho b^3} + i\left(\frac{1}{k}\right)\right]\alpha + \left[-\frac{\bar{M}}{\pi\rho b^2}\left(1 - \frac{\omega_h^2}{\omega^2}\right)\right]\frac{h}{b} = 0 \tag{17}$$

Since there is no circulation about the airfoil, the Kutta condition becomes

$$V\alpha + h + b(1/2 - a)\dot{\alpha} = 0 \tag{18}$$

In nondimensional form

$$\left[(1/2 - a) - i\left(\frac{1}{k}\right)\right]\alpha + [1]\frac{h}{b} = 0 \tag{19}$$

From Eqs. (16) and (17),

$$\begin{vmatrix} + [X + (1/k^2)] & [Z + i(1/k)] \\ [Z - i(1/k)] & Y \end{vmatrix} = 0 \tag{20}$$

and from Eqs. (17) and (19)

$$\begin{vmatrix} (1/2 - a) - i(1/k) & 1 \\ [Z - i(1/k)] & Y \end{vmatrix} = 0 \tag{21}$$

where

$$X = (\bar{I}_\alpha/\pi\rho b^4)\,[1 - (\omega_\alpha^2/\omega^2)]$$
$$Y = (\bar{M}/\pi\rho b^2)\,[1 - (\omega_h^2/\omega^2)]$$
$$Z = \bar{S}_\alpha/\pi\rho b^3$$

Eq. (20) becomes

$$Y[X + (1/k^2)] - [Z^2 + (1/k^2)] = 0 \tag{22}$$

while Eq. (21) becomes:

$$\left.\begin{aligned}(1/2 - a)Y - Z &= 0\\ (1/k)(1 - Y) &= 0\end{aligned}\right\} \tag{23}$$

Eqs. (23) are identically satisfied for all values of $1/k$ if

$$\left.\begin{aligned}Y &= 1\\ (1/2) - a &= 0\end{aligned}\right\} \tag{24}$$

Substituting Eq. (24) into the determinant, Eq. (20),

$$X = (1/2 - a)^2 \tag{25}$$

as the condition for flutter. Since Eq. (25) is independent of $1/k$, it is seen that this type of instability will persist at all air speeds—i.e., flutter will occur at any speed from 0 to ∞.

From Eq. (19) it is seen that, when $1/k = 0$ ($V = 0$),

$$h/b + (1/2 - a)\alpha = 0 \tag{26}$$

which is the condition that the nodal point be at the three-quarter chord. A further examination of the Kutta condition, Eq. (18), reveals that the motion of the airfoil during this vortexless flutter is one of sinusoidal gliding at the three-quarter chord point as portrayed in Fig. 5.

We have then the following conditions for vortexless flutter:

$$X = \frac{\bar{I}_\alpha}{\pi\rho b^4}\left(1 - \frac{\omega_\alpha^2}{\omega^2}\right) = \left(\frac{1}{2} - a\right)^2 \tag{i}$$

$$Y = \frac{\bar{M}}{\pi\rho b^2}\left(1 - \frac{\omega_h^2}{\omega^2}\right) = 1 \tag{ii}$$

$$Z = \frac{\bar{S}_\alpha}{\pi\rho b^3} = \frac{S_\alpha}{\pi\rho b^3} - a = \frac{1}{2} - a \tag{iii}$$

Node at three-quarter chord (iv)

However, conditions (iv) and (iii) imply Eqs. (i) and (ii); therefore, the necessary and sufficient conditions for vortex-free flutter are, from Eqs. (iii) and (iv), that

FIG. 5. Motion of the wing in vortex-free flutter.

the node is at the three-quarter chord point and that the static moment about the elastic axis is a small value determined by

$$S_\alpha = {}^1/_2\pi\rho b^3 \tag{27}$$

The frequency of flutter ω is independent of the velocity, and the frequency ratio ω_h/ω_α is near unity. Therefore, when, in addition to a three-quarter chord location of the nodal line, the frequency ratio is near unity, the flutter speed will be extremely sensitive to changes in the frequency ratio.

Three-Dimensional Considerations

We must realize that a wing may be assumed to be composed of a continuous distribution of two-dimensional sections of the type we have been describing. Each of these sections would have its own flutter characteristics if it were separated from the rest of the wing and placed in a two-dimensional stream. For example, section A of Fig. 1, whose nodal line is at 40 per cent of the chord, would have a high flutter speed, but section B, whose nodal line is close to the three-quarter chord, would have a low flutter speed. At a given speed, section A would be dissipating energy to the stream, while section B would be absorbing energy from the stream. At the air speed at which the amount of energy lost by such sections as A equals that absorbed by those such as B, flutter occurs. The obvious guide is to design the wing so that the nodal line is as far from the three-quarter chord as is practicable at all spanwise stations of the wing.

During the early stages of design, the nodal line and the effect of various design changes on its location can be determined analytically.

Another important consequence of the present point of view is the tendency of vortex-free flutter to be independent of aspect ratio. It is to be expected that certain types of flutter occur at or near the vortex-free régime. In this case, correction of three-dimensional aerodynamic effects will have little influence on the flutter speed.

It should also be noted that vortex-free flutter involves only perfect fluid theory and does not introduce the action of viscosity since no circulation is produced. This is probably a contributing factor to the remarkable experimental verification of the theory which has been frequently observed. It may well be that the substitution of experimental aerodynamic coefficients measured on oscillating models can lead to less reliable predictions of flutter in certain cases.

Conclusions

(a) It is recommended that a study of locations of nodal lines be employed to ensure against the occurrence of flutter.

(b) The designer should attempt to locate the nodal line as far from the three-quarter chord as is practicable.

(c) A limiting case of flutter without vorticity may occur. This may account for the small effect that aspect ratio corrections have had on flutter in many cases studied.

(d) The importance of the theoretical aerodynamic coefficients should be emphasized, since it is entirely possible that in certain types of flutter they may lead to more reliable predictions of the flutter speed than the experimental coefficients.

Reference

[1] Theodorsen, T., *General Theory of Aerodynamic Instability and the Mechanism of Flutter*, N.A.C.A. T.R. No. 496, 1940.

Letter to the Editor

Dear Sir:

I wish to make two corrections in the article written by myself and Mr. C. D. D. Pancu in the November, 1947, issue of the Journal of the Aeronautical Sciences, entitled "Use of Vectors in Vibration Measurement and Analysis."

First (through no fault of the publisher), the heading is misleading, since it gives the impression that I am at Consolidated Vultee Aircraft Corporation. I am not connected with Consolidated Vultee and have not been connected with any other aircraft concern since I left the Curtiss-Wright Research Laboratory in 1944.

Second, the titles of Figs. 3 and 6 should be interchanged. Fig. 3 should read "Lissajous ellipse," and Fig. 6, "Force equilibrium."

Charles Kennedy

The Analysis of a Circular Ring with Propped Floor Beam

J. S. TAYLOR* AND S. S. GILL*

A. V. Roe and Company Ltd.

ABSTRACT

The paper sets out a method of analyzing a circular fuselage former with a floor crossbeam supported by four vertical struts. The structure has eight redundancies, but from symmetry of loading and geometry there are only five unknowns to be evaluated by strain-energy methods.

The general equation for the bending moment and the partial differential coefficients with respect to the unknowns are stated in tabular form to assist computation.

INTRODUCTION

THE TREND OF DESIGN of cabin aircraft has more or less standardized a type of fuselage former which consists of a ring and transverse floor beam. The loading of the fuselage consists in part of the loads applied to each floor beam by the internal equipment, etc. These loads are carried to the fuselage skin through the floor beam and ring and are counterbalanced by shear loads from the skin to the ring.

In the case of noncircular rings, a graphical analysis is often necessary or convenient, but the advent of pressurized fuselages has required the use of circular rings of which there are many analytical solutions.[1–3]

An example of an economical design of a former for an aircraft with circular fuselage is shown in Fig. 1. In this particular case, the floor beam is propped by four supports. It is assumed that these four vertical supports are pin-jointed at their ends and that the floor crossbeam is pin-jointed to the ring. However, note that the ring is considered continuous for bending at this point. This is consistent with practical design. The main ring would be a continuous ring, and the crossbeam and vertical struts would be riveted to it.

This structure has eight redundancies, and, at first sight, its analysis by strain-energy methods along the lines of existing analyses[4,5] presents formidable arithmetical difficulties because of the work entailed. This paper presents a method of tabular layout of equations and computations which simplifies the otherwise tedious work. Combined with the fact that symmetry of loading and geometry reduces the unknowns to five, the solution by this method becomes tractable.

The loading will be assumed to be a uniformly distributed load over the floor beam, but the use of a similar analysis for other symmetric and antisymmetric loadings would make it possible to solve a former of this type for any loading.[6]

In this analysis the strain energy of the structure due to end loads, shear forces, and curvature of the ring is neglected. This is customary practice and is justified for large rings of small cross section.[4]

The ring is cut at the top centerline, and the restoring end load, X_1, and end moment, M_1, are applied. The vertical struts have loads W_1 and W_2 in them, and the floor beam acts as a tie as well as a beam. The end load in the beam, X_2, is the fifth unknown to be evaluated.

The total down load on the structure is $2wc$. This is resisted by shear loads from the aircraft skin. It will be assumed that the distribution of this shear load (acting tangentially to the ring) is sinusoidal, representing a reasonable approximation. In actual fact, its distribution will depend on the relative stiffnesses of the ring and the aircraft skin and their attachments, but widely different assumptions of this distribution do not appreciably affect the final result. The moment due to the offset of the aircraft skin from the centroidal axis of the former is ignored because this is small.

NOTATION

- x = horizontal distance of point on the former from point A (top centerline)
- y = vertical distance of point on former from point A (top centerline)
- M_1 = restoring couple at cut at A
- X_1 = restoring load at cut at A
- X_2 = end load in crossbeam
- W_1 = load in inner floor support strut
- W_2 = load in outer floor support strut
- w = uniformly distributed floor load per in. run
- I_1 = moment of inertia of former cross section
- I_2 = moment of inertia of floor beam cross section
- k = I_1/I_2
- R = radius of neutral axis of former
- θ = angle between point on former under consideration and vertical centerline
- M_s = bending moment at any point of the former caused by shear load from aircraft skin applied to former between A and the point under consideration.
- M = bending moment at any point caused by all loads applied to the former
- U = total strain energy

Other symbols used are obvious from the sketches of the former or from their context.

Received August 27, 1947.

* Now on the Lecturing Staff of the College of Technology, University of Manchester, Manchester, England.

TABLE 1

Part	Bending Moment Due to M_1	X_1	X_2	W_1	W_2	w	s	$\frac{\partial M}{\partial M_1}$	$\frac{\partial M}{\partial X_1}$	$\frac{\partial M}{\partial X_2}$	$\frac{\partial M}{\partial W_1}$	$\frac{\partial M}{\partial W_2}$
AB	1	y	...	...	...	...	M_s	1	y	...	...	...
BC	1	y	$y-d$	$x-c$	$x-c$	$c(c-x)$	M_s	1	y	$y-d$	$x-c$	$x-c$
CD	1	y	$y-d$	$x-c$	$b-c$	$c(c-x)$	M_s	1	y	$y-d$	$x-c$	$b-c$
DE	1	y	$y-d$	$a-c$	$b-c$	$c(c-x)$	M_s	1	y	$y-d$	$a-c$	$b-c$
FG	...	...	...	$a-c$	$b-c$	$(c^2-x^2)/2$	...	...	...	...	$a-c$	$b-c$
GH	...	...	...	$x-c$	$b-c$	$(c^2-x^2)/2$	...	...	...	...	$x-c$	$b-c$
HB	...	...	...	$x-c$	$x-c$	$(c^2-x^2)/2$	...	...	...	...	$x-c$	$x-c$

TABLE 2

Part	$(M/I)(\partial M/\partial M_1)$: M_1	X_1	X_2	W_1	W_2	w	s	$(M/I)(\partial M/\partial X_1)$: M_1	X_1	X_2	W_1	W_2	w	s
AB	1	y	...	...	...	...	M_s	y	y^2	...	...	...	...	$M_s y$
BC	1	y	$y-d$	$x-c$	$x-c$	$c(c-x)$	M_s	y	y^2	$y(y-d)$	$y(x-c)$	$y(x-c)$	$cy(c-x)$	$M_s y$
CD	1	y	$y-d$	$x-c$	$b-c$	$c(c-x)$	M_s	y	y^2	$y(y-d)$	$y(x-c)$	$y(b-c)$	$cy(c-x)$	$M_s y$
DE	1	y	$y-d$	$a-c$	$b-c$	$c(c-x)$	M_s	y	y^2	$y(y-d)$	$y(a-c)$	$y(b-c)$	$cy(c-x)$	$M_s y$
FG	...	...	...	...	...	...	...	...	...	...	...	...	...	...
GH	...	...	...	...	...	...	...	...	...	...	...	...	...	...
HB	...	...	...	...	...	...	...	...	...	...	...	...	...	...

TABLE 3

Part	$(M/I)(\partial M/\partial X_2)$: M_1	X_1	X_2	W_1	W_2	w	s
AB	...	...	...	...	...	...	...
BC	$y-d$	$y(y-d)$	$(y-d)^2$	$(y-d)(x-c)$	$(y-d)(x-c)$	$c(c-x)(y-d)$	$M_s(y-d)$
CD	$y-d$	$y(y-d)$	$(y-d)^2$	$(y-d)(x-c)$	$(y-d)(b-c)$	$c(c-x)(y-d)$	$M_s(y-d)$
DE	$y-d$	$y(y-d)$	$(y-d)^2$	$(y-d)(a-c)$	$(y-d)(b-c)$	$c(c-x)(y-d)$	$M_s(y-d)$
FG	...	...	...	...	...	...	...
GH	...	...	...	...	...	...	...
HB	...	...	...	...	...	...	...

TABLE 4

Part	$(M/I)(\partial M/\partial W_1)$: M_1	X_1	X_2	W_1	W_2	w	s
AB	...	...	...	...	...	...	...
BC	$x-c$	$y(x-c)$	$(y-d)(x-c)$	$(x-c)^2$	$(x-c)^2$	$-c(c-x)^2$	$M_s(x-c)$
CD	$x-c$	$y(x-c)$	$(y-d)(x-c)$	$(x-c)^2$	$(x-c)(b-c)$	$-c(c-x)^2$	$M_s(x-c)$
DE	$a-c$	$y(a-c)$	$(y-d)(a-c)$	$(a-c)^2$	$(a-c)(b-c)$	$c(c-x)(a-c)$	$M_s(a-c)$
FG	...	...	...	$k(a-c)^2$	$k(a-c)(b-c)$	$\frac{k(a-c)(c^2-x^2)}{2}$	...
GH	...	...	...	$k(x-c)^2$	$k(x-c)(b-c)$	$\frac{k(x-c)(c^2-x^2)}{2}$	...
HB	...	...	...	$k(x-c)^2$	$k(x-c)^2$	$\frac{k(x-c)(c^2-x^2)}{2}$	...

TABLE 5

Part	$(M/I)(\partial M/\partial W_2)$: M_1	X_1	X_2	W_1	W_2	w	s
AB	...	...	...	...	...	...	...
BC	$x-c$	$y(x-c)$	$(y-d)(x-c)$	$(x-c)^2$	$(x-c)^2$	$-c(c-x)^2$	$M_s(x-c)$
CD	$b-c$	$y(b-c)$	$(y-d)(b-c)$	$(b-c)(x-c)$	$(b-c)^2$	$c(c-x)(b-c)$	$M_s(b-c)$
DE	$b-c$	$y(b-c)$	$(y-d)(b-c)$	$(b-c)(a-c)$	$(b-c)^2$	$c(c-x)(b-c)$	$M_s(b-c)$
FG	...	...	...	$k(b-c)(a-c)$	$k(b-c)^2$	$\frac{k(b-c)(c^2-x^2)}{2}$	...
GH	...	...	...	$k(b-c)(x-c)$	$k(b-c)^2$	$\frac{k(b-c)(c^2-x^2)}{2}$	...
HB	...	...	...	$k(x-c)^2$	$k(x-c)^2$	$\frac{k(x-c)(c^2-x^2)}{2}$	...

DERIVATION OF EQUATIONS

The equations for the bending moment at any point in the ring and floor beam are given in tabular form in Table 1.

The bending moment (B.M.) at any point on the ring between C and D, for example, equals

$$M_1 + X_1 y + X_2(y-d) + (x-c)W_1 + (b-c)W_2 + wc(c-x) + M_s$$

and the bending moment at any point of the floor beam between G and H, for example, equals

$$(x-c)W_1 + (b-c)W_2 + [w(c^2-x^2)/2]$$

The coefficient of each applied load or redundancy is tabulated in the appropriate column for each part of the ring or beam. The tables of $\partial M/\partial M_1$, $\partial M/\partial X_1$, $\partial M/\partial X_2$, $\partial M/\partial W_1$, $\partial M/\partial W_2$ for each part of the structure in the same table are self-explanatory.

The next step is to tabulate $M(\partial M/\partial M_1)$, etc., for each part of the former.

The coefficients of the unknowns and applied loads for each part of the ring are multiplied by the appropriate differential coefficient (see Table 1), giving the Tables 2 to 5.

Each "block" of coefficients gives one of the five equations

$$EI_1\partial U/\partial M_1 = 0, \quad EI_1\partial U/\partial X_1 = 0,$$
$$EI_1\partial U/\partial X_2 = 0, \quad EI_1\partial U/\partial W_1 = 0,$$
$$EI_1\partial U/\partial W_2 = 0$$

As an example from Table 2

$$EI_1\partial U/\partial M_1 = M_1 \int_A^E ds + X_1 \int_A^E y ds + X_2 \int_B^E \times (y - d)ds + W_1[\int_B^D (x - c)ds + \int_D^E (a - c)ds] + W_2[\int_B^C (x - c)ds + \int_C^E (b - c)ds] + \int_B^E wc \times (c - x)ds + \int_A^E M_s ds$$

Each coefficient is multiplied by ds and is integrated over the appropriate range. Note that integrals for the beam are multiplied by k, the ratio of the moments of inertia of the ring and the beam.

Examination will show that all these coefficients are multiples, or the addition of multiples, of the following standard "geometric" and "loading" integrals, which must be evaluated for each part of the ring or beam:

For the ring:

$$\int ds, \int xds, \int yds, \int y^2ds, \int xyds, \int x^2ds, \int M_s ds, \int M_s yds, \int M_s xds$$

For the beam:

$$\int ds, \int xds, \int x^2ds, \int x^3ds$$

Integrals for the ring are required over the ranges AB, BC, CD, DE. Integrals for the beam are required over the ranges FG, GH, HB. All other ranges can be found from these basic ones by addition.

Note that in practice it is simpler and more convenient to write the Tables 1 to 5 side by side on a long sheet of paper. The tables are split up for convenience in printing.

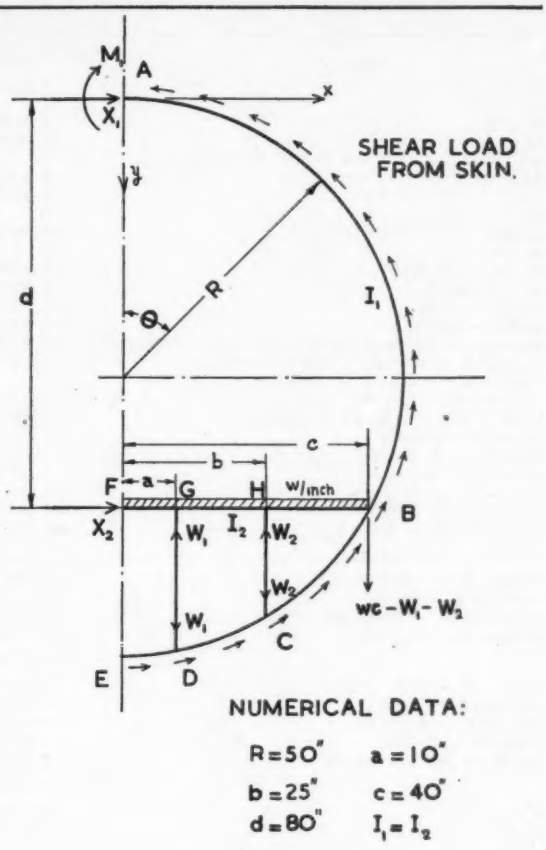

FIG. 1.

The various integrals are evaluated for a ring whose dimensions, etc., are given in Fig. 1. First they are evaluated analytically for any range θ_1 to θ_2. The general mathematical analysis is given below. On Tables 6 and 7, θ_1 and θ_2 and x_1 and x_2 are taken at their appropriate values for the different ranges, and the trigonometric functions and integrals for each range are tabulated.

Note that these tables are considerably abbreviated. In practice it is easier to tabulate a large number of small items, as is done in the first eleven lines, thus keeping all the calculations in tabular form and avoiding separate calculations.

ANALYTICAL EVALUATION OF THE INTEGRALS

For the Ring

$$\int_{\theta_1}^{\theta_2} ds = R(\theta_2 - \theta_1)$$
$$\int_{\theta_1}^{\theta_2} yds = R^2[(\theta_2 - \theta_1) - (\sin\theta_2 - \sin\theta_1)]$$
$$\int_{\theta_1}^{\theta_2} xds = -R^2(\cos\theta_2 - \cos\theta_1)$$
$$\int_{\theta_1}^{\theta_2} xyds = R^3[1/2(\cos^2\theta_2 - \cos^2\theta_1) - (\cos\theta_2 - \cos\theta_1)]$$
$$\int_{\theta_1}^{\theta_2} y^2ds = R^3[3/2(\theta_2 - \theta_1) - 2(\sin\theta_2 - \sin\theta_1) + 1/4(\sin 2\theta_2 - \sin 2\theta_1)]$$
$$\int_{\theta_1}^{\theta_2} x^2ds = R^3[1/2(\theta_2 - \theta_1) - 1/4(\sin 2\theta_2 - \sin 2\theta_1)]$$

TABLE 6

Item	Range AB	BC	CD	DE
θ_2	2.2143	2.6180	2.9403	3.1416
θ_1	0	2.2143	2.6180	2.9403
$\theta_2 - \theta_1$	2.2143	0.4037	0.3223	0.2013
θ_2^2	4.9031	6.8539	8.6454	9.8697
θ_1^2	0	4.9031	6.8539	8.6454
$\theta_2^2 - \theta_1^2$	4.9031	1.9508	1.7915	1.2243
$2\theta_2$	4.4286	5.2360	5.8806	6.2832
$2\theta_1$	0	4.4286	5.2360	5.8806
$\sin 2\theta_2$	−0.9600	−0.8660	−0.3918	0
$\sin 2\theta_1$	0	−0.9600	−0.8660	−0.3918
$\sin 2\theta_2 - \sin 2\theta_1$	−0.9600	0.0940	0.4742	0.3918
$\sin \theta_2 - \sin \theta_1$	0.8000	−0.3000	−0.3000	−0.2000
$\cos \theta_2 - \cos \theta_1$	−1.6000	−0.2660	−0.1138	−0.0202
$\cos^2 \theta_2 - \cos^2 \theta_1$	−0.6400	0.3899	0.2101	0.0400
$(\theta_2 - \theta_1) - (\sin \theta_2 - \sin \theta_1)$	1.4143	0.7037	0.6223	0.4013
$\frac{1}{2}(\cos^2 \theta_2 - \cos^2 \theta_1) - (\cos \theta_2 - \cos \theta_1)$	1.2800	0.4609	0.2188	0.0402
$\frac{3}{2}(\theta_2 - \theta_1) - 2(\sin \theta_2 - \sin \theta_1) + \frac{1}{4}(\sin 2\theta_2 - \sin 2\theta_1)$	1.4815	1.2291	1.2020	0.79995
$\frac{1}{2}(\theta_2 - \theta_1)^3 - \frac{1}{4}(\sin 2\theta_2 - \sin 2\theta_1)$	1.34715	0.17835	0.04265	0.00270
$\theta_2 \cos \theta_2 - \theta_1 \cos \theta_1$	−1.3286	−0.9368	−0.6137	−0.2607
$\theta_2 \sin 2\theta_2 - \theta_1 \sin 2\theta_1$	−2.1257	−0.1415	1.1152	1.152
$\theta_2 \cos 2\theta_2 - \theta_1 \cos 2\theta_1$	−0.6202	1.9211	1.3961	0.4365
Total: $A = (\theta_2 - \theta_1)$	2.2143	0.4037	0.3223	0.2013
$-\frac{3}{2}(\sin \theta_2 - \sin \theta_1)$	−1.2000	0.4500	0.4500	0.3000
$+\frac{1}{2}(\theta_2 \cos \theta_2 - \theta_1 \cos \theta_1)$	−0.6643	−0.4693	−0.30685	−0.13035
A	0.3500	0.3844	0.46545	0.37095
Total: $B = -2(\theta_2^2 - \theta_1^2)$	−9.8062	−3.9016	−3.5830	−2.4486
$-16(\cos \theta_2 - \cos \theta_1)$	25.6000	4.2560	1.8208	0.3232
$+2(\theta_2 \sin 2\theta_2 - \theta_1 \sin 2\theta_1)$	−4.2514	−0.2830	2.2304	2.3040
$+5(\cos 2\theta_2 - \cos 2\theta_1)$	−6.4005	3.9005	2.1000	0.4000
B	5.1419	3.9719	2.5682	0.5786
Total: $C = 24(\theta_2 - \theta_1)$	53.1430	9.6889	7.7352	4.8312
$-40(\sin \theta_2 - \sin \theta_1)$	−32.0000	12.0000	12.0000	8.0000
$8(\theta_2 \cos \theta_2 - \theta_1 \cos \theta_1)$	−10.6288	−7.5088	−4.9096	−2.0856
$5(\sin 2\theta_2 - \sin 2\theta_1)$	−4.8000	0.4700	2.3710	1.9590
$-2(\theta_2 \cos 2\theta_2 - \theta_1 \cos 2\theta_1)$	1.2404	−3.8422	−2.7922	−0.8730
C	6.9546	10.8079	14.4044	11.8320
$\int ds$	110.715	20.185	16.115	10.065
$\int y ds$	3,535.75	1,759.25	1,555.25	1,003.25
$\int x ds$	4,000.0	665.0	284.5	50.5
$\int xy ds$	160,000.0	57,612.5	27,350.0	5,025.0
$\int y^2 ds$	185,187.5	153,637.5	150,250.0	99,993.75
$\int x^2 ds$	168,393.75	22,293.75	5,331.25	337.5
$\int M_s ds = \frac{2wcR^2}{\pi} \times A$	−22,282.0	−24,472.0	−29,631.0	−23,615.0
$\int M_s x ds = \frac{2wcR^2}{16\pi} \times B$	−1,022,950.0	−790,186.0	−510,928.0	−115,109.0
$\int M_s y ds = \frac{2wcR^2}{16\pi} \times C$	−1,383,576.0	−2,150,167.0	−2,865,669.0	−2,353,905.0

For the Beam

$$\int_{x_1}^{x_2} ds = x_2 - x_1, \qquad \int_{x_1}^{x_2} x ds = (x_2^2 - x_1^2)/2$$
$$\int_{x_1}^{x_2} x^2 ds = (x_2^3 - x_1^3)/3, \qquad \int_{x_1}^{x_2} x^3 ds = (x_2^4 - x_1^4)/4$$

INTEGRALS DUE TO SHEAR LOAD

Distribution of Shear Load

Assume the distribution varies as sin ϕ (see Fig. 2) equals $f \sin \phi$. Then vertical component equals $f \sin^2 \phi$. Therefore, total vertical force $= \int_0^\pi f \sin^2 \phi \, R d\phi = f(R\pi)/2 = wc$
Therefore,

$$f = 2wc/R\pi$$

The bending moment at θ due to the shear force at ϕ equals $-\frac{2wc}{R\pi} \sin \phi \{R[1 - \cos(\theta - \phi)]\} R d\phi$

Therefore,

$$-M_s = \frac{2wc}{R\pi} \int_0^\theta R^2 \sin \phi [1 - \cos(\theta - \phi)] d\phi = \frac{2wcR}{\pi} \left(1 - \frac{\theta \sin \theta}{2} - \cos \theta\right)$$

Hence, we have

$$\int_{\theta_1}^{\theta_2} M_s ds = \int_{\theta_1}^{\theta_2} M_\theta R d\theta$$

where $M_\theta = M_s$ at angle θ. Therefore,

$$-\int_{\theta_1}^{\theta_2} M_s ds = \frac{2wcR^2}{\pi}\int_{\theta_1}^{\theta_2}\left(1 - \frac{\theta \sin\theta}{2} - \cos\theta\right)d\theta = \frac{2wcR^2}{\pi}\left[(\theta_2 - \theta_1) - \frac{3}{2}(\sin\theta_2 - \sin\theta_1) + \frac{1}{2}(\theta_2\cos\theta_2 - \theta_1\cos\theta_1)\right]$$

Similarly,

$$-\int_{\theta_1}^{\theta_2} M_s x ds = \frac{2wcR^3}{16\pi}\left[-2(\theta_2^2 - \theta_1^2) + 5(\cos 2\theta_2 - \cos 2\theta_1) + 2(\theta_2 \sin 2\theta_2 - \theta_1 \sin 2\theta_1) - 16(\cos\theta_2 - \cos\theta_1)\right]$$

and

$$-\int_{\theta_1}^{\theta_2} M_s y ds = \frac{2wcR^3}{16\pi}\left[24(\theta_2 - \theta_1) - 40(\sin\theta_2 - \sin\theta_1) + 5(\sin 2\theta_2 - \sin 2\theta_1) + 8(\theta_2\cos\theta_2 - \theta_1\cos\theta_1) - 2(\theta_2\cos 2\theta_2 - \theta_1\cos 2\theta_1)\right]$$

TABLE 7

Item	FG	GH	HB
x_1	0	10	25
x_2	10	25	40
$\int ds = x_2 - x_1$	10	15	15
$\int x ds = \frac{1}{2}(x_2^2 - x_1^2)$	50	262.5	487.5
$\int x^2 ds = \frac{x_2^3 - x_1^3}{3}$	333.33	4,875	16,125
$\int x^3 ds = \frac{1}{4}(x_2^4 - x_1^4)$	2,500	95,156.25	542,344

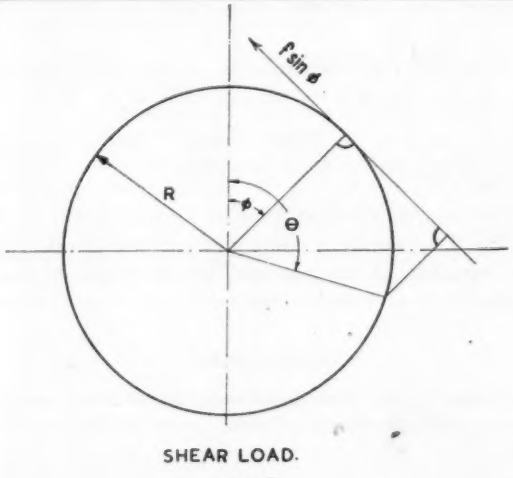

FIG. 2.

From these basic integrals we can evaluate numerically the coefficients of the partial differential coefficient equations as tabulated in Tables 2 to 5.

The layout is identical, each square representing the coefficient. For example, coefficient of W_1 in $EI_1(\partial U/\partial W_1) = 0$ is:

$$\int_B^C (x-c)^2 ds + \int_C^D (x-c)^2 ds + \int_D^E (a-c)^2 ds + k\int_F^G (a-c)^2 ds + k\int_G^H (x-c)^2\, ds + k\int_H^B (x-c)^2 ds$$

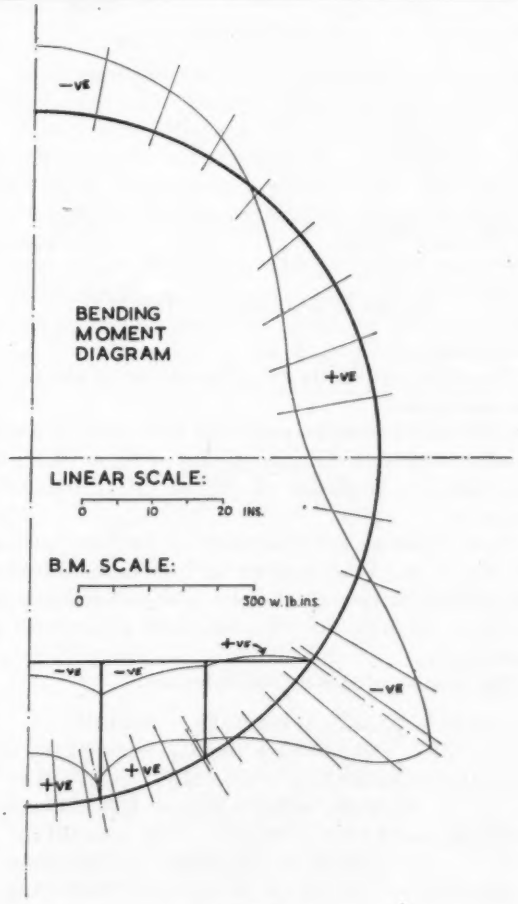

FIG. 3.

This is the sum of multiples of $\int x^2 ds$, $\int x ds$, and $\int ds$ over ranges BC, CD, DE, FG, GH, HB.

TABLE 8

	$(M/I)(\partial M/\partial X_1)$						
Part	M_1	X_1	X_2	W_1	W_2	w	s
AB	3,535.75	185,187.5	...	...	...	...	−1,383,576
BC	1,759.25	153,637.5	+153,637.5	+57,612.5	+57,612.5	+2,214,800	−2,150,167
			−140,740.0	−70,370.0	−70,370.0	−2,304,500	
CD	1,555.75	150,250.0	+150,250.0	+27,350.0	−23,336.0	+2,489,200	−2,865,669
			−124,460.0	−62,230.0		−1,094,000	
DE	1,003.25	99,993.75	+99,993.75	−30,097.5	−15,048.0	+1,605,200	−2,353,905
			− 80,260.0			− 201,000	
TOTAL	7,854.0	589,068.75	+ 50,421.0	−77,735.0	−51,142	+3,309,700	−8,753,317

TABLE 9

	$(M/I)(\partial M/\partial W_1)$						
Part	M_1	X_1	X_2	W_1	W_2	w	s
AB	...	...	...	...	...	...	...
BC	+665.0	+57,612.5	+64,592.0	+22,293.75	+22,293.75	−1,291,840	−790,186
			−53,200.0	−53,200.0	−53,200.0	+2,128,000	+978,880
	−807.4	−70,370.0	+57,612.5	+32,296.0	+32,296.0	−891,750	
			−70,370.0				
CD	+254.5	+27,350.0	+51,568.0	+5,331.25	−4,267.5	−1,031,360	−510,928
			−22,760.0				
	−645.6	−62,230.0	+27,350.0	−22,760.0	+9,669.0	+910,400	+1,185,240
			−62,230.0	+25,784.0		−213,250	
DE	−301.95	−30,097.5	−30,097.5	+9,058.5	+4,529.25	+60,600	+708,450
			+24,155.0			−483,120	
FG	...	...	...	+9,000k	+4,500k	−240,000k	...
						+5,000k	
GH	...	...	...	+4,875k	−3,937k	−47,578k	...
				−21,000k	+9,000k	+210,000k	
				−24,000k		−480,000k	
						+97,500k	
HB	...	...	...	+16,125k	+16,125k	−271,172k	...
				−39,000k	−39,000k	+390,000k	
				+24,000k	+24,000k	−480,000k	
						+322,500k	
TOTAL	−805.45	−77,735	−13,379	+18,803.5	+11,320.5	−812,320	+1,571,456
				+18,000k	+10,688k	−493,750k	

$$\text{coefficient} = 18{,}803.5 + 18{,}000\,k$$

(See Table 9.)

The other coefficients are tabulated and evaluated in the same manner.

Note that Maxwell's reciprocal theorem is a useful check on this work—e.g., coefficient of W_1 in $(M/I) \times (\partial M/\partial W_2)$ = coefficient of W_2 in $(M/I_1)(\partial M/\partial W_1)$ and so on.

Table 8 shows the computations for the equation $\partial U/\partial X_1 = 0$. Table 9 shows the computations for the equation $\partial U/\partial W_1 = 0$. Similar tables are required for $\partial U/\partial M_1$, $\partial U/\partial X_2$, $\partial U/\partial W_2$, but these are omitted to save space.

The five simultaneous equations are:

$$157.08M_1 + 7{,}854X_1 + 609.05X_2 - 805.45W_1 - 535.10W_2 + 34{,}184w - 100{,}000w = 0$$

$$7{,}854M_1 + 589{,}068.75X_1 + 58{,}421X_2 - 77{,}735W_1 - 51{,}142W_2 + 3{,}309{,}700w - 8{,}753{,}317w = 0$$

$$609.05M_1 + 58{,}421X_1 + 9{,}472.25X_2 - 13{,}379W_1 - 8{,}305W_2 + 573{,}800w - 1{,}152{,}301w = 0$$

$$-805.45M_1 - 77{,}735X_1 - 13{,}379X_2 + (18{,}803.5 + 18{,}000k)W_1 + (11{,}320 + 10{,}688k)W_2 - (812{,}320 + 493{,}750k)w + 1{,}571{,}456w = 0$$

$$-535.10M_1 - 51{,}142X_1 - 8{,}305X_2 + (11{,}320 + 10{,}688k)W_1 + (7{,}280 + 6{,}750k)W_2 - (482{,}910 + 299{,}610k)w + 987{,}384w = 0$$

These five equations may be solved simultaneously for M_1, X_1, X_2, W_1, W_2 for any value of k. If $k = 1$,

$$M_1 = -95.62w, \quad X_1 = +9.44w, \quad X_2 = +50.05w$$
$$W_1 = +22.54w, \quad W_2 = +10.52w$$

The bending moment diagram for this case is shown in Fig. 3. Positive bending moment tends to decrease the curvature of the ring and, for the beam, tends to make the beam concave upward.

REFERENCES

[1] Ruffner, B. F., *Monocoque Fuselage Circular Ring Analysis*, Journal of the Aeronautical Sciences, Vol. 6, No. 3, p. 114, January, 1939.

[2] Wise, J. A., *Analysis of Circular Rings for Monocoque Fuselages*, Journal of the Aeronautical Sciences, Vol. 6, No. 11, p. 460, September, 1939.

[3] Greenwood, E. J. A., *A Method of Stress Analysis of Monocoque Fuselage Circular Rings*, Journal of the Aeronautical Sciences, Vol. 3, No. 12, p. 440, October, 1936.

[4] Lundquist, E. E., and Burke, W. F., *The General Equations for the Stress Analysis of Rings*, N.A.C.A. Tech. Report No. 509, August, 1934.

[5] Pippard, A. J. S., and Baker, J. F., *The Analysis of Engineering Structures*, 1st Ed., p. 265; Edward Arnold & Co., London, 1936.

[6] Newell, J. S., *The Use of Symmetric and Anti-Symmetric Loadings*, Journal of the Aeronautical Sciences. Vol. 6, No. 6. p. 235, April, 1939.

High-Speed Flow Through Cambered Rotating Grids

FRANK L. WATTENDORF*

Air Materiel Command, Wright Field

SUMMARY

In a previous paper,[1] an analysis was given for the ideal performance of rotating blades in curved lattice arrangement. The lattice type of blading represents an approach to higher stage pressures by utilizing blades that are more closely spaced and highly cambered than airfoil theory permits. The blades exert a predominant guiding action on the flow, and the direction of flow relative to the trailing edge of a blade is essentially determined by the angular setting of the trailing edge itself.

For incompressible flow, ideal pressure coefficients based on blade tip speed can be computed as a function of the flow coefficient. Experimental results of several investigators show good comparison with the theory in the neighborhood of the design point.

For compressor application, the stage temperature ratio or pressure ratio replaces the pressure coefficient in significance. The temperature ratio can also be expressed in terms of the velocity diagram and Euler's equation.

The present paper shows various configurations of flow diagram which result in considerable increases in the ideal stage pressure ratio, and the following four cases are considered:

(1) Subsonic flow throughout.

(2) Subsonic axial flow, subsonic flow in the rotor, supersonic flow in the downstream stator.

(3) Subsonic axial flow, supersonic flow in rotor and stator.

(4) Supersonic flow throughout.

In all cases considerations are limited to ideal adiabatic flow through curved lattice types of blading.

It is the purpose of this paper to show the extremely large potential increases in ideal stage pressure ratio theoretically possible in axial compressors, with a view toward stimulating experimental investigation of the losses involved and of possible methods of decreasing these losses. Application would be especially promising for cases where simplicity and compactness outweigh efficiency in importance.

INTRODUCTION

AXIAL COMPRESSORS are becoming increasingly important as components of gas-turbine propulsion systems and other applications because of their small frontal area in relation to their output. Their chief disadvantage, as compared for instance with the centrifugal compressor, lies in the many stages and resulting length of the unit required to obtain a given pressure ratio. A subsonic axial-flow compressor designed by airfoil theory seldom has a stage pressure ratio of more than 1.25; therefore, such a compressor would need many stages to equal a centrifugal compressor having a stage pressure ratio of 3 or 4 to 1.

Received September 22, 1947.

*Scientific Consultant

It is the purpose of this paper to show how, disregarding for the moment the question of efficiency, the stage pressure ratio of an axial compressor can be raised to compete with the centrifugal compressor. This particular discussion is based on the utilization of closely spaced, highly cambered blades, and the four cases mentioned in the Summary are considered.

Ideal adiabatic flow will be assumed in this study, and none of the cases considered should be assumed competitive with other methods from the point of view of efficiency.

AIRFOIL THEORY

Axial compressors are usually designed by the application of single-airfoil theory, whereby each blade element is treated as an airfoil and the pressure produced is obtained by suitable resolution and integration of the component forces acting on the blade element. A typical vector diagram showing the forces acting on a blade element is shown in Fig. 1, where W_i and W_o are the relative inlet and the relative outlet velocities of the rotating blades, W_{ouc} is the absolute outlet velocity of the upstream contravane or stator, and W_{idc} is the absolute inlet velocity of the downstream contravane.

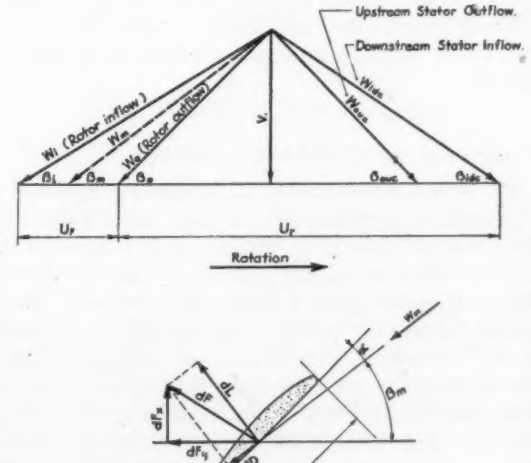

FIG. 1. Velocity diagram for a single-stage compressor (airfoil theory).

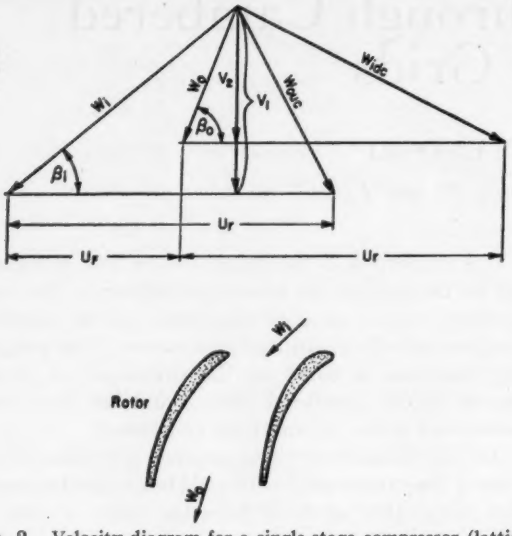

FIG. 2. Velocity diagram for a single-stage compressor (lattice theory).

U_r is the circumferential velocity of the rotating blade element, and W_m is the mean relative velocity through the rotating blades. Since the pressure rise is essentially proportional to the lift force acting on the airfoil, it follows that increased stage pressure should be obtained in two principal ways—namely, increase of the relative velocity, W_m, or increase of blade area.

The relative velocity is usually limited by approach to the speed of sound in normal compressor design. Utilization of supersonic velocity in the airfoil type of compressor will not be discussed in this paper.

Increase of blade area involves increase of the ratio of blade chord to spacing. When this ratio essentially exceeds unity, mutual interference between the blades seriously impedes the applicability of single-airfoil theory, and a different approach becomes necessary, as follows.

Curved Lattice Theory

The curved lattice theory, as discussed in reference 1, represents an approach to high stage pressures for any given relative velocity by utilizing higher values of the ratio of chord to spacing than airfoil theory permits. This is done by using a system of cambered, closely spaced blades, the passages between which represent curved expanding channels and are analyzed as such. The blades exert a predominant guiding action on the flow, and the direction of flow relative to the trailing edge of a blade is essentially determined by the angular setting of the trailing edge itself, as discussed, for instance, by Constant.[2]

A typical vector flow diagram for a lattice system is shown in Fig. 2, where the notations for the velocities are the same as that of Fig. 1. Here, U_F is the change in the circumferential component of the velocity relative to the rotating blades. In reference 1 the pressure coefficient was expressed in terms of the flow coefficient and was integrated over the effective disc area. In this way, ideal characteristic curves could be calculated for a series of curved lattice systems. Experimental results showed good comparison with the theory in the neighborhood of the design point.

Stage Temperature Ratio

For compressor application, the stage pressure ratio or temperature ratio replaces the incompressible pressure coefficient in significance. For compressible flow, the adiabatic temperature head developed by a compressor stage can be expressed in terms of Euler's equation, which ties directly into the velocity diagram, shown in Fig. 2. The force acting against the direction of motion of the rotating blades per unit mass flow per second is $1 \cdot U_F$. The work done per unit mass flow per second by the rotating blades is then $1 \cdot U_F \cdot U_r$. If the absolute inlet velocity to the rotating blades is equal to the absolute outlet velocity from the stationary blades, there is no change in the kinetic energy of the gas stream in passing through the stage. According to the energy equation for gas flow, this work done, $U_F U_r$, must appear as increase in enthalpy of the gas. Thus,

$$JgC_p\Delta T = U_F U_r$$

where J is the mechanical equivalent of heat, g is the gravitational constant, C_p is the specific heat of the gas at constant pressure, and ΔT is the stage temperature rise. The stage temperature ratio then becomes

$$\frac{T_2}{T_1} = \frac{T_1 + \Delta T}{T_1} = 1 + \frac{U_F U_r}{JgC_p T_1}$$

Since isentropic flow is assumed, the pressure ratio p_2/p_1 across the stage must be given by

$$p_2/p_1 = [1 + (U_F U_r / JgC_p T_1)]^{K/(K-1)}$$

where K is the adiabatic exponent.

Limits for Subsonic Flow Throughout

It is of interest to consider a special case that will indicate limiting ideal conditions for subsonic flow. The

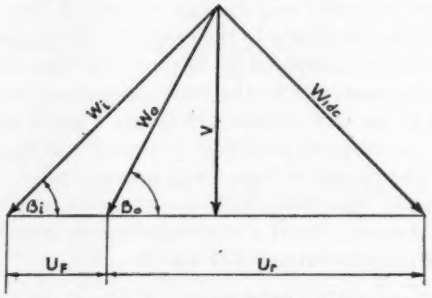

FIG. 3. Velocity diagram where velocity relative to rotor inlet equals velocity relative to inlet of downstream stator ($W_i = W_{ide}$).

following assumptions are made: (1) constant axial velocity (i.e., by suitable area change); (2) Mach Number relative to rotor inlet approaches unity; and (3) Mach Number relative to downstream stator inlet approaches unity.

In Fig. 3 is shown the vector diagram whereby the relative velocities approaching the rotor blades and downstream stator vanes are equal. This condition can be satisfied by a wide combination of rotor speed and rotational velocity imparted to the air.

Thus,

$$T_2/T_1 = 1 + (U_F U_r/JgC_pT_1)$$
$$(U_F + U_r)/2 = W_i \cos \beta_i$$
$$U_F = 2W_i \cos \beta_i - U_r$$
$$U_F U_r = 2W_i \cos \beta_i U_r - U_r^2 =$$
$$2W_i U_r[\sqrt{1 - (V/W_i)^2}] - U_r^2$$

By introducing the speed of sound, a, and the gas constant, R_0, it follows that

$$T_1 = a^2/KgR_0$$
$$\frac{T_2}{T_1} = 1 + (K-1)\left[2M_iM_r\sqrt{1 - \left(\frac{M_a}{M_i}\right)^2} - M_r^2\right]$$

where

$$M_i = W_i/a, \qquad M_r = U_r/a, \qquad M_a = V/a$$

The combination for maximum ideal temperature rise can be found by differentiating. Thus:

$$T_2/T_1 = 1 + (U_F U_r/JgC_pT_1)$$
$$U_F U_r = 2W_i \cos \beta_i U_r - U_r^2$$

For max. T_2/T_1, $U_F U_r$ = max.

$$\partial(U_F U_r)/\partial U_r = 2W_i \cos \beta_i - 2U_r = 0$$
$$U_r = W_i \cos \beta_i = U_F$$
$$T_2/T_1 = 1 + (W_i^2 \cos^2 \beta_i/JgC_pT_1)$$
$$T_1 = a^2/KgR_0$$
$$\frac{T_2}{T_1} = 1 + \frac{KR_0}{JC_p} M_i^2 \cos^2 \beta_i = 1 + \frac{KR_0}{JC_p} M_r^2 =$$
$$1 + (K-1)M_r^2$$

where $M_i = W_i/a$ and $M_r = U_r/a$. It is seen that the theoretical maximum occurs when the absolute inflow into the rotor is axial (Fig. 4) and the circumferential

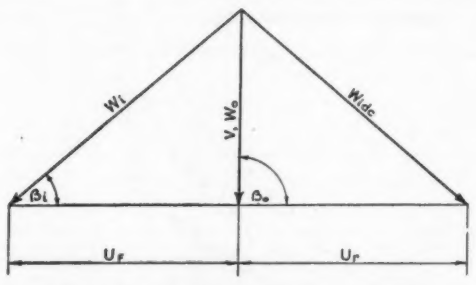

FIG. 4. Velocity diagram for maximum stage pressure for case when $W_i = W_{ide}$.

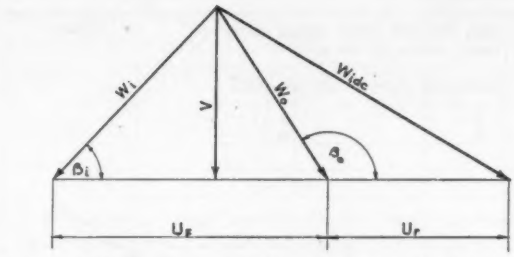

FIG. 5. Velocity diagram for impulse-type rotor blading and supersonic velocity entering downstream stator.

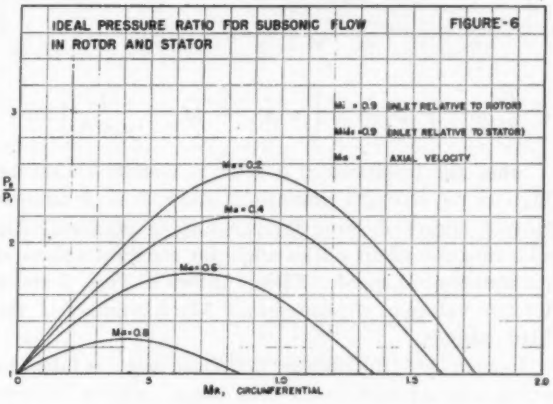

velocity of the rotor blade element is equal to the rotational velocity imparted to the air by the rotor blade element.

The general case represented by Fig. 3 can be illustrated by plotting ideal temperature ratio against rotational tip speed, as shown in Fig. 6. As an illustrative case, specific values were assigned to the relative velocity entering the rotor blades and downstream stator vanes.

SUPERSONIC FLOW IN STATOR VANES

In the previous section, special cases of limiting ideal stage pressure ratios were considered, whereby velocities relative to both rotor and stator were limited by the speed of sound. Further increase of stage pressure would involve lengthening the horizontal vector, which would give rise to supersonic velocities entering either the rotor or stator. The special case that will now be considered is the case of limiting subsonic flow in the rotor and supersonic flow entering the downstream stator.[3] The corresponding vector diagram is shown in Fig. 5, where β_0 is taken greater than 90° as an example. For this more general case,

$$T_2/T_1 = 1 + (U_F U_r/jgC_pT_1)$$
$$U_F = W_i \cos \beta_i - (W_i \sin \beta_i/\tan \beta_0)$$
$$= W_i\sqrt{1 - (V/W_i)^2} - (V/\tan \beta_0)$$
$$T_1 = a^2/KgR_0$$

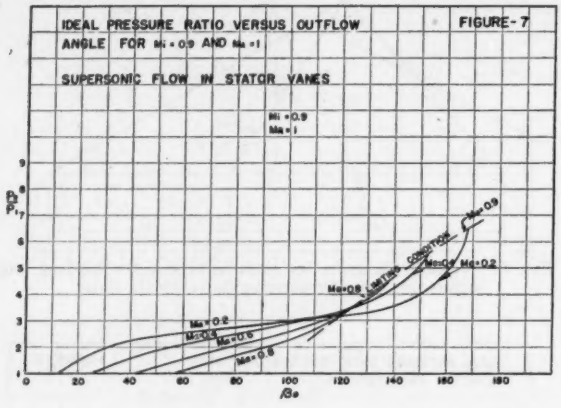

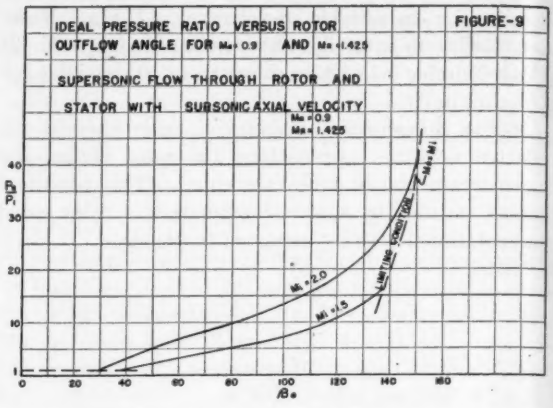

$$\frac{T_2}{T_1} = 1 + (K-1)\left[\sqrt{M_i^2 - M_a^2} - \frac{M_a}{\tan \beta_0}\right] M_r$$

Since the tip speed of a rotor is usually chosen as high as the strength limitations allow, it is of interest to plot curves showing temperature or pressure ratio as a function of air outlet angle for constant values of circumferential speed. This is shown in Figs. 7 and 8 for two values of circumferential Mach Number of the blade element.

In each case, the limiting deflection angle is taken as equal and opposite to the inlet angle, and the relative exit velocity is equal to the limiting relative inlet velocity; in other words, the compressor would be analogous to the pure impulse turbine.

Supersonic Flow Through Rotor and Stator: Subsonic Axial Velocity

If the restriction of subsonic flow is removed from both rotor and stator, still further increase of ideal stage pressure is theoretically possible. Limitations then are associated chiefly with the axial velocity and rotor tip speed. A family of curves is plotted in Fig. 9 for subsonic axial velocity and a blade element circumferential speed of 1,600 ft. per sec.

This general case was proposed by Tsien[4] who worked out a specific illustrative example as follows.

The rotor blade is a pure impulse type, whereby the entrance angle of the rotor blade referred to the plane of rotation is 29° and the trailing edge, 151°. The Mach Number of the axial approach flow is 0.92. The Mach Number of the relative flow entering the rotor blade is 1.62 and that of the flow leaving the blade is 1.55. The flow entering the downstream stator vanes has a Mach Number of 3 at an entrance angle of 14.5°. Dr. Tsien estimated the pressure rise for the entire stage by first computing the pressure drop in accelerating the axial flow from atmospheric stagnation pressure to the section immediately preceding the rotor; then assuming no pressure change in the rotor blades; and, finally, estimating the pressure recovery in a special design of downstream stator vanes utilizing multiple oblique shock waves. Dr. Tsien's calculations made in this manner show a possible compression ratio of 15 in a single stage with an estimated adiabatic compression efficiency of 65 per cent, which would not seem unfavorable in the light of the extremely high compression ratio involved.

Completely Supersonic Flow

In this case the axial flow entering the compressor is assumed supersonic, as well as the flow relative to both rotor and stator. The only limitations on the stage

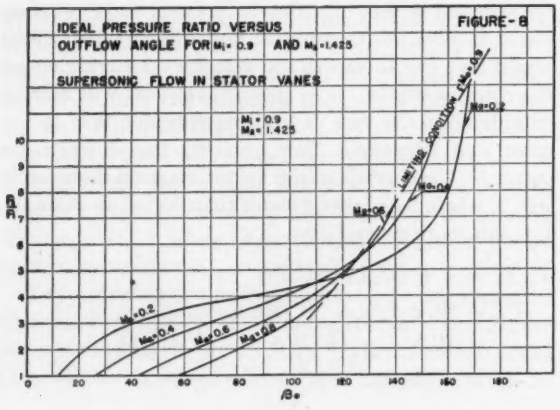

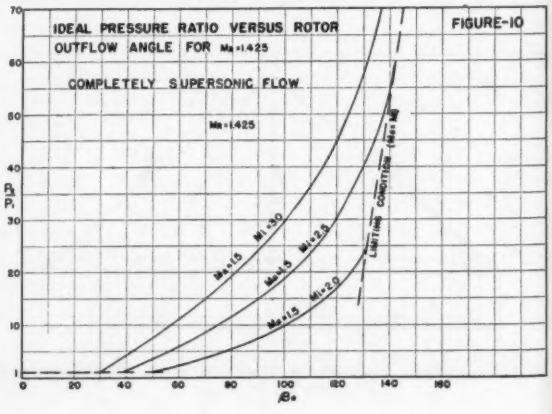

pressure or temperature ratio will be the structural limitation on the rotor tip speed. Again taking an assumed constant value of 1,600 ft. per sec. for the blade element circumferential speed, several calculated ideal curves are shown in Fig. 10.

Conclusion

In conclusion, it is emphasized that the present discussion intends only to point out that theoretically high ideal stage pressure ratios are attainable with the use of highly cambered blades of the curved lattice type. It is realized that highly cambered blades are not widely used in practice because of the tendency toward lower efficiency. However, it seemed worth while to point out the large potential increase in stage pressure ratio theoretically possible with a view toward stimulating experimental investigations of the losses involved in such a system and of possible methods of decreasing these losses. Application would be especially promising for cases where simplicity and compactness outweigh efficiency in importance.

References

[1] Wattendorf, F. L., *The Ideal Performance of Curved Lattice Fans*, Theodore von Kármán Anniversary Volume, 1941.

[2] Constant, H., *Performance of Cascades of Airfoils*, R.A.E. Note No. E.3696, 1939.

[3] Weise, A., *Ueberschallaxialverdichter*, Bericht 171, Lilienthal Gesellschaft.

[4] Tsien, H. S., *Axial Compressors with Supersonic Exit Velocities from Rotating Buckets*, December, 1945 (unpublished).

Errata

An incorrect graph (Fig. 9, page 63) appeared in the paper "The Kinematics of Turbulence" by F. N. Frenkiel in the Journal of the Aeronautical Sciences, Vol. 15, No. 1, pp. 57–64, January, 1948. The correct figure is reproduced here.

The following errors also appeared in the paper:

(1) Table 1, column 3, "instant" should be "instant t."

(2) Table 1, column 4, "$R_x(x) = R_x(x)$" should be "$R_x(x) = R_x^{\%}(x)$."

(3) Page 59, in Eq. (6), "$\Re_x$" should be "R_x."

(4) Page 61, line 9, "$\int^{\rho_0}$" should be "$\int_{\rho_0}$."

(5) Page 62, column 1, line 5, "$A_0m^2 + 1 \div m^2 + 1$" should be "$(A_0m^2 + 1)/(m^2 + 1)$."

(6) Page 63, line 3, "β exp" should be "B exp."

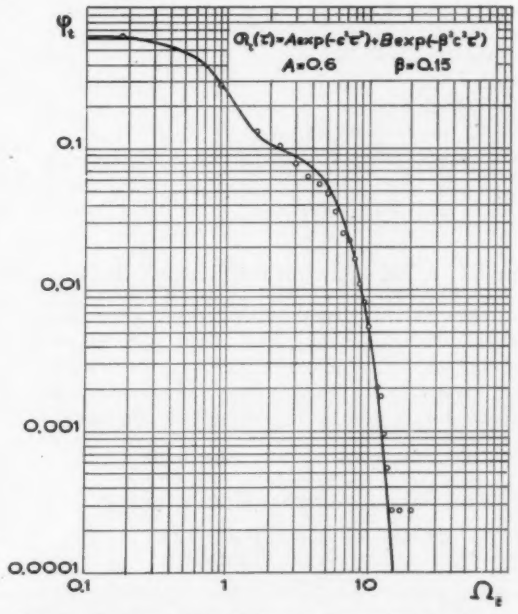

Fig. 9. Spectrum of turbulence measured by Dryden.[13]

Services of the Libraries of the Institute of the Aeronautical Sciences

The services of the Libraries are available to all members of the Institute, to Corporate Members, to advertisers in the AERONAUTICAL ENGINEERING REVIEW and AERONAUTICAL ENGINEERING CATALOG, and, under usual library limitations, to the public. Four specialized services are available.

The Paul Kollsman Lending Library

This lending library service makes available, *without charge*, the latest and more important aeronautical books.

Members may request the loan of any aeronautical or technical book they wish to borrow. Through an exchange agreement with the Engineering Societies Library, any book on general engineering may be borrowed from its great collection of over 160,000 volumes.

A photostating service is available at usual library rates.

Applications for membership in the library and further information will be sent on request.

The W. A. M. Burden Reference Library

This reference library contains over 12,000 aeronautical books, magazines, pamphlets, and reports gathered from world-wide sources and is one of the most complete aeronautical libraries in the world. Material from this library is not available for loan but may be used for reference purposes.

The Pacific Aeronautical Library

6715 Hollywood Boulevard
Los Angeles 28, California

Established in cooperation with the aircraft companies the library serves. The leading aircraft companies in or near Los Angeles participate in its support and operation.

This service library for aeronautical research is available to the public for reading privileges. Source material includes aerodynamic and structural research reports, as well as books on drafting, production methods, history, and allied sciences. It furnishes books, periodicals, and pamphlet material to the participating aircraft companies to supplement their engineering libraries.

Technical Information Service

This service has experienced personnel under the supervision of trained aeronautical engineers to compile any information desired. The services range from listing specialized reference books to the preparation of exhaustive bibliographies, digesting of reports, and general surveys of any aeronautical subject. Some of the available services are:

Bibliographies on any aeronautical subject.
Reports on any aeronautical subject.
Digests of aeronautical books, papers, periodicals, and references.
Translations.
Engineering investigations of special aeronautical subjects.
Biographies of individuals engaged in aeronautics.
Photostats of any aeronautical or general engineering material.
Microfilms made on special order.
Photographs made from the Institute's photographic collection.
Drawings and tracings made.

In addition to the services mentioned any commission which comes within the scope of the Service will be accepted. Special arrangements may be made for work requiring several weeks or months.

Translators are available for accurate transcriptions of all foreign language data. Translations are carefully edited by trained engineers.

Reproductions of any material in the collections of the Institute may be ordered at standard photostat rates.

INSTITUTE OF THE AERONAUTICAL SCIENCES, INC.
2 EAST 64TH STREET, NEW YORK 21, N.Y.